Modulating Tumor Promotion by Targeting Inflammation and Endoplasmic Reticulum Stress

Doctoral thesis

to obtain a doctorate (PhD)

from the Faculty of Medicine

of the University of Bonn

Peng Chen

from Chongqing, China

2025

Written with authorization of

the Faculty of Medicine of the University of Bonn

First reviewer: Prof. Dr. Ingo Schmidt-Wolf

Second reviewer: Prof. Dr. Hans Weiher

Day of oral examination: 26/06/2025

From the Department of Integrated Oncology, CIO Bonn, University Hospital of Bonn

Table of Contents

List of abbreviations

ACT	Adoptive cellular immunotherapy
ANOVA	Analysis of variance
ATF6	Activating transcription factor 6
ATG3	Autophagy related 3
bFGF	Basic fibroblast growth factor
BiP	Binding immunoglobulin protein
CAFs	Cancer-associated fibroblasts
CCK-8	Cell counting kit-8
CHOP	C/EBP homologous protein
CIK	Cytokine-induced killer cells
CM	Conditioned-meidum
CRC	Colorectal cancer
CSCs	Cancer stem cells
CTLA-4	Cytotoxic T-lymphocyte-associated protein
CXCL1/2	C-X-C motif chemokine ligand 1/2
DCs	Dendritic cells
eIF2α	eukaryotic initiation factor 2α
ELISA	Enzyme-linked immunosorbent assay
EMT	E pithelial-to-mesenchymal transition
ER	Endoplasmic reticulum

ERAD	ER-associated degradation
ERK	Extracellular signal-regulated kinase
FAD	Flavin adenosine dinucleotide
FBS	Fetal bovine serum
G-CSF	Granulocyte colony-stimulating factor
GPx8	Glutathione peroxidase 8
GRP78	Glucose-regulated protein 78
HIF-1α	Hypoxia-inducible factor-1 alpha
HUVEC	Human umbilical vein endothelial cell
ICAM-1	Intracellular cell adhesion molecule 1
ICD	Immunogenic cell death
ICIs	Immune checkpoint inhibitors
IRE1	Inositol requiring enzyme 1
JNK	c-Jun N-terminal kinase
KIRs	Killer immunoglobulin-like receptors
LFA-1	Lymphocyte function associated antigen 1
LSD-1	Lysine specific demethylase 1
MAO-A/B	Monoamine oxidases A and B
MAPK	Mitogen-activated protein kinase
MDSCs	Myeloid-derived suppressor cells
MHC	Major histocompatibility complex

MICA/B	MHC class I chain-related protein A and B
MM	Multiple myeloma
MMPs	Matrix metalloproteinases
NF-κB	Nuclear factor kappa B
NK	Natural killer
NKG2D	Natural killer group 2D
NOS	Nitric oxide synthase
OD	Optical density
PBMC	Peripheral blood mononuclear cells
PD-1	Programmed cell death protein 1
PDGF	Platelet-derived growth factor
PDI	Protein disulfide isomerase
PD-L1	Programmed Cell Death Ligand 1
PERK	Protein kinase-like ER kinase
POI	Protein of interest
PPP	Pentose phosphate pathway
PRDX4	Peroxiredoxin 4
PROTAC	Proteolysis-targeting chimera
PrxIV	Peroxiredoxin IV
RNS	Reactive nitrogen species
ROS	Reactive oxygen species

STAT3	Signal transducer and activator of transcription 3
TAMs	Tumor-associated macrophages
TIM-3	T-cell immunoglobulin and mucindomain containing-3
TLR	Toll-like receptor
TME	Tumor microenvironment
TRAIL	Tumor necrosis factor-related apoptosis-inducing ligand
Tregs	Regulatory T cells
ULK1	Unc-51-like kinase 1
UPR	Unfolded protein response
UPS	Ubiquitin proteasome system
VEGF	Vascular endothelial growth factor
VKOR	Vitamin K epoxide reductase
XBP1	X-box protein 1

1. Introduction

1.1 Cytokine-induced killer (CIK) cells

1.1.1 Introduction

Cytokine-induced killer (CIK) cells were first reported by Schmidt-Wolf I.G.H. and colleagues in 1991 (Schmidt-Wolf et al., 1991). Derived from peripheral blood mononuclear cells (PBMCs) and being incubated with indicated cytokines for 14-21 days, CIK cells become a heterogeneous population of exceptional T lymphocytes with $CD3^+CD56^+$ cells as the primary effectors, which is rare (around 3%) in peripheral blood of healthy individuals and possess both functional characteristics of T cells and a major histocompatibility complex (MHC)-unrestricted cytolysis of natural killer (NK) cells (Schmeel et al., 2015; Schmidt-Wolf et al., 1991). In addition, CIK cells also contain a minor fraction of $CD3^+CD56^-$ T cells and $CD3^-CD56^+$ NK cells. Similar to NK cells, CIK cells are well-documented to be triggered by the natural killer group 2D (NKG2D) to exert lytic effects against tumors (Wu et al., 2020). Engaging with its ligands, NKG2D transmits activating signals into CIK cells to polarize and release lytic granules, and consequently kill malignant cells.

CIK cells are originally generated from freshly isolated PBMCs with the treatment of IFN-γ, anti-CD3, IL-1β, and IL-2. Importantly, it has been demonstrated that the usage of IFN-γ can enhance the cytotoxicity of CIK cells only if added 24 h before the addition of IL-2, probably due to the induction of IL-2 receptors on the effector cells, resulting in a more efficient activation or recruitment of additional cell populations that are not activated by IL-2 alone (Itoh et al., 1985; Teichmann et al., 1989). In addition, CIK cells can also be generated from both peripheral blood and cord blood (Schmidt-Wolf et al., 1991).

1.1.2 CIK cell-mediated tumor cell lysis

As mentioned above, among the heterogeneous populations of CIK cells, the abundant $CD3^+CD56^+$ subset is considered to exert cytotoxic activity. The mechanisms involved in the cytotoxicity of CIK cells have not yet been completely clarified, however, some crucial molecules have been identified. CIK cell-mediated cytotoxicity is cell-cell contact dependent as studies revealed that the blockade of lymphocyte function associated antigen 1 (LFA-1) and intracellular cell adhesion molecule 1 (ICAM-1) inhibited the

cytotoxicity of CIK cells (Schmidt-Wolf et al., 1993). Cell contact subsequently activates the polarization and the release of lytic granules, such as perforin, granzymes, and cytokines (Wu et al., 2021; Wu et al., 2020).

The activation of CIK cells depends on the recognition and engagement of ligands and receptors on the surface of CIK cells and tumor cells. The contact between CIK cells and tumor cells provides a reliable physical environment for the activation of CIK cells. NK receptors on CIK cells are the main recognition structure, including NKG2D, DNAX accessory molecule-1 (DNAM-1), NKp30, CD16 (Pievani et al., 2011; Verneris et al., 2004). Both NKG2D and DNAM-1 are highly expressed in CIK cells, while NKp30 is present at low density and CD16 expression is donor-dependent. The corresponding ligands in tumor cells include MHC class I chain-related protein A and B (MICA/B) and UL16 binding proteins (ULBPs) (Raulet et al., 2013), which are mainly expressed on tumor cells and a few on normal cells. Engagement of these receptors and ligands can trigger and activate CIK cells, exerting cell lysis in an MHC-unrestricted pattern.

In addition, programmed cell death system Fas-FasL and tumor necrosis factor-related apoptosis-inducing ligand (TRAIL) signaling are also found to mediate the cytotoxicity of CIK cells (Cappel et al., 2016; Durrieu et al., 2014). Research also found that inhibitory receptors, such as killer immunoglobulin-like receptors (KIRs), are usually absent from CIK cells. However, other immuue checkpoint molecules, including programmed cell death protein 1 (PD-1), T-cell immunoglobulin and mucindomain containing-3 (TIM-3), and cytotoxic T-lymphocyte-associated protein 4 (CTLA-4) have been shown to be expressed in CIK cells with various extents and may incur functional inhibition of CIK cells.

1.2 Tumor microenvironment (TME)

1.2.1 Introduction

TME is a complex ecosystem, surrounding and feeding tumor cells. TME is composed of cancer cells, stromal components (such as immune cells, fibroblasts, and blood vessels), and extracellular matrix (ECM) (Bozyk et al., 2022). The mutual interaction between the TME and tumor cells facilitates the tumor-supportive evolution of TME and promotes tumor cell growth (Whiteside, 2008). Tumor cells can reshape TME to a tumor-supportive condition by releasing extracellular signals, while educated TME in turn supports the growth and invasion of tumor cells (Pickup et al., 2014).

1.2.2 Inflammation in the TME

The inflammation in the TME is a hallmark of cancers (Balkwill and Mantovani, 2001; Zhao et al., 2021). It represents a complex physiological response of the body to internal and external environmental stimuli and is closely linked to tumor initiation and progression. As a double-edged sword, inflammation plays both pro-tumor and anti-tumor roles, largely determined by the type, intensity, and duration of the inflammation. Pro-inflammatory cytokines, as key mediators of inflammation, can promote tumor progression through various mechanisms, while, under certain conditions, they can also inhibit tumor growth.

Acute inflammation in tumors typically occurs during the early stages of inflammation, which reflects an adaptive, anti-tumor physiological mechanism aimed at limiting tumor progression (Balkwill and Mantovani, 2001). For instance, TNF-α can induce tumor cell death by activating apoptosis-related signaling pathways, such as the FADD-caspase 8 pathway (Wang et al., 2008). In addition, cytokines like IL-1 and IFN-γ can directly or indirectly enhance the activity of effector T cells and NK cells, thereby boosting the immune surveillance of tumors (Castro et al., 2018; Ikeda et al., 2002). Certain pro-inflammatory cytokines can also modulate the TME to downregulate the expression of immune inhibitory molecules, thereby inhibiting tumor progression (Zhao et al., 2021).

However, acute inflammation gradually transitions into chronic inflammation and switches to a critical promoter of cancer (Grivennikov et al., 2010). Pro-inflammatory cytokines, such as IL-6, IL-8, and TNF-α, activate signaling pathways like nuclear factor kappa B (NF-κB) and signal transducer and activator of transcription 3 (STAT3), driving increased cell proliferation and enhanced anti-apoptotic capacity, thus promoting the survival and expansion of tumor cells (Guo et al., 2024). Furthermore, inflammation generates substantial reactive oxygen species (ROS) and reactive nitrogen species (RNS), which can induce DNA damage and mutation, leading to genomic instability and a heightened risk of carcinogenesis (Chen and Zhou, 2015; Grivennikov et al., 2010). Within the TME, pro-inflammatory cytokines also promote tumor progression by inducing angiogenesis. For example, the upregulation of IL-1 and vascular endothelial growth factor (VEGF) enhances new blood vessel formation, providing essential oxygen and nutrients for tumor growth (Aguilar-Cazares et al., 2019; Voronov et al., 2014). Concurrently, pro-inflammatory cytokines may regulate the immune microenvironment by recruiting

regulatory T cells (Tregs) and myeloid-derived suppressor cells (MDSCs), thereby suppressing effector immune responses and enabling tumors to evade immune surveillance (Rahma and Hodi, 2019; Wang and DuBois, 2015).

In summary, inflammation in the TME exhibits dual effects on tumor biology. Although acute inflammation may contribute to tumor control, chronic inflammation facilitates tumor growth and immune evasion, highlighting its dualistic and context-dependent nature in tumor progression.

1.2.3 Tumor-associated macrophages (TAMs)

Macrophages are the major cellular component of the TME, occupying 60 % of the TME parenchyma (Bied et al., 2023; Chevrier et al., 2017). Macrophages in the TME can exhibit very different or even opposite phenotypes, depending on the microenvironment in which they are located. Activated macrophages are generally divided into classically activated M1 macrophages, induced by lipopolysaccharide (LPS), IFN-γ, or colony-stimulating factor 2 (CSF-2); or alternatively activated M2 macrophages, induced by IL-4, IL-13, or CSF-1 (Lin et al., 2019; Qian and Pollard, 2010). In addition, M2 macrophages are further divided into M2a, M2b, M2c, and M2d cells. In general, M1 macrophages promote inflammatory responses against invading pathogens and tumor cells, while M2 macrophages tend to exhibit an immunosuppressive phenotype that favors tissue repair and tumor progression. The markers, metabolic characteristics, and gene expression profiles of these two types of macrophages are different. M1 macrophages secrete pro-inflammatory cytokines such as IL-12, TNF-α, CXCL-10, and IFN-γ and produce high levels of nitric oxide synthase (NOS), while M2 macrophages secrete anti-inflammatory cytokines such as IL-10, IL-13, and IL-4 and express abundant arginase-1 (ARG-1), mannose receptor (MR, CD206), and scavenger receptors (Movahedi et al., 2010; Qian and Pollard, 2010). A notable feature of macrophages is their high plasticity, meaning that M1 and M2 macrophages can transition between each other in response to TME signals, a process known as macrophage polarization (Mantovani et al., 2002). Although studies have found that TAMs can exhibit both M1 and M2 polarization phenotypes, TAMs are generally considered to be M2-like macrophages (Mantovani et al., 2002; Zhang et al., 2014). Importantly, due to the plasticity, reprogramming M2-like TAMs in the TME into M1-like macrophages with anti-tumor efficacy using various approaches, including small

molecule compounds, nanomedicines, and gene editing, has emerged as an important strategy of targeting TAMs for anti-tumor therapy in recent years.

TAMs contribute to tumor progression through multiple mechanisms (Yang et al., 2020). Firstly, TAMs promote tumor growth by secreting a range of cytokines, including VEGF, TGF-β, platelet-derived growth factor (PDGF), and basic fibroblast growth factor (bFGF), which enhance cancer cell proliferation. Furthermore, TAMs suppress the cytotoxic effects of normal macrophages by downregulating the iNOS pathway in M1 macrophages (Rigo et al., 2010; Zeisberger et al., 2006). Secondly, TAMs facilitate tumor invasion and metastasis by releasing ECM-degrading enzymes, such as matrix metalloproteinases (MMPs) and cathepsins, which degrade the basement membrane and connective tissue surrounding tumors. Additionally, TAM-derived factors, such as TNF-α, induce epithelial-to-mesenchymal transition (EMT), thereby enhancing metastatic potential (Olmeda et al., 2007). Thirdly, TAMs play a central role in angiogenesis by secreting pro-angiogenic factors such as VEGF, IL-8, and bFGF, which promote neovascularization and increase microvessel density in tumor tissues. Hypoxic conditions within the TME further stimulate TAMs to upregulate additional pro-angiogenic molecules, thereby amplifying this effect (Joimel et al., 2010; Yuri et al., 2015). Lastly, TAMs contribute to immune suppression by secreting immunosuppressive cytokines such as IL-10, TGF-β, and PGE2, which impair the cytotoxic function of T cells and NK cells. Together, these mechanisms underscore the multifaceted role of TAMs in tumor progression and highlight their potential as therapeutic targets in tumor treatment.

1.3 Endoplasmic reticulum (ER) stress

1.3.1 ER

The ER in eukaryotic cells is the largest organelle of an interconnected membrane system with diverse functions, including protein synthesis, transport and folding, lipid and steroid synthesis, calcium storage, and crosstalk with other organelles (Schwarz and Blower, 2016). The ER is classified as rough ER and smooth ER, depending on the presence of ribosomes. The rough ER is defined by the presence of membrane-bound ribosomes and mainly performs functions associated with the biosynthesis of membrane and secretory proteins, including their proper folding and modification. The smooth ER, where ribosomes are absent, is primarily involved in lipid and steroid synthesis, carbohydrate metabolism,

and calcium ion storage (Schwarz and Blower, 2016). However, there is little evidence to suggest that the rough ER is excluded from performing functions typically associated with the smooth ER. For instance, the rough ER is also involved in calcium homeostasis in the ER (Walton et al., 1991). With the assistance of chaperones, nascent unfolded proteins synthesized by ribosomes are subjected to the ER quality control mechanisms (Kopito, 1997). Qualified proteins are subsequently packaged into vesicles and trafficked to the Golgi apparatus for further processing, while misfolded proteins are degraded in the cytosol through ER-associated degradation (ERAD). ERAD is a process mediated by proteasomes, in which misfolded proteins are retrotranslocated from the ER to the cytosol for degradation by proteasomes, facilitated by channel proteins in an energy-consuming manner (Kopito, 1997; Rao et al., 2023).

1.3.2 ER stress and unfolded protein response (UPR)

Given the complex and pivotal functions, the ER is strictly and intricately regulated to meet cellular biological activities. Protein homeostasis is a distinctive feature of a properly functioning ER, where protein synthesis is compatible with processing (Jayaraj et al., 2020). However, when cells are exposed to stressful conditions such as nutrient shortage, hypoxia, calcium dyshomeostasis, and oxidative stress, the protein-folding capacity of cells is disrupted, leading to the accumulation of unfolded and misfolded proteins in the ER lumen, thereby provoking ER stress (Chen and Cubillos-Ruiz, 2021). In reaction to ER dysfunction, cells initiate an adaptive defense mechanism known as UPR to reinforce protein folding and degradation capacities, ultimately tackling the ER stress and restoring protein homeostasis (Schroder, 2008). Therefore, the UPR is a protective response by which cells to mitigate ER stress.

The UPR is initiated by three transmembrane sensors: inositol requiring enzyme 1 (IRE1), protein kinase (PKR)-like ER kinase (PERK), and activating transcription factor 6 (ATF6) (Chang et al., 2018; Chen and Cubillos-Ruiz, 2021). The accumulation of unfolded and misfolded proteins binds more chaperone proteins, such as glucose-regulated protein 78 (GRP78, also known as binding immunoglobulin protein (BiP)), resulting in the dissociation of BiP from these three sensors. Upon BiP release, ATF6 is transported to the Golgi apparatus where it is processed into its active form and subsequently translocated to the nucleus to promote the transcription of chaperone and ERAD-related

genes. Dimerization and autophosphorylation occur when PERK and IRE1 decouple from BiP. Activated PERK in turn phosphorylates eukaryotic initiation factor 2α (eIF2α), which leads to transient inhibition of global protein translation to restore abnormal ER but selectively induces ATF4. AFT4 then enters the nucleus and activates the transcription of genes related to chaperone, apoptosis and amino acid metabolism. Activation of IRE1 induces the splicing of X-box protein 1(XBP1) mRNA and then the formation of its active form, sXBP1. sXBP1 is translocated to the nucleus to initiate the transcription of genes responsible for chaperone, ERAD and lipid synthesis. Collectively, UPR contributes to restore ER protein homeostasis by retarding general protein translation and increasing the translation of ER resident chaperones and components of the protein degradative machinery to prevent the aggregation of unfolded and misfolded proteins.

Moderate ER stress can be dispelled by proper collaboration among the respective UPR branches, therefore maintaining cell survival, however, persistent or excessive ER stress eventually induces cell death (Mohamed et al., 2017). Ample evidence supports that unrelievable ER stress leads to cell apoptosis, and two UPR branches, PERK and IRE1, control cell fate under ER stress (Chang et al., 2018; Lu et al., 2014). In the face of overwhelming ER stress, ATF4, which is selectively activated in the PERK branch, has been shown to induce apoptosis by both inhibiting the anti-apoptotic protein Bcl-2 (McCullough et al., 2001) and promoting the pro-apoptotic proteins BIM (Puthalakath et al., 2007) and PUMA (Galehdar et al., 2010) through the activation of the transcription factor C/EBP homologous protein (CHOP). On the other hand, IRE1 can offset the apoptosis signals from the PERK/ATF4/CHOP branch by degrading apoptosis-dependent components (Chang et al., 2018). However, IRE1 has also been revealed to promote apoptosis and autophagy by activating the c-Jun N-terminal kinase (JNK) pathway (Han et al., 2009; Urano et al., 2000).

1.3.3 ER stress in tumors

ER stress has been documented in most major types of human cancer, especially in solid tumor (Wang and Kaufman, 2014). Of importance, amounting evidence has shown that ER stress and the subsequent UPR modulate various pro-tumoral properties, including angiogenesis, metabolism, metastasis, and chemoresistance, while reprogramming the function of immune cells in the TME (Chen and Cubillos-Ruiz, 2021; Urra et al., 2016). In

addition, ER stress has also been identified in cancer stem cells (CSCs) and dormant tumor cells, which are mostly to blame for relapse, contributing to their stemness maintenance, quiescence, and chemoresistance (Calvo et al., 2023; Liang et al., 2021; Ranganathan et al., 2006). Targeting UPR, the adaptive response of ER stress, induces the differentiation of CSCs, increases cell death and sensitivity to chemotherapy in CSCs and dormant tumor cells (Calvo et al., 2023; Ranganathan et al., 2006). Overall, adaptation to ER stress confers a survival advantage to tumor cells, but also renders them vulnerable to environmental perturbations. Therefore, targeting the UPR to disturb the ER homeostasis has emerged as an attractive approach for anti-tumor therapy in recent years (Salvagno et al., 2022).

1.4 Endoplasmic reticulum oxidoreductase 1 alpha (ERO1L)

1.4.1 Introduction

ERO1L, also known as ERO1A or ERO1α, is a flavin adenosine dinucleotide (FAD)-containing ER-resident thiol oxidoreductase responsible for catalyzing disulfide bond formation in nascent polypeptides, working in conjunction with protein disulfide isomerase (PDI) (Inaba et al., 2010). ERO1L is expressed ubiquitously in all cell types as its crucial role in oxidative protein folding. Of note, in addition to oxidative protein folding, ERO1L is also implicated in various biochemical pathways, such as calcium release and regulation of nicotinamide adenine dinucleotide phosphate oxidase (NOX) activity. In addition, an interesting finding is that ERO1L knockout in mammals is not as fatal as in yeast, and mice with ERO1L knockout exhibit a mere retardation in disulfide bond formation (Zito et al., 2012). Indeed, it has been demonstrated that ERO1L function in oxidative protein folding can be compensated by other redundant oxidoreductases, such as peroxiredoxin 4 (PRDX4), glutathione peroxidase 8 (GPx8), peroxiredoxin IV (PrxIV) and vitamin K epoxide reductase (VKOR) (Bulleid, 2012; Kanemura et al., 2020; Nguyen et al., 2011; Zito, 2013).

Human ERO1L protein is functionally composed of two regions: a four antiparallel alpha-helices core region containing a binding site for the FAD coenzyme and an adjacent inner active-site, as well as a shuttle loop with an outer active-site (Araki and Inaba, 2012). In addition, ERO1L features a protruding β-hairpin responsible for docking with PDI. ERO1L

functions as an exchange center for disulfide bonds and electrons to assist PDI in the de novo disulfide bond formation in nascent polypeptides.

1.4.2 Expression profile of ERO1L in tumors

In our prior research, we conducted an integrative analysis of expression data derived from cell lines, tumor tissues, and publicly available gene expression databases. The findings revealed that ERO1L expression was significantly upregulated in a range of cancers, including bile duct cancer, cervical cancer, lung cancer, pancreatic cancer, breast cancer, liver cancer, and gastric cancer. Notably, prostate cancer was the exception, as ERO1L expression levels in both tumor tissues and cell lines did not show a significant difference compared to their normal counterparts (Chen et al., 2024).In addition, a pan-cancer expression analysis from the Oncomine database revealed upregulated ERO1L in 10 cancer types while reduced in esophageal cancer, head and neck cancer, and leukemia (Liu et al., 2021). Taken together, these data support that ERO1L is highly expressed in the vast majority of tumors, implying a potential role in tumor biology.

1.4.3 ERO1L mediates tumor progression

1.4.3.1 Roles in tumor growth and aggression

ERO1L is widely implicated in tumor progression. Most studies have shown that inhibition of ERO1L impairs tumor cell proliferation, migration, and invasion, whereas its overexpression enhances these malignant traits (Chen et al., 2024). Additionally, ERO1L facilitates EMT in various cancers, including lung, liver, colorectal, bile duct, and cervical cancer. Mechanistically, ERO1L promotes the oxidative folding of integrin β1 and MMPs, which are crucial for ECM degradation and tumor cell dissemination (Cornelius et al., 2021; Han et al., 2018; Lee et al., 2018).

1.4.3.2 Roles in angiogenesis

ERO1L primarily promotes tumor angiogenesis by facilitating VEGF maturation. By facilitating the oxidative folding of VEGF and stabilizing hypoxia-inducible factor-1 alpha (HIF-1α), ERO1L also enhances endothelial cell proliferation and vascular network formation (Tanaka et al., 2016; Varone et al., 2021; Zilli et al., 2021). Studies in breast

and liver cancer have demonstrated that ERO1L increases human umbilical vein endothelial cell (HUVEC) migration and tube formation, as well as blood vessel density in tumor tissues (Tanaka et al., 2016; Varone et al., 2021; Zilli et al., 2021).

1.4.3.3 Roles in the TME

ERO1L plays a pivotal role in establishing an immunosuppressive TME by modulating both immune and stromal components. High ERO1L expression is associated with reduced levels of cytotoxic immune cells, such as $CD8^+$ T cells, B cells, and NK cells, while being positively correlated with immunosuppressive components, including cancer-associated fibroblasts (CAFs), MDSCs, and TAMs. (Liu et al., 2023; Liu et al., 2021). Moreover, ERO1L directly enhances the oxidative folding and stability of PD-L1, promoting immune evasion of tumor cells (Tanaka et al., 2017).

Furthermore, ERO1L facilitates the recruitment and differentiation of myeloid-derived cells. It enhances MDSC chemotaxis by increasing the oxidative folding of key chemokines, such as granulocyte colony-stimulating factor (G-CSF) and C-X-C motif chemokine ligand 1/2 (CXCL1/2), which drive immunosuppressive myeloid infiltration (Tanaka et al., 2015). In pancreatic cancer, ERO1L knockdown promotes monocyte infiltration and their differentiation into dendritic cells (DCs), thereby improving antigen presentation (Tay et al., 2023). Single-cell RNA sequencing (scRNA-seq) analysis further indicates that ERO1L drives TAM polarization from an M1 to an M2 phenotype, reinforcing immunosuppression (Liu et al., 2023; Liu et al., 2021).

In T cells, ERO1L triggers ER stress transmission from tumor cells, leading to CHOP-dependent apoptosis and functional exhaustion of CD8+ T cells (Liu et al., 2023). Notably, high ERO1L expression correlates with resistance to immune checkpoint inhibitors (ICIs), whereas its deletion enhances tumor sensitivity to anti-PD-1 therapy (Liu et al., 2023; Liu et al., 2021).

1.4.3.4 Roles in metabolism and chemoresistance

ERO1L contributes to metabolic reprogramming by promoting aerobic glycolysis (the Warburg effect) and pentose phosphate pathway (PPP) activity, thereby increasing NADPH and glutathione (GSH) production to enhance antioxidant defenses (Han et al., 2018; Zhang et al., 2020). In pancreatic and cervical cancer, ERO1L has been shown to

enhance glycolytic flux, and its inhibition suppresses tumor cell proliferation (Zhang et al., 2020). Moreover, ERO1L plays a role in chemoresistance by supporting adaptive mechanisms under hypoxia and ER stress. In gastric and breast cancer, ERO1L knockdown increases tumor cell sensitivity to 5-fluorouracil (5-FU) and paclitaxel (Seol et al., 2016; Varone et al., 2022). This effect is likely due to heightened susceptibility to lethal ER stress upon ERO1L inhibition, ultimately compromising cellular survival under therapeutic pressure.

1.5 Multiple myeloma (MM) and colorectal cancer (CRC)

According to cancer statistics, CRC ranks as the third most common cancer globally in terms of incidence but the second leading cause of cancer-related mortality, with 1.9 million new cases and 900,000 deaths annually (Bray et al., 2024). By 2040, CRC incidence is projected to reach 3.2 million new cases annually, with 1.6 million related deaths (Morgan et al., 2023). Despite advances in treatment modalities, including surgery, chemotherapy, radiotherapy, and immunotherapy, challenges such as recurrence, drug resistance, and off-target toxicity remain significant hurdles (Dekker et al., 2019). Therefore, there remains an urgent need for more effective therapeutic strategies. Similarly, MM is a malignant disorder of plasma cells characterized by their abnormal proliferation in the bone marrow and excessive production of monoclonal immunoglobulins, leading to destructive bone lesions, anemia, renal impairment, and immune dysfunction (Cowan et al., 2022). The introduction of proteasome inhibitors, immunomodulatory drugs, and monoclonal antibodies has significantly advanced MM treatment. However, MM remains incurable, with frequent relapses and persistent drug resistance.

1.6 Aims of the thesis

Inflammation and ER stress are the two features of the TME, both of which exhibit dual roles in tumor progression. Depending on their intensity and duration, they can either promote or limit tumor growth. Regulating these processes to enhance their anti-tumor effects may contribute to the development of novel therapeutic strategies. This study aims to:

1. Investigate whether pro-inflammatory cytokines derived from M1 macrophages enhance the anti-tumor activity of CIK cells and elucidate the underlying mechanisms.

2. Examine the role of the PD-1/PD-L1 axis in the pro-inflammatory cytokine-mediated enhancement of CIK cell cytotoxicity.

3. Assess the feasibility and necessity of combining PD-1/PD-L1 blockade with macrophage reprogramming therapy for cancer treatment.

4. Analyze the expression of ERO1L in tumors and its regulatory relationship with ER stress.

5. Investigate the role of ERO1L in programmed cell death in tumor cells.

6. Evaluate the therapeutic potential of combining ERO1L inhibition with ER stress-inducing agents.

2. Material and methods

2.1 Materials

2.1.1 Table 1: Cell lines

Cell name	Cell type	Source	Culture medium
CCD18-Co	Human normal colon epithelia	ATCC	MEM
Colo201	Colorectal cancer	ATCC	RPMI-1640
Colo205	Colorectal cancer	ATCC	RPMI-1640
HCT116	Colorectal cancer	DSMZ	McCoy's 5A
HT29	Colorectal cancer	ATCC	McCoy's 5A
NCI-H929	Multiple myeloma	ATCC	RPMI-1640
OPM2	Multiple myeloma	DSMZ	RPMI-1640
SW480	Colorectal cancer	ATCC	RPMI-1640
THP-1	Human monocyte	ATCC	RPMI-1640
U266	Multiple myeloma	ATCC	RPMI-1640

2.1.2 Table 2: Antibodies

Name	Colne	Catalog number	Source
Anti- Mouse IgG1, κ	P3.6.2.8.1	16-4714-82	Invitrogen
Anti- Rat IgG1, κ	eBRG1	14-4301-82	Invitrogen
Anti-AMPKα	A20017A	600651	BioLegend
Anti-ATF4	-	11815	CST
Anti-ATF6	-	65880	CST
Anti-Bax	-	2772	CST
Anti-Bcl-2	-	4223	CST
Anti-Beclin1	-	3495	CST
Anti-CD16/32	93	101320	BioLegend
Anti-ERK1/2	-	4695	CST
Anti-ERO1L	-	3264	CST
Anti-GRP78	-	610978	BD Bioscience
Anti-IL1β	CRM56	14-7018-81	Invitrogen

Anti-IL6	MQ2-13A5	16-7069-81	Invitrogen
Anti-IRE1α	-	3294	CST
Anti-LC3A/B	-	1247	CST
Anti-PD-L1/Durvalumab	-	A2013	Selleckchem
Anti-PERK	-	3192	CST
Anti-p-ERK1/2	-	4370	CST
Anti-TNFα	Mab1	16-7348-81	Invitrogen
Anti-β-Actin	-	4967	CST
Anti-β-Tubulin	-	MA5-16308	Thermo Scientific
APC anti-CD86	BU63	374208	BioLegend
APC anti-MICA/B	6D4	320908	BioLegend
APC anti-mouse IgG	Poly4053	405308	BioLegend
APC anti-mouse IgG1, κ	MOPC-21	981806	BioLegend
APC anti-mouse IgG2a, κ	MOPC-173	981906	BioLegend
APC anti-PD-1	EH12.2H7	329908	BioLegend
APC anti-p-NF-κB	14G10A21	653005	BioLegend
FITC anti-NKG2D	1D11	320820	BioLegend
FITC anti-p-p53	DO-7	645803	BioLegend
HRP Goat anti-Mouse Secondary antibody	-	SA0000I-I	Proteintech
HRP Goat anti-Rabbit Secondary antibody	-	RGAR001	Proteintech
PE anti-CD206	15-2	321106	BioLegend
PE anti-mouse IgG1, κ	MOPC-21	981804	BioLegend
PE anti-p-AKT	A21001C	606553	BioLegend
PE anti-PD-L1	MIH2	393608	BioLegend
PE anti-p-ERK1/2	6B8B69	369505	BioLegend
PE anti-p-JNK1/2	N9-66	562480	BD Biosciences
PE anti-p-mTOR	O21-404	563489	BD Biosciences
PE anti-p-p38 MAPK	A16016A	690203	BioLegend
PE anti-p-STAT3	13A31	651004	BioLegend

PE anti-rat IgG2a, κ	RTK2758	400508	BioLegend

2.1.3 Table 3: Chemicals, reagents, and kits

Name	Catalog number	Source
0.5 M Stacking Gel Buffer	1610799	Bio-Rad
1.5 M Resolving Gel Buffer	1610798	Bio-Rad
10X AnnexinV Binding Buffer	556454	BD Bioscience
10X Laemmli Buffer	42556.01	SERVA
10X TBS	1706435	Bio-Rad
10X Tris/Glycine Buffer	1610734	Bio-Rad
1X PBS 1% Casein Blocker	1610783	Bio-Rad
4X Roti-Load 1	K929.2	CarRoth
4μ8c	HY-19707	MCE
ACA-28	HY-147855	MCE
Accutase	423201	BioLegend
Acrylamid/Bis-acrylamide (29:1)	A124.1	CarRoth
AKT Inhibitor X	14863	Cayman
Ammoniumperoxodisulfat (APS)	9592.3	CarRoth
Caspase 3/7 Dye	C10740	Thermo Scientific
Caspase 9 Dye	AB65615	Abcam
CCK-8 Solution	CK04-20	Dojindo
Ceapin-A7	HY-108434	MCE
Carboxyfluorescein succinimidyl ester (CFSE)	C34554	Thermo Scientific
Clarity Western ECL Substrate	170-5060	Bio-Rad
Cyto-ID Green Autophagy Kit	ENZ-KIT175	Enzo Life Science
Dimethyl Sulfoxide (DMSO)	A994.2	CarRoth
DPBS	P04-36500	Pan-Biotech
DuoSet ELISA Ancillary	DY008	R&D system
DuoSet Human MICA ELISA Kit	DY1300	R&D system
DuoSet Human MICB ELISA Kit	DY1599	R&D system

Ethanol	K928.4	CarRoth
Fetal Bovine Serum (FBS)	P240501	Pan-Biotech
FITC Annexin V	640906	BioLegend
Fixation Buffer	420901	BioLegend
Gossypetin	Cay33840	Biomol
GSK2606414	HY-18072	MCE
Halt Protease Inhibitor Cocktail (100X)	1860932	Thermo Scientific
HEPES 1M	7365-45-9	Pan-Biotech
High-Capacity cDNA Reverse Transcription Kit	4368814	Applied Biosystems
Hoechst 33258	Cay16756-50	Cayman
Human IL-1β ELISA Kit	88-7261-22	Invitrogen
Human IL-6 ELISA Kit	88-7066-22	Invitrogen
Human TNF-α ELISA Kit	88-7346-22	Invitrogen
IC Fixation Buffer	00-8222-49	Thermo Scientific
JAK Inhibitor I	420097	Biomol
Lipofectamine RNAiMAX	100014472	Invitrogen
Lipopolysaccharides (LPS)	L4391	Sigma-Aldrich
LY-294002	L9908	Biomol
McCoy’s 5A	P04-05500	Pan-Biotech
MEM Eagle	P04-08056	Pan-Biotech
Methanol	P717.1	CarRoth
MG132	HY-13259	MCE
p38 MAP Kinase Inhibitor III	506148	Merck
PageRuler Prestained Protein Ladder	26616	Thermo Scientific
Pancoll Human	P04-36500	Pan-Biotech
Penicillin-Streptomycin	15140122	Gibco
PerCP 7-AAD	420404	BioLegend
Permeation Buffer	425401	BioLegend
Phorbol 12-myristate 13-acetate (PMA)	P8139	Sigma-Aldrich
Pierce BCA Protein Assay Kit	A55865	Thermo Scientific

PowerTrack SYBR Master Mix	A46110	Applied Biosystems
PVDF membrane	22860	Invitrogen
RBC Lysis Buffer	420301	BioLegend
rh-IFN-γ	1134534	ImmunoTools
rh-IL-1β	11340015	ImmunoTools
rh-IL-2	11340025	ImmunoTools
rh-IL-6	11340064	ImmunoTools
rh-TNFα	1134015	ImmunoTools
RIPA Buffer	89900	Thermo Scientific
RNeasy Plus Mini Kit	74134	Qiagen
RPMI-1640	P04-16500	Pan-Biotech
SDS Solution 10 % (w/v)	1610416	Bio-Rad
SP600125	HY-12041	MCE
TaqMan Gene Expression Assay (FAM)	4351368	Applied Biosystems
TaqMan Gene Expression Master Mix	4369016	Applied Biosystems
Tetramethylethylenediamine (TEMED)	161-0800	Bio-Rad
Trypan Blue Satin (0.4 %)	15250-061	Gibco
Trypsin-EDTA	25300054	Gibco
Tauroursodeoxycholic Acid (TUDCA)	HY-19696	MCE
Tunicamycin	12819	CST
Tween-20	9127.2	CarRoth
Zombie Aqua Dye	423102	BioLegend

2.1.4 Table 4: Primer list

ATF4	Forward	CTCCGGGACAGATTGGATGTT
	Reverse	GGCTGCTTATTAGTCTCCTGGAC
ATF6	Forward	TCCTCGGTCAGTGGACTCTTA
	Reverse	CTTGGGCTGAATTGAAGGTTTTG
CHOP	Forward	GGAAACAGAGTGGTCATTCCC
	Reverse	CTGCTTGAGCCGTTCATTCTC
ERO1L	Forward	GGCTGGGGATTCTTGTTTGG

	Reverse	AGTAACCACTAACCTGGCAGA
GAPDH	Forward	GCACCGTCAAGGCTGAGAAC
	Reverse	TGGTGAAGACGCCAGTGGA
GRP78	Forward	GCCGTCCTATGTCGCCTTC
	Reverse	TGGCGTCAAAGACCGTGTTC
IRE1α	Forward	AGAGAAGCAGCAGACTTTGTC
	Reverse	GTTTTGGTGTCGTACATGGTGA
PERK	Forward	ACGATGAGACAGAGTTGCGAC
	Reverse	ATCCAAGGCAGCAATTCTCCC
GAPDH	TaqMan (FAM)	Hs99999905_m1
MICA	TaqMan (FAM)	Hs07292198_gH
MICB	TaqMan (FAM)	Hs00792952_m1
PD-L1	TaqMan (FAM)	Hs00204257_m1

2.1.5 Table 5: Equipment and software

Name	**Source**
BD FACSCanto II	BD Bioscience
Centrifuge	Eppendorf
ChemiDox XRS+ Imaging System	Bio-Rad
Diva software	BD Bioscience
FlowJo software	TreeStar
GraphPad Prism software	GraphPad Software Inc.
ImageJ software	National Institutes of Health, USA
Incubator	Thermo Scientific
Mastercycler gradient	Eppendorf
Microplate reader	Thermo Scientific
Microscope	Carl Zeiss
Nanodrop1000	NanoDrop
QuantStudio 3	Applied Biosystems
Water bath	Memmert

2.2 Methods

2.2.1 Cell culture

All cell lines were cultured in in a humidified incubator with 5 % CO2 at 37 °C. All media were supplemented with 10 % FBS and 1 % penicillin–streptomycin. All cell lines were mycoplasma free, as tested by mycoplasma detection kit.

2.2.2 siRNA-mediated gene knockdown

For ERO1L knockdown, a pre-designed ERO1L specific siRNA (#hs.Ri.ERO1L.13.1) or a negative control scramble siRNA (#51-01-14-04) was purchased from Integrated DNA Technologies (IDT, Coralville, IA, USA). 3 x 10^5 HCT116 or 4 x 10^5 SW480 cells were seeded in 6-well plates and incubated overnight, then cells were transfected with ERO1L siRNA (siERO1L) or scramble siRNA (siNC) using Lipofectamine RNAiMAX according to the manufacturer's instructions. Two days after transfection, cells were harvested for use.

2.2.3 Generation of CIK cells

PBMC-derived CIK cells were generated as previously described (Schmidt-Wolf et al., 1991). The non-adherent cells were collected and stimulated by 1000 U/mL IFN-γ for 24 h. As next, 50 ng/mL anti-CD3 monoclonal antibody, 600 U/mL IL-2, and 100 U/ml IL-1β were added to induce CIK cells. Cells were then incubated at 37 °C in a humidified atmosphere of 5 % CO_2. Fresh medium with 600 U/mL IL-2 was replenished every 2-3 days.

2.2.4 Macrophage polarization and characterization

The protocol of macrophages polarization from THP-1 cells has been described previously, with our minor modifications (Nyiramana et al., 2020). Briefly, 5 x 10^5 THP-1 cells were seeded to 6-well plates and stimulated to M0 macrophages by adding 100 ng/mL PMA for 24 hours. For the polarization of M1 macrophages, M0 macrophages were then treated with 100 ng/mL LPS and 20 ng/mL IFN-γ for 48 hours in the presence of 50 ng/mL PMA.

2.2.5 Flow cytometry-based phenotype measurement

2.2.5.1 Surface proteins

For the measurement of surface proteins, cells with or without treatments were collected and washed once followed by surface staining with fluorescence conjugated antibodies at 4 °C for 30 minutes. Next, cells were washed twice and resuspended in 200 μL DPBS for analyses. Hoechst 333258 was immediately added to tubes before the analysis to recognize dead cells. Of note, for Fc receptors blockade, macrophages were incubated with CD16/32 antibodies at 4 °C for 10 minutes prior to the staining of surface markers. For the inhibition of signaling pathways, cells were pre-treated with the inhibitors for 20 minutes prior to the treatment of cytokines. Conditioned-medium (CM) from macrophages was pre-incubated with cytokine antibodies at 4 °C for 3 hours for cytokines neutralization before the use.

2.2.5.2 Apoptosis measurement

The Annexin V/7-AAD double staining was used for apoptosis measurement. Tumor cells, including supernatants were collected and washed with DPBS for twice. Next, cells were resuspended and stained in 1x Binding Buffer with Annexin V and 7-AAD dyes in the dark for 15 minutes at room temperature. Then, the percentages of apoptotic cells (Annexin V+/7-AAD-) were analyzed.

For caspase staining, cells were harvested and washed with DPBS for twice. Then, tumor cells were stained in DPBS with Caspase 3/7 Dye in the dark at room temperature for 1 hour, or in culturing medium with Caspase 9 Dye in 37 °C for 1 hour. Next, dead cell indicator SYTOX dye was added to cells followed by analyses.

2.2.5.3 Autophagy measurement

For autophagy measurement, tumor cells were collected and washed twice with DPBS. Cells were then stained in DPBS with CYTO-ID Green Dye in the dark for 30 minutes at room temperature, followed by flow cytometry analyses.

2.2.5.4 Intracellular staining

Intracellular staining was performed for the measurement of phosphorylation levels of signaling molecules. Briefly, cells were fixed with Fixation Buffer for 15 minutes in 37 °C.

After washed twice using wash buffer, cells were permeated using Permeation Buffer while vortex, followed by incubation at -20 °C for 2 hours. Cells then were stained in wash buffer with phosphorylation specific antibodies in the dark for 30 minutes. After washed twice, cells were analyzed using flow cytometry

2.2.6 Flow cytometry-based cytotoxicity measurement

For cytotoxicity assays, 1 x 10^4 of CFSE-labeled tumor cells were seeded with cytokines or macrophage-derived CM for 24 hours. CIK cells were then added to tumor cells and co-cultured for 24 hours followed by analysis. For the neutralizing and blocking experiments, prior to the co-culturing with CIK cells, cytokine antibodies or PD-L1 antibody were pre-incubated with tumor cells at 4 °C for 3 hours or at 37 °C for 2 hours, respectively. The formula used for cytotoxicity calculation is as follows: Cytotoxicity = CL-TL. CL, live tumor cells percentage in tumor cells alone group; TL, live tumor cells percentage in tumor cells and CIK cells groups, with or without treatments. Effector to target (E:T) ratio was 10:1 in this study.

2.2.7 Enzyme-linked immunosorbent assay (ELISA)

Supernatants from tumor cells and M1 macrophages were collected for the measurement of shed MICA, shed MICB, and cytokines, respectively. For cytokines measurement, supernatants were 10 folds diluted prior to the use. ELISA assays were conducted according to the manufacturer’s instructions.

2.2.8 Western-blotting

Total proteins were extracted using RIPA Buffer supplemented with protease and phosphatase inhibitors. Protein samples were quantified using BCA Kit, separated by SDS-PAGE and transferred onto PVDF membranes. Membranes were blocked with blocking buffer (1x PBS with 1 % Casein) or BSA (5 % w/v, for phosphorylated proteins) for 1 hour at room temperature and then incubated with indicated primary antibodies overnight at 4 °C. On the next day, the membranes were incubated with secondary antibodies at room temperature for 1 hour. The visualization of the immunoreactive complexes was performed using ECL Kit and a ChemiDoc XRS+ Imaging System.

2.2.9 Reverse transcription-quantitative PCR (RT-qPCR)

Total RNA was isolated using RNeasy Plus Mini Kit. Quality of the RNA samples was confirmed using Nanodrop1000 system and cDNA was synthesized using High-Capacity cDNA Reverse Transcription Kit. Gene quantification was performed on a QuantStudio3 Real-Time PCR system with PowerTrack SYBR Master Mix reagent or TaqMan Gene Expression Master Mix. Gene expression levels were normalized to GAPDH. $2^{-\Delta\Delta Ct}$ method was used to calculate gene relative expression. Primers used in this study were purchased from Eurofins or IDT. The primer sequences were listed in Table 4.

2.2.10 Cell counting kit-8 (CCK-8) assay

For the viability assays in study 1, 5 x 10^4 U266 or NCI-H929 cells well seeded with or without cytokines or macrophage-derived CM. After 24 hours, 10 µL of CCK-8 solution was added to each well and incubated for 1 hour (U266) or 3 hours (NCI-H929). For proliferation assays in study 2, 2 x 10^3 HCT116 or SW480 cells were seeded in 96-well plates. After 0, 24, 48, and 72 hours of incubation, 10 µL of CCK-8 reagent was added to wells and incubated for 1 hour (SW480) or 2 hours (HCT116). For the incubation with Tunicamycin or ER stress-inducing agents, 2 x 10^4 HCT116 or SW480 cells were seeded in 96-well plates and incubated with corresponding agents for 24 hours. 10 µL of CCK-8 was then added to cells and incubated for 1 hour followed by optical density (OD) value measurement. The OD values at 450 nm and 600 nm were measured using a microplate reader.

2.2.11 Scratch assay

Tumor cells were seeded in 24-well plates, and wounds were scratched using 200 µL sterile tips. At 0, 24, 48 hours after scratch, the wounds were observed and documented using microscopy. The wound-healing rates were analyzed by ImageJ software.

2.2.12 Transwell assay

Tumor cells were washed twice with DPBS and resuspended using FBS-free medium. Then, 5 x10^4 HCT116 or 1 x 10^5 SW480 cells in 200 µL FBS-free medium were seeded in upper chamber, while 750 µL of culture medium containing 20 % FBS were added to lower chambers. For migration assays, tumor cells were transferred to upper chamber

and incubated for 2 days. For invasion assay, tumor cells were seeded to upper chamber pre-coated with Matrigel and incubated for 3 days. Cells then were fixed with 4 % paraformaldehyde and stained with 0.1 % crystal violet. The results were observed and documented using microscopy.

2.2.13 Colony formation assay

Tumor cells were seeded in 6-well plates at a density of 500 cells per well. After 8 days (HCT116) or 14 days (SW480) of incubation, cells were fixed with 4 % paraformaldehyde and stained with 0.1 % crystal violet. The results were then photographed and documented.

2.2.14 Public database analysis

The ERO1L mRNA and protein expression profile in CRC patients was analyzed using the Gene Expression Profiling Interactive Analysis 2 (GEPIA2) database (http://gepia2.cancer-pku.cn) and the Human Protein Atlas (HPA) database (http://proteinatlas.org), respectively.

2.2.15 Statistical analysis

Data were statistical analyzed with GraphPad Prism software. Flow cytometry data sets were analyzed using FlowJo software. Quantitative data were presented as mean ± standard deviation (SD). Statistical differences between groups were analyzed with either two-tailed Student's unpaired t test or one-/two-way analysis of variance (ANOVA) with Bonferroni's post-hoc test. Each experiment was performed for three times. Significance was indicated as $P \leq 0.05$.

3. Results

3.1 Study 1: Pro-inflammatory cytokines augment the cytotoxicity of CIK cells

3.1.1 Pro-inflammatory cytokines upregulate MICA/B expression in MM cells

To investigate whether pro-inflammatory cytokines influence MICA/B expression in MM cells, we first incubated three MM cell lines (U266, OPM2, and NCI-H929) with 50 ng/mL of cytokines and measured surface MICA/B expression. The results showed that U266 cells were sensitive to all cytokines, whereas OPM2 and NCI-H929 cells responded only to IL-6 (Fig. 1).

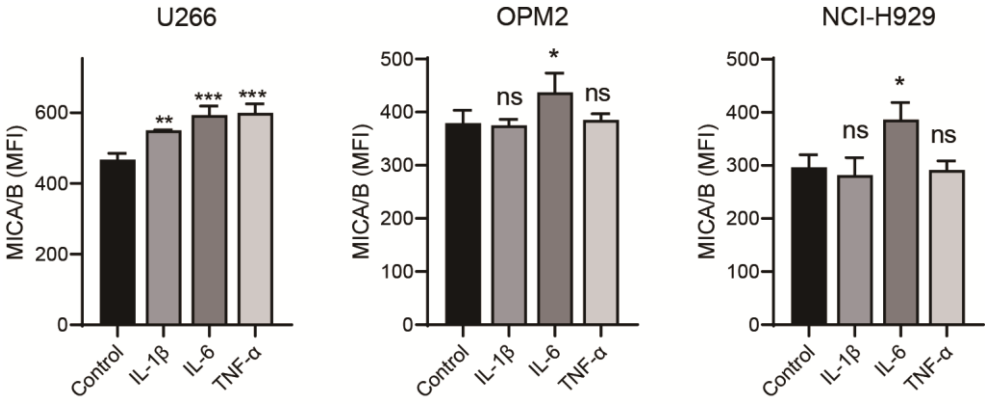

Figure 1: Pro-inflammatory cytokines upregulate MICA/B expression. Pro-inflammatory cytokines enhanced the expression of MICA/B in U266 cells, while only IL-6 worked in OPM2 and NCI-H929 cells. Data are shown as mean ± SD of three independent experiments. *P < 0.05, **P < 0.01, ***P < 0.001, ns, not significant, calculated by one-way ANOVA, Bonferroni's post-hoc test.

To optimize cytokine concentrations, U266 and NCI-H929 cells were treated with a gradient of cytokine concentrations. For U266 cells, 50 ng/mL of IL-6 and TNF-α exhibited significantly higher MICA/B expression than 25 ng/mL or 100 ng/mL, whereas IL-1β showed no significant differences across concentrations (Fig. 2). For NCI-H929 cells, IL-6 elicited comparable effects at all tested concentrations (Fig. 2). In addition, when U266 cells were treated with combined cytokines, 50 ng/mL proved more effective than 25 ng/mL but showed no significant difference compared to 100 ng/mL (Fig. 2). For convenience and consistency, 50 ng/mL was chosen as the working concentration for subsequent experiments.

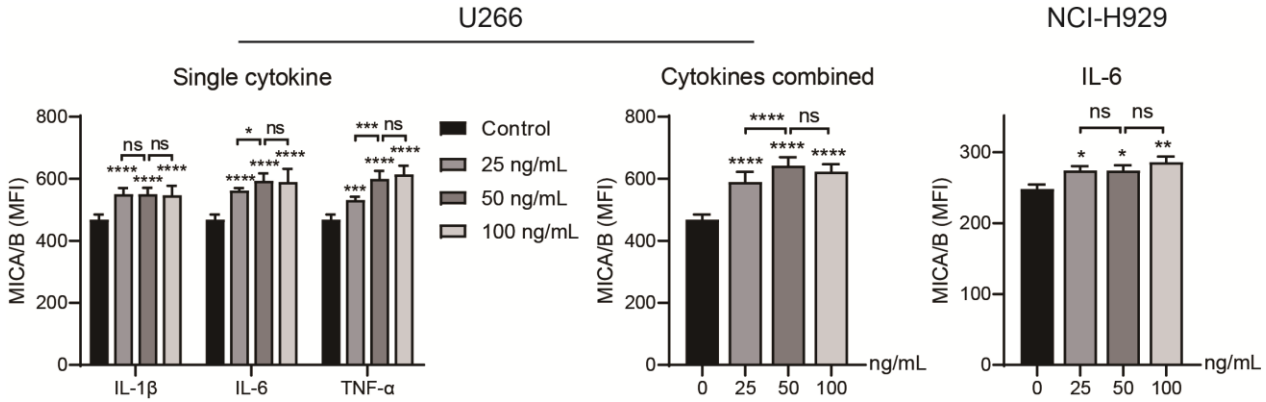

Figure 2: The effect of combined cytokines on MICA/B expression. In U266 cells, 50 ng/mL of single (left) or combined (right) cytokines exhibited the highest effect on MICA/B expression. In NCI-H929 cells, there was no significant difference among the IL-6 concentrations. Data are shown as mean ± SD of three independent experiments. *P < 0.05, **P < 0.01, ***P < 0.001, ****P < 0.0001, ns, not significant, calculated by one-way or two-way ANOVA, Bonferroni's post-hoc test.

3.1.2 Pro-inflammatory cytokines enhance CIK cell-mediated cytotoxicity

To determine whether pro-inflammatory cytokines enhance the cytotoxicity of CIK cells against MM cells via modulating the expression of MICA/B, we first assessed the potential direct cytotoxic effects of cytokines. Cell viability and live cell percentages were measured and confirmed that the cytokines themselves had no cytotoxicity on MM cells (Fig. 3).

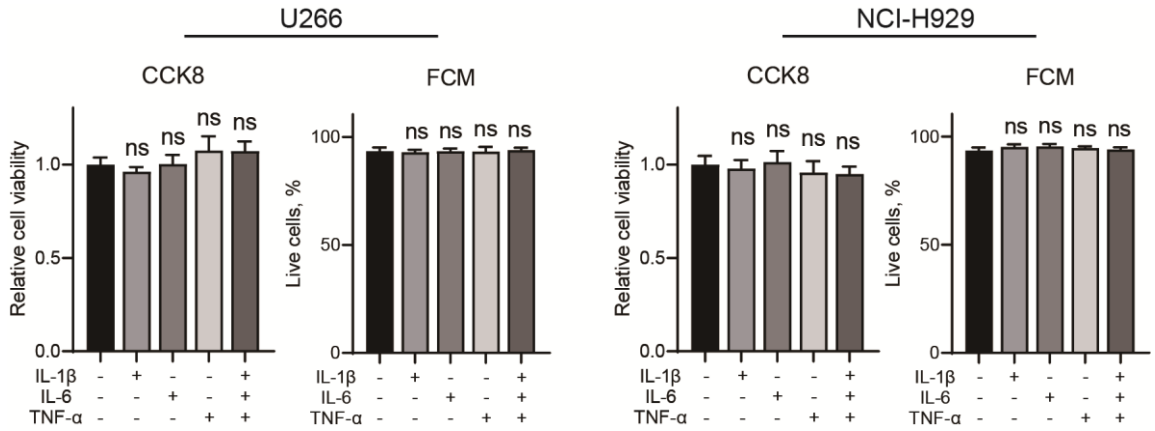

Figure 3: Pro-inflammatory cytokines have no cytotoxic effect on tumor cells. Potential cytotoxic effects of cytokines on tumor cells were excluded by flow cytometry (FCM) and CCK-8 assays. Data are shown as mean ± SD of three independent experiments. ns, not significant, calculated by one-way ANOVA, Bonferroni's post-hoc test.

Subsequently, we co-incubated cytokine-treated MM cells with CIK cells, and observed that cytokine treatment significantly enhanced the cytotoxicity of CIK cells against MM cells (Fig. 4).

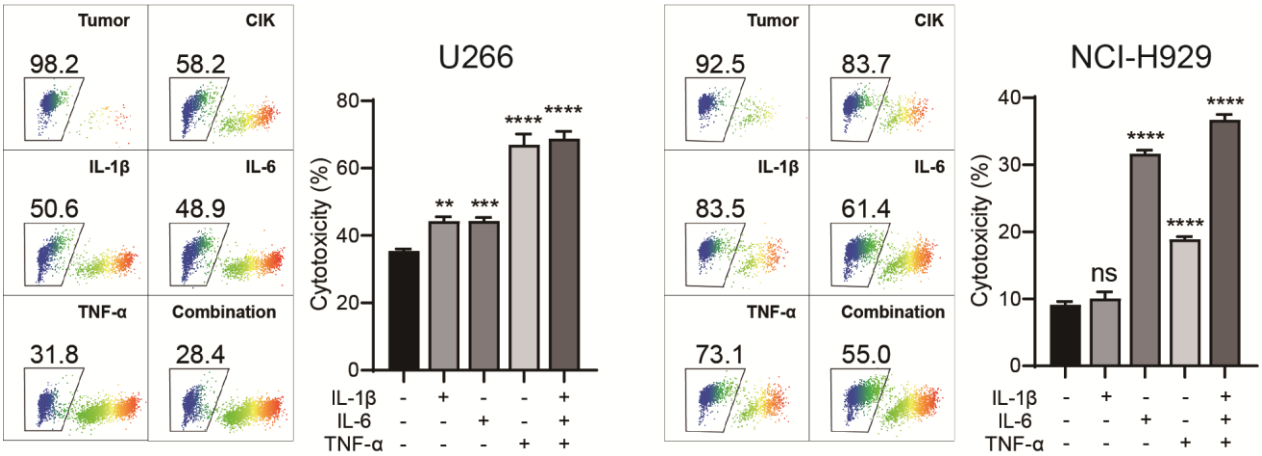

Figure 4: Pro-inflammatory cytokines enhance the cytotoxicity of CIK cells. In U266 cells, all cytokines increased the cytotoxicity of CIK cells, whereas only IL-6 and TNF-α enhanced the cytotoxic activity of CIK cells in NCI-H929 cells. Data are shown as mean ± SD of three independent experiments. **P < 0.01, ***P < 0.001, ****P < 0.0001, ns, not significant, calculated by one-way ANOVA, Bonferroni's post-hoc test.

Interestingly, in U266 cells, TNF-α treatment significantly enhanced the cytotoxicity of CIK cells compared to IL-1β and IL-6, although their similar effects on MICA/B modulation. In NCI-H929 cells, TNF-α also promoted CIK cell-mediated killing, despite having no effect on MICA/B expression (Fig. 2 and 4). These findings suggest that TNF-α exhibits an unique and potent effect on boosting the cytotoxicity of CIK cells, likely via mechanisms beyond MICA/B.

To explore this hypothesis, we examined the expression of NKG2D, the receptor for MICA/B, on CIK cells after cytokine treatment. Results demonstrated that TNF-α, but not IL-1β and IL-6, significantly increased NKG2D expression on CIK cells (Fig. 5A). Meanwhile, we also assessed PD-1 and PD-L1 expression on CIK and MM cells. Interestingly, all cytokines elevated PD-L1 expression in U266 cells, whereas only IL-6 acted in NCI-H929 cells (Fig. 5B). However, none of the cytokines influenced PD-1 expression in CIK cells (Fig. 5A).

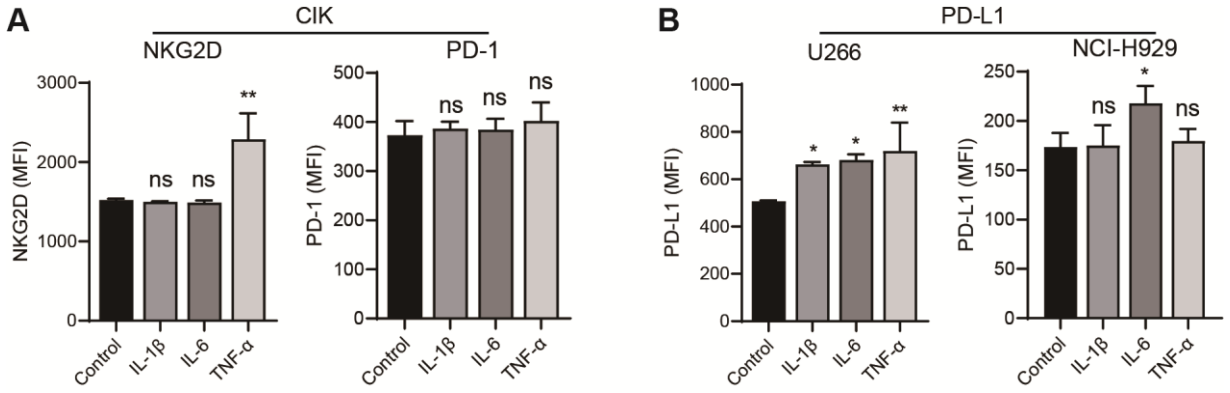

Figure 5: Pro-inflammatory cytokines modulate PD-L1 and NKG2D. (A) In CIK cells, TNF-α upregulated NKG2D expression in tumor cells, whereas none of the cytokines affected PD-1 expression. **(B)** In tumor cells, all cytokines augmented PD-L1 expression in U266 cells, while only IL-6 acted in NCI-H929 cells. Data are shown as mean ± SD of three independent experiments. *P < 0.05, **P < 0.01, ns, not significant, calculated by one-way ANOVA, Bonferroni's post-hoc test.

Given the upregulation of PD-L1 in MM cells, we further investigated whether PD-L1 blockade could enhance CIK cell-mediated cytotoxicity. As anticipated, treatment with a PD-L1 antibody significantly increased the cytotoxicity of CIK cells against both U266 and NCI-H929 cells compared to cytokine treatment alone (Fig. 6).

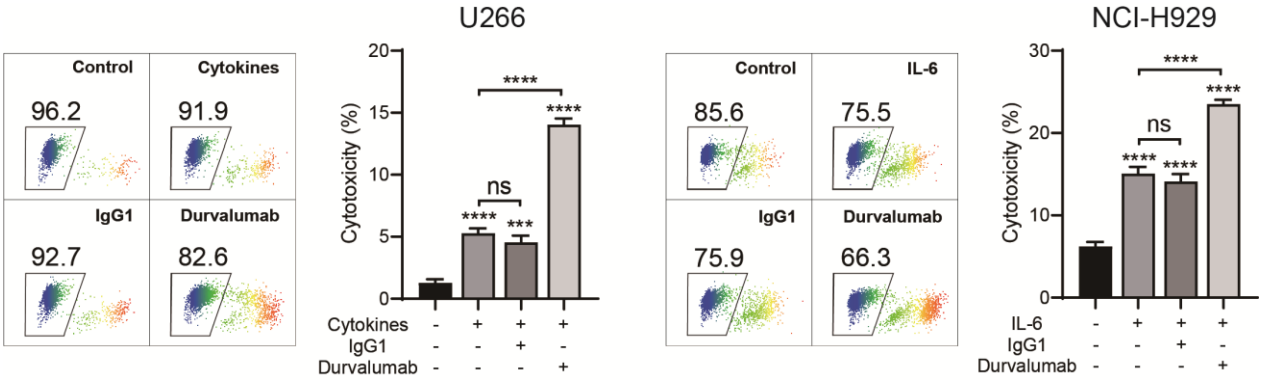

Figure 6: PD-L1 blockade enhances the cytokine-induced cytotoxicity of CIK cells. 10 µg/mL of Durvalumab facilitated the CIK cells' cytotoxicity against MM cells. Data are shown as mean ± SD of three independent experiments. ***P < 0.001, ****P < 0.0001, calculated by one-way ANOVA, Bonferroni's post-hoc test.

Taken together, these data indicate that pro-inflammatory cytokines enhance the cytotoxicity of CIK cells, with TNF-α showing a particularly pronounced effect compared to IL-1β and IL-6, as it simultaneously reinforces both components of the NKG2D pathway.

In addition, these cytokines also elevate PD-L1 expression, while PD-L1 blockade significantly promotes the cytotoxic potential of CIK cells.

3.1.3 IL-1β, IL-6 and TNF-α promote the transcription of MICA/B and PD-L1 via the PI3K/AKT, JAK/STAT3, and MKK/p38 MAPK pathways

To identify the mechanisms by which pro-inflammatory cytokines modulate MICA/B and PD-L1, we first evaluated the transcription levels of MICA, MICB, and PD-L1. The results revealed that cytokine treatment promoted the mRNA levels of MICA and PD-L1, while only TNF-α upregulated MICB mRNA levels (Fig. 7).

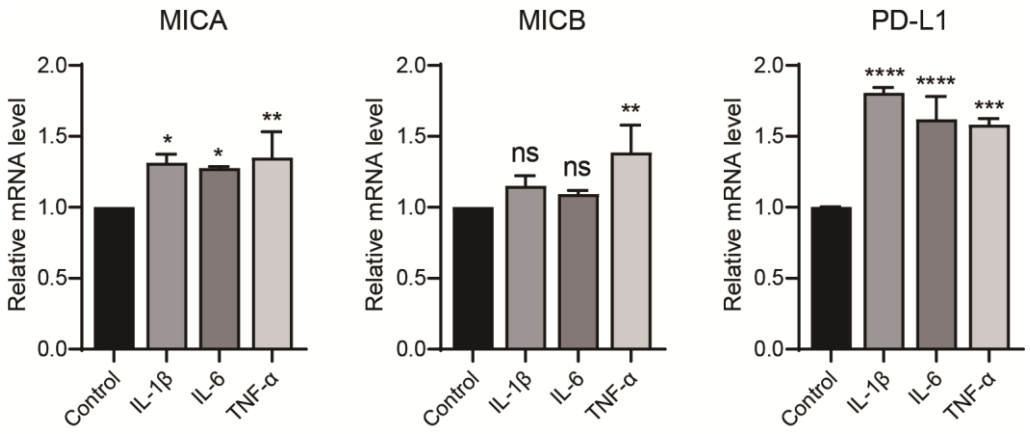

Figure 7: Pro-inflammatory cytokines induce the transcription of MICA/B and PD-L1. RT-qPCR assays showed that pro-inflammatory cytokines enhanced the transcription of MICA and PD-L1 genes, while only TNF-α upregulated MICB transcription. Data were shown as mean ± SD of three independent experiments. *P < 0.05, **P < 0.01, ***P < 0.001, ****P < 0.0001, ns, not significant, calculated by one-way ANOVA, Bonferroni's post-hoc test.

ELISA assays were then performed to assess shed MICA and MICB after cytokine treatment. The results showed that the levels of shed MICA and MICB remained comparable to those in the control group, suggesting that the elevated expression of MICA/B was not attributable to altered shedding (Fig. 8).

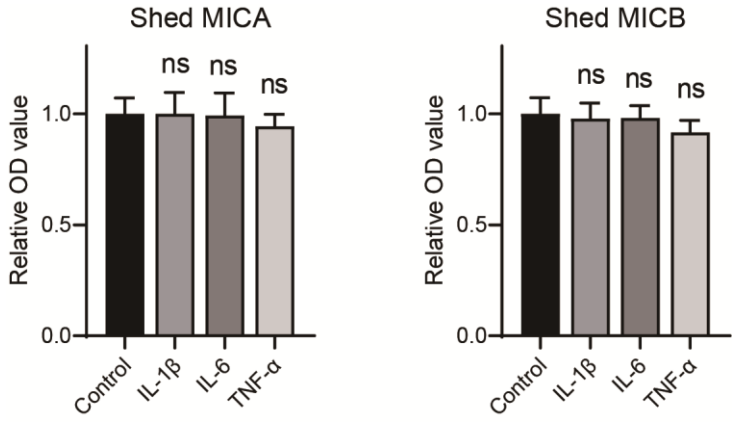

Figure 8: Pro-inflammatory cytokines have no effect on MICA/B shedding. ELISA assays showed that the levels of shed MICA and MICB remianed unchanged upon cytokines treatment. Data were shown as mean ± SD of three independent experiments. ns, not significant, calculated by one-way ANOVA, Bonferroni's post-hoc test.

To elucidate the specific signaling pathways activated by cytokines, we examined several pathways commonly associated with cytokine signaling, including the JAK/STAT, NF-κB, MAPK, and PI3K/AKT. Upon cytokine treatment, we observed increased phosphorylation levels of AKT, STAT3, and p38 MAPK, while JNK1/2, ERK1/2, and NF-κB remained unchanged (Fig. 9).

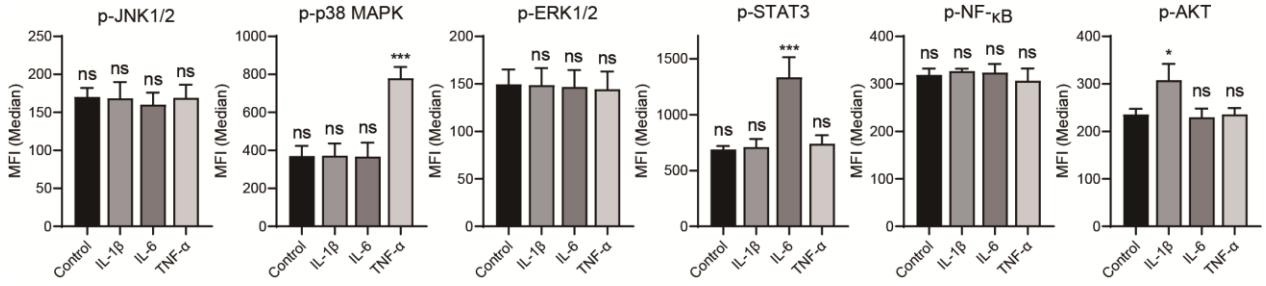

Figure 9: Pro-inflammatory cytokines activate the phosphorylation of the p38 MAPK, STAT3, and AKT pathways. The phosphorylation levels of AKT, p38 MAPK, and STAT3 increased upon the treatment of IL-1β, TNF-α, and IL-6, respectively, while ERK1/2, NF-κB, and JNK remained unchanged. Data were shown as mean ± SD of three independent experiments. *P < 0.05, ***P < 0.001, ns, not significant, calculated by one-way ANOVA, Bonferroni's post-hoc test.

To further identify the involvement of these pathways, we evaluated MICA/B and PD-L1 expression in the presence of their specific inhibitors. The upregulated MICA/B and PD-L1 induced by cytokines was completely abolished when the JAK (Fig. 10A), PI3K (Fig. 10B), and MAPK (Fig. 10C) inhibitors were applied.

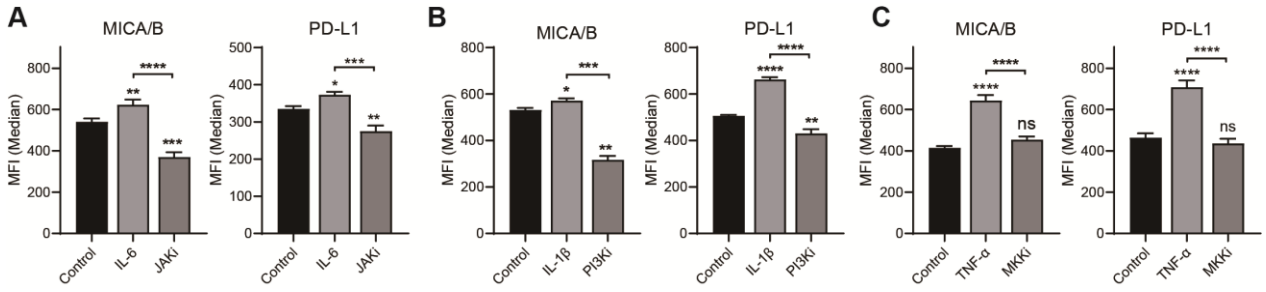

Figure 10: Signaling inhibitors restore the upregulation of MICA/B and PD-L1. Inhibitors of JAK **(A)**, PI3K **(B)**, and MAPK**(C)** completely reversed the upregulation of MICA/B and PD-L1 caused by cytokines. PI3Ki, LY-294002, 10 μM; MMKi, Gossypetin, 60 μM; JAKi, JAK inhibitor I, 1 μM. Data were shown as mean ± SD of three independent experiments. *P < 0.05, **P < 0.01, ***P < 0.001, ****P < 0.0001, ns, not significant, calculated by one-way ANOVA, Bonferroni's post-hoc test.

Interestingly, the inhibition of JAK and PI3K reduced MICA/B and PD-L1 expression to levels even lower than those in the control groups (Fig. 10), suggesting a constitutive activation of these pathways in MM. Consistent with this observation, basal levels of STAT3 and AKT phosphorylation were notably high in the absence of cytokine stimulation (Fig. 11).

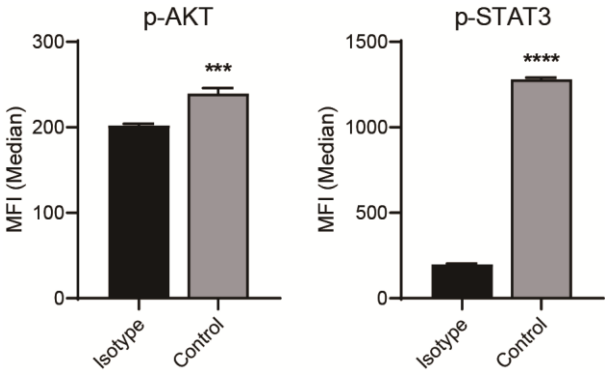

Figure 11: The basal phosphorylation levels of the AKT and STAT3 pathways. The AKT and STAT3 signaling pathways were constructively activated in MM cells. Data were shown as mean ± SD of three independent experiments. ***P < 0.001, calculated by student's unpaired t test.

Given that TNF-α upregulated NKG2D expression in CIK cells, we next explored the underlying signaling pathways in CIK cells. The results demonstrated that TNF-α also activated the p38 MAPK pathway in CIK cells (Fig. 12).

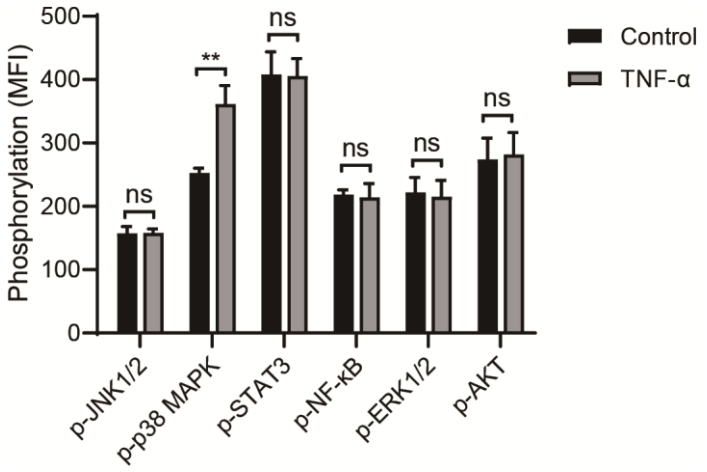

Figure 12: The phosphorylation levels of signaling pathways in CIK cells. The p38 MAPK pathways was significantly activated upon TNF-α treatment. Data were shown as mean ± SD of three independent experiments. **P < 0.01, ns, no significance, calculated by student's unpaired t test.

Overall, our findings reveal that pro-inflammatory cytokines elevate MICA/B and PD-L1 expression via transcription, and identify the signaling pathways through which cytokines function.

3.1.4 Macrophage-derived pro-inflammatory cytokines increase MICA/B and PD-L1 expression and the cytotoxicity of CIK cells

Considering that M1 macrophages are the primary source of pro-inflammatory cytokines in the TME (Wynn et al., 2013), we induced M1 macrophages from THP-1 cells and investigated whether the cytokines secreted from M1 macrophages exert comparable effects to those human recombinant cytokines. The polarization of M1 macrophages was initially identified based on their morphologic features and the CD86/CD206 expression patterns. Morphologically, M1 macrophages displayed a mixture of dendritic-like and spindle-shaped cells and were predominantly $CD86^{+}CD206^{-}$ (Fig. 13A and B). The secretion of pro-inflammatory cytokines was subsequently confirmed using ELISA assay. The results showed that IL-1β, IL-6, and TNF-α were highly secreted by M1 macrophages (Fig. 13C).

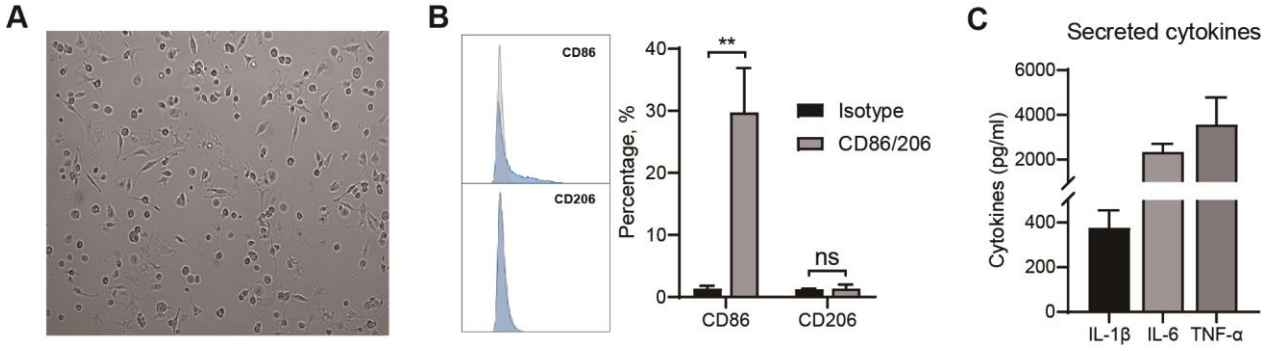

Figure 13: The polarization of M1 macrophages. (A) Representative brightfield microscope image of morphological features of M1 macrophages. **(B)** M1 macrophages expressed CD86 but not CD206. **(C)** M1 macrophages highly secreted IL-1β, IL-6, and TNF-α. Data are shown as mean ± SD of three independent experiments. **P < 0.01, ns, not significant, calculated by student's unpaired t test.

For MICA/B and PD-L1 measurement, tumor cells were co-cultured with CM from M1 macrophages, with or without cytokine neutralizing antibodies. The results showed that CM significantly upregulated MICA/B and PD-L1 expression, while cytokine antibodies partially or completely reversed this effect (Fig. 14).

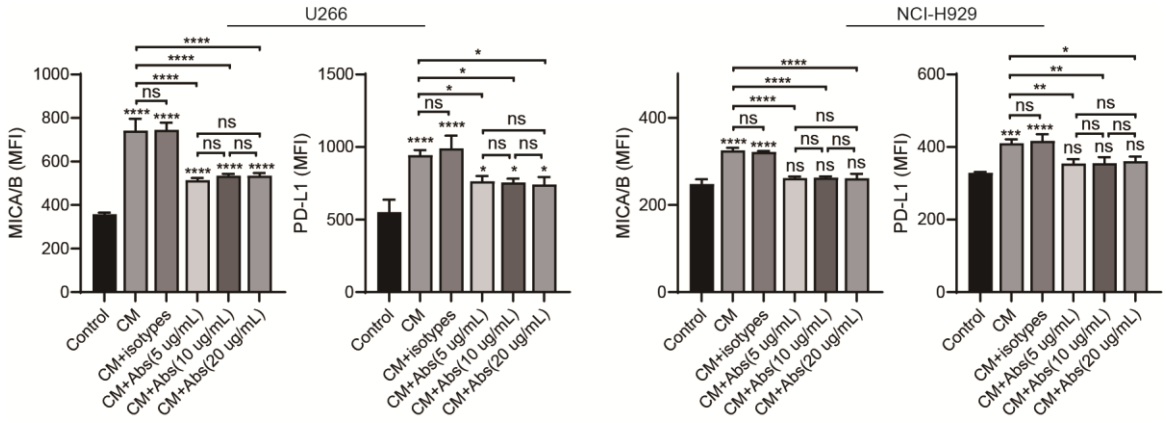

Figure 14: Macrophage-derived pro-inflammatory cytokines upregulate MICA/B and PD-L1. The CM from M1 macrophages upregulated the expression of MICA/B and PD-L1, and cytokine antibodies partially or completely eliminated this upregulation in MM cells.

For cytotoxicity assessment, we first confirmed that CM itself exhibited no cytotoxicity against tumor cells (Fig. 15A). Co-culture of tumor cells with CM enhanced the cytotoxicity of CIK cells, whereas cytokine antibodies partially reversed this enhanced cytotoxicity (Fig. 15B). Notably, PD-L1 blockade further augmented the cytotoxic activity of CIK cells against MM (Fig. 15C).

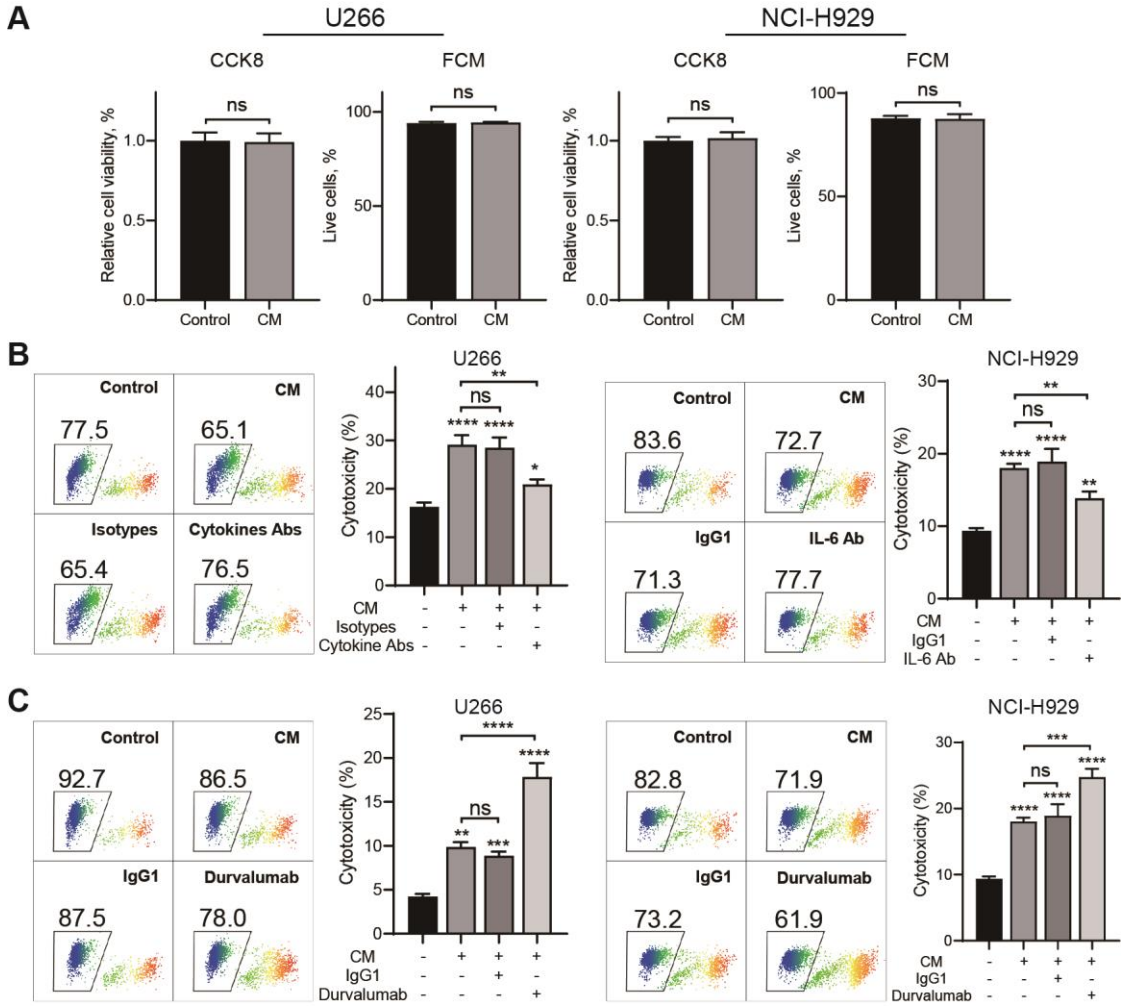

Figure 15: Macrophage-derived pro-inflammatory cytokines enhance the cytotoxicity of CIK cells. (A) The CM had no cytotoxic effect on tumor cells. **(B)** The CM promoted the cytotoxicity of CIK cells against MM cells, while the use of cytokine antibodies partially abolished this cytotoxicity. **(C)** Blockade of PD-L1 enhanced the cytotoxicity of CIK cells. Durvalumab, PD-L1 antibody, 10 μg/mL. Data are shown as mean ± SD of three independent experiments. *P < 0.05, **P < 0.01, ***P < 0.001, ****P < 0.0001, ns, not significant, calculated by one-way ANOVA, Bonferroni's post-hoc test (B and C) or student's unpaired t test (A).

3.2 Study 2: Inhibition of ERO1L mediates autophagy and apoptosis via ER stress

3.2.1 The expression profile and prognostic significance of ERO1L in pan-cancers

To evaluate the expression profile of ERO1L in pan-cancers, we analyzed the transcription data of ERO1L using the GEPIA2 database, in which contains the TCGA and GTEx data. The results showed that ERO1L expression in tumor tissiues was elevated in 9 out of 33 cancer types (Red), however, data also showed that ERO1L expression was downregulated in ESCA and THYM (Green) (Fig. 16).

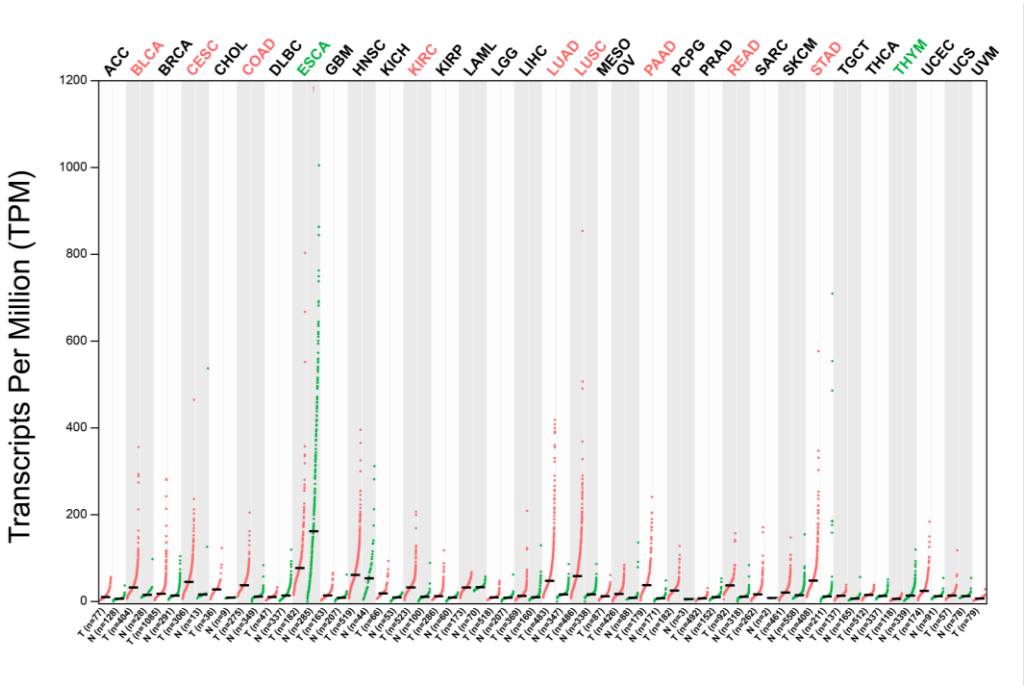

Figure 16: The expression profile of ERO1L in pan-cancers. ERO1L expression is upregulated in 9 and downregulated in 2 out of 33 different cancer types. ACC, adrenocortical carcinoma; BLCA, bladder Urothelial Carcinoma; BRCA, breast invasive carcinoma; CESC, cervical squamous cell carcinoma and endocervical adenocarcinoma; CHOL, cholangio carcinoma; COAD, colon adenocarcinoma; DLBC, diffuse large B-cell; ESCA, esophageal carcinoma; GBM, glioblastoma multiforme; HNSC, head and neck squamous cell carcinoma; KICH, kidney chromophobe; KIRC, kidney renal clear cell carcinoma; KIRP, kidney renal papillary cell carcinoma; LAML, acute myeloid leukemia; LGG, lower grade glioma; LIHC, liver hepatocellular carcinoma; LUAD, lung adenocarcinoma; LUSC, lung squamous cell carcinoma; MESO, mesothelioma; OV, ovarian serous cystadenocarcinoma; PAAD, pancreatic adenocarcinoma; PCPG, pheochromocytoma and paraganglioma; PRAD, prostate adenocarcinoma; READ, rectum adenocarcinoma; SARC, sarcoma; SKCM, skin cutaneous melanoma; STAD, stomach adenocarcinoma; TGCT, testicular germ cell tumors; THCA, thyroid carcinoma; THYM, thymoma; UCEC, uterine corpus endometrial carcinoma; UCS, uterine carcinosarcoma; UVM, uveal melanoma.

The high expression of ERO1L implies the clinical significance in tumor patients. We retrieved prognostic data of ERO1L in tumor patients from public online databases. From the Gene Expression Profiling Interactive Analysis 2 (GEPIA2) database, an integrated result showed that ERO1L expression was negatively associated with patients' overall survival (OS) with a hazard ratio (HR) of 1.7 ($p < 0.0001$) across 33 cancer types (Fig. 17A). Specifically, data from the Kaplan-Meier Plotter database showed that ERO1L was identified as an indicator of poor prognosis in 9 out of 20 different cancer types (Fig. 17B).

A

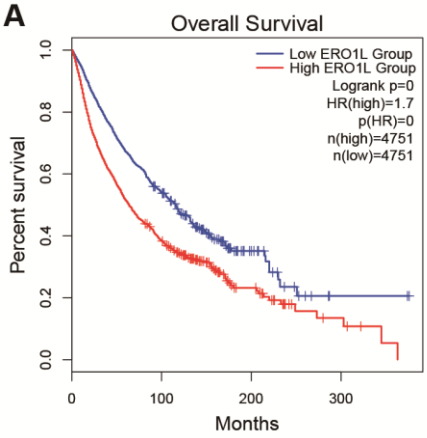

B

Cancer type	High	Low	HR	p-value	Cancer type	High	Low	HR	p-value
BLCA	357	1118	1.42	0.054	LUSC	1416	456	0.71	0.077
BRCA	1582	2992	3.06	< 0.001	OV	1103	460	0.73	0.19
CESC	373	795	2.66	0.001	PDAC	142	464	2.17	< 0.001
EAC	184	84	1.41	0.43	PCPG	187	495	7.98	0.033
ESCC	82	183	1.59	0.31	READ	275	366	0.52	0.26
HNSC	1349	611	1.39	0.075	SARC	332	767	2.28	0.002
KIRC	555	1716	1.51	0.081	STAD	443	804	1.23	0.26
KIRP	285	897	4.55	< 0.001	TGCT	158	448	5.48	0.12
LIHC	527	849	1.72	0.0092	THCA	552	1653	3.08	0.02
LUAD	684	1328	2.91	< 0.001	UCEC	1606	706	0.59	0.074

Figure 17: Overexpressed ERO1L indicates poor prognosis. (A) Integrated Kaplan-Meier curves from the GEPIA2 database showing the prognostic effect of ERO1L expression with patients' survival across 33 types of cancers. **(B)** Prognostic analyses from the Kaplan-Meier Plotter database indicating the correlations of ERO1L with survival in specific cancers.

In addition, ERO1L was also included into multi-gene models as a predictor for poor prognosis of tumor patients. Differentially expressed genes (DEGs) between tumor patients and normal individuals were computationally identified and then screened to construct risk score models. In these models, ERO1L was found to be associated with poor prognosis and was proposed for the prognosis prediction in lung cancer (Liu et al., 2022; Zhu et al., 2020) and pancreatic cancer (Nie et al., 2021).

3.2.2 ERO1L is overexpressed in CRC

To explore the mRNA expression of ERO1L in CRC patients, we analyzed datasets from the GEPIA2 database. The results showed that ERO1L mRNA was significantly higher in CRC tissues than normal tissues (Fig. 18A). For ERO1L protein expression, we utilized

data from the HPA database. Immunohistochemistry (IHC) results revealed that ERO1L protein was negative to weak in normal tissues, but moderate to strong in most CRC tissues (Fig. 18B).

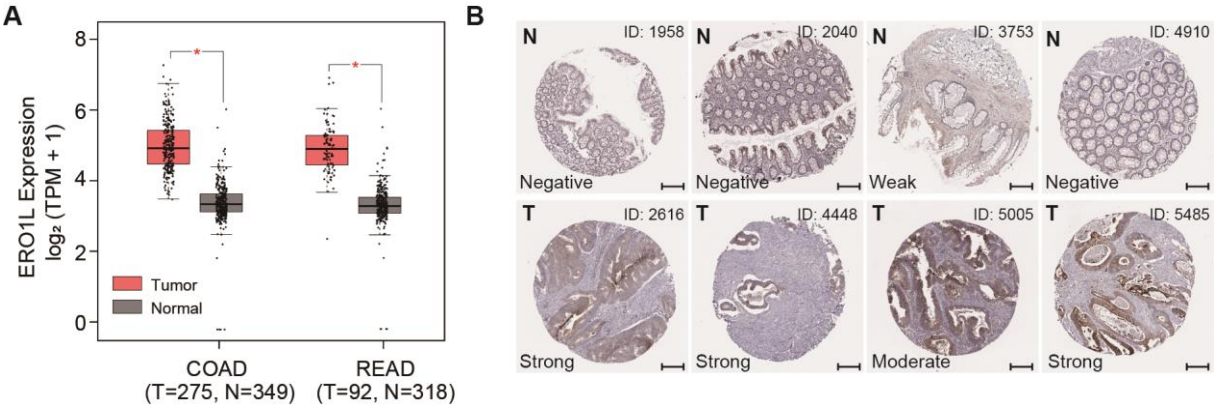

Figure 18: The expression profile of ERO1L in CRC tissues. (A) ERO1L mRNA was elevated in CRC tissues, including COAD and READ, compared to their normal counterparts. Data were from the GEPIA2 database. **(B)** ERO1L protein was highly expressed in CRC tissues. Representative four normal tissues (N) and four CRC tissues (T) from the HPA database. Scale bar, 200 μm. COAD: colon adenocarcinoma; READ: rectal adenocarcinoma.

Additionally, ERO1L expression analysis in cell lines revealed markedly upregulated mRNA and protein levels in CRC cell lines compared to the normal epithelial cell line (Fig. 19A and B).

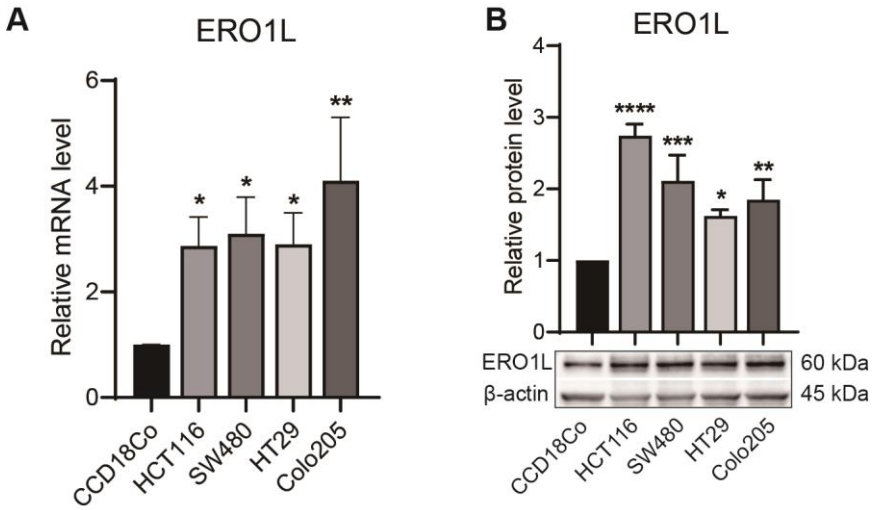

Figure 19: ERO1L expression in CRC cell lines. ERO1L mRNA **(A)** and protein **(B)** were overexpressed in CRC cell lines compared with normal colon epithelial cell line

(CCD18Co). Data are shown as mean ± SD of three independent experiments. *P < 0.05, **P < 0.01, ***P < 0.001, ****P < 0.0001, calculated by one-way ANOVA, Bonferroni's post-hoc test.

Together, these findings indicate that ERO1L is overexpressed in CRC, implicating its potential role in tumor progression.

3.2.3 ERO1L is regulated by ER stress and contributes to mitigate ER stress

To investigate the relationship between ER stress and ERO1L, we first examined whether ERO1L could be modulated by ER stress. Tunicamycin (Tm), a widely used ER stress-inducing agent that interferes with N-linked glycosylation in glycoprotein synthesis [24], was employed to induce ER stress. Successful induction of ER stress in CRC cells was validated by the upregulation of ER stress-related genes, including GRP78, CHOP, PERK, IRE1, ATF4, and ATF6 (Fig. 20).

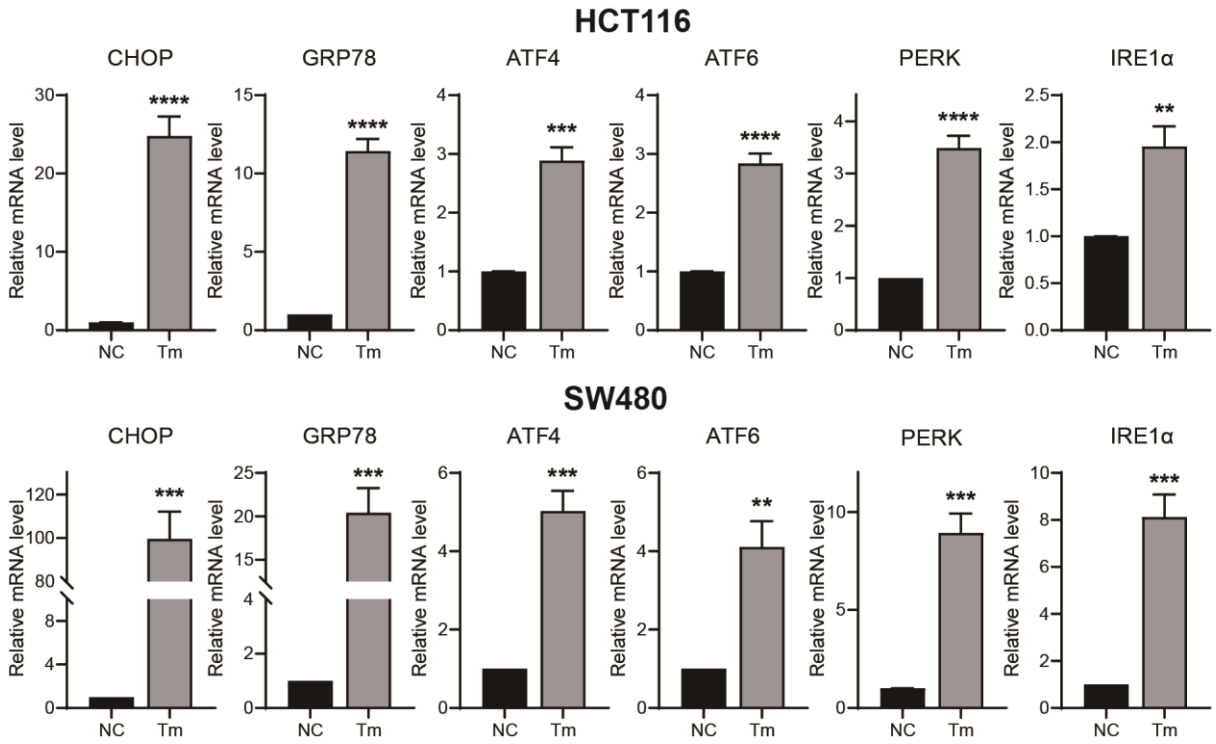

Figure 20: Tunicamycin induces ER stress in CRC. RT-qPCR analysis showed that ER stress-related genes were upregulated in CRC cells following tunicamycin treatment. CRC cells were treated with 2 µg/mL of Tm for 6 hours. Data are shown as mean ± SD of three independent experiments. **P < 0.01, ***P < 0.0001, ****P < 0.0001, calculated by student's unpaired t test.

Following Tm treatment, ERO1L expression was significantly enhanced at both mRNA and protein levels (Fig. 21A and B).

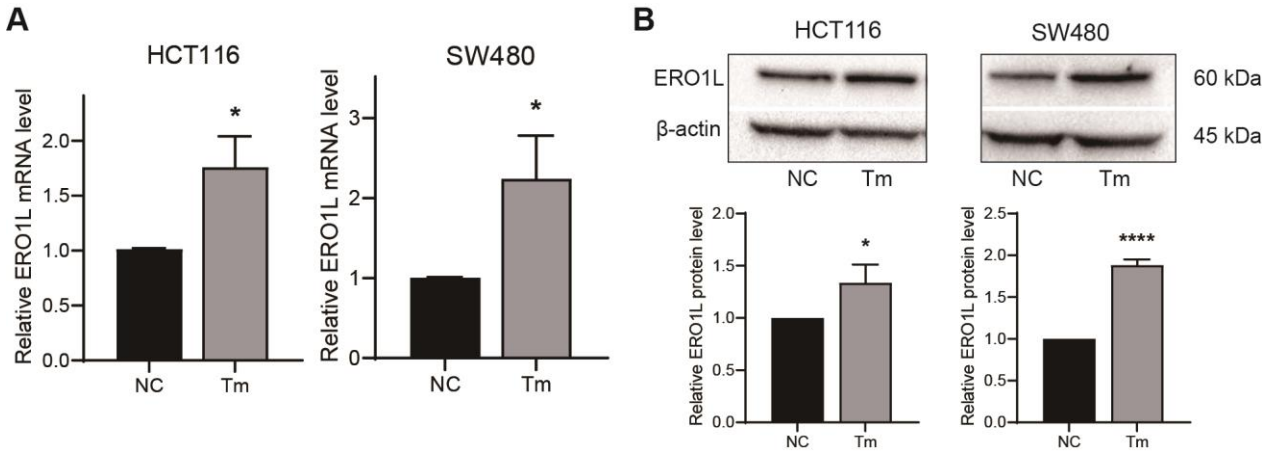

Figure 21: Tunicamycin upregulates the expression of ERO1L. The mRNA **(A)** and protein **(B)** levels of ERO1L in CRC cells were up-regulated upon Tm treatment. CRC cells were treated with 2 ug/mL of Tm for 24 hours. Data are shown as mean ± SD of three independent experiments. *P < 0.05, ****P < 0.0001, calculated by student's unpaired t test.

Next, we explored whether ERO1L inhibition could induce ER stress. Using siRNA-mediated knockdown of ERO1L, we confirmed knockdown efficiency (Fig. 22 A and B).

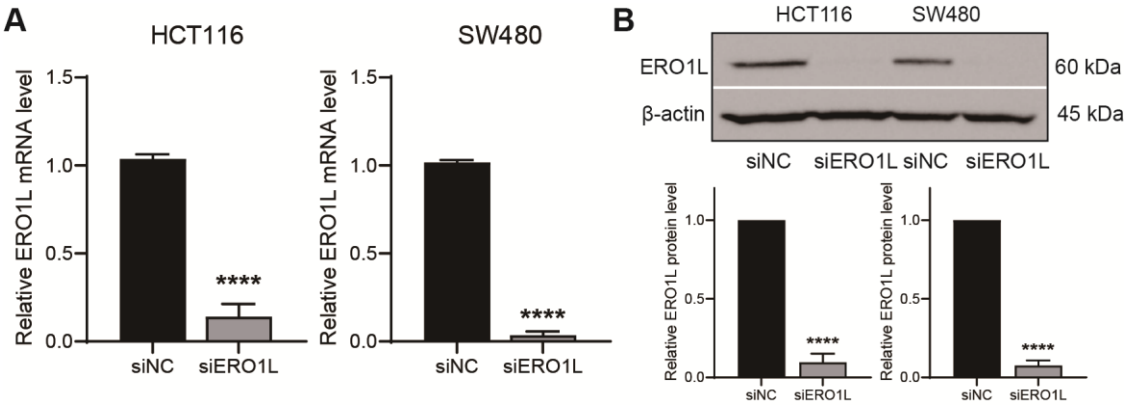

Figure 22: siRNA-mediated ERO1L knockdown. ERO1L mRNA **(A)** and protein **(B)** levels were significantly inhibited using ERO1L-specific siRNA. Data are shown as mean ± SD of three independent experiments. ****P < 0.0001, calculated by student's unpaired t test.

Upon ERO1L knockdown, we found that ER stress was induced in CRC cells. The mRNA and protein levels of ER stress-related genes were upregulated upon ERO1L knockdown (Fig. 23 A and B).

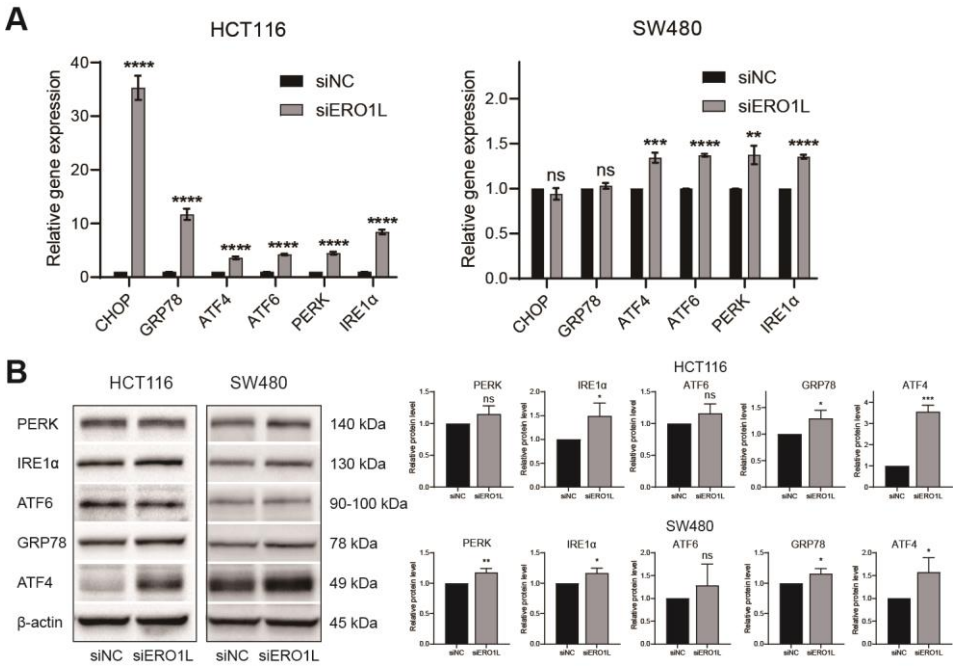

Figure 23: ERO1L inhibition induces ER stress in CRC. The mRNA **(D)** and protein **(E)** levels of ER stress-related genes were increased in ERO1L knockdown CRC cells. Data are shown as mean ± SD of three independent experiments. *P < 0.05, **P < 0.01, ****P < 0.0001, calculated by student's unpaired t test.

To assess the role of ERO1L in modulating ER stress, we treated ERO1L knockdown cells with Tm and found that ERO1L-deficient CRC cells exhibited heightened sensitivity to Tm compared to control cells, indicating that ERO1L plays a protective role in CRC cell survival under ER stress (Fig. 24).

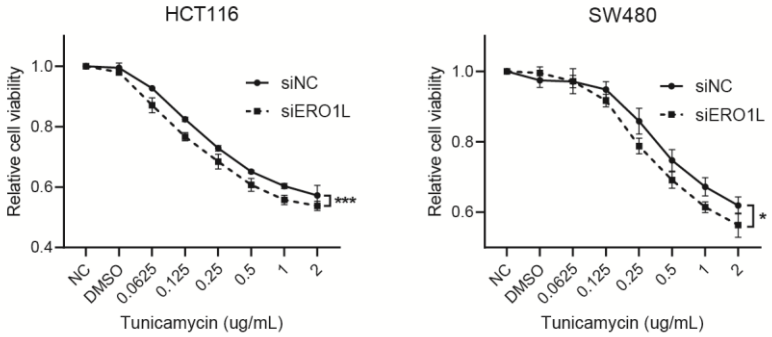

Figure 24: ERO1L contributes to the resistance of CRC to ER stress. Knockdown of ERO1L increased the susceptibility of CRC cells to tunicamycin. CRC cells were incubated with tunicamycin for 24 hours. Data are shown as mean ± SD of three independent experiments. *P < 0.05, **P < 0.01, ****P < 0.0001, calculated by two-way ANOVA, Bonferroni's post-hoc test.

Collectively, our findings suggest a bidirectional relationship between ERO1L and ER stress, and highlight the critical regulatory role of ERO1L in ER stress. The upregulation of ERO1L in response to ER stress contributes to cell survival, while the deficiency of ERO1L could induce ER stress in CRC.

3.2.4 ERO1L contributes to the malignant behaviors of CRC

Since ERO1L was elevated in CRC, we next assessed its role in driving the malignant phenotypes of CRC cells. First, we assessed the effect of ERO1L on cell proliferation using CCK-8 assays. ERO1L knockdown significantly retarded the proliferation of CRC cells compared to control cells (Fig. 25).

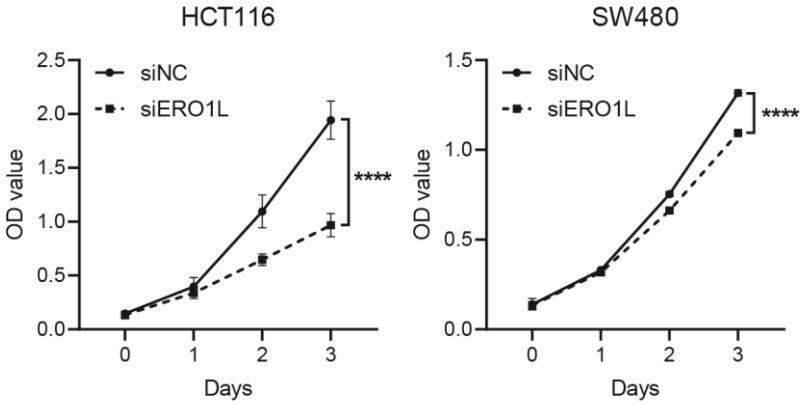

Figure 25: ERO1L inhibition retards the proliferation of CRC cells. Knockdown of ERO1L inhibited the proliferation of CRC cells. Data are shown as mean ± SD of three independent experiments. ****P < 0.0001, calculated by student's unpaired t test.

By comparing wound-healing rates, we found that ERO1L knockdown reduced the migration ability of CRC cells (Fig. 26).

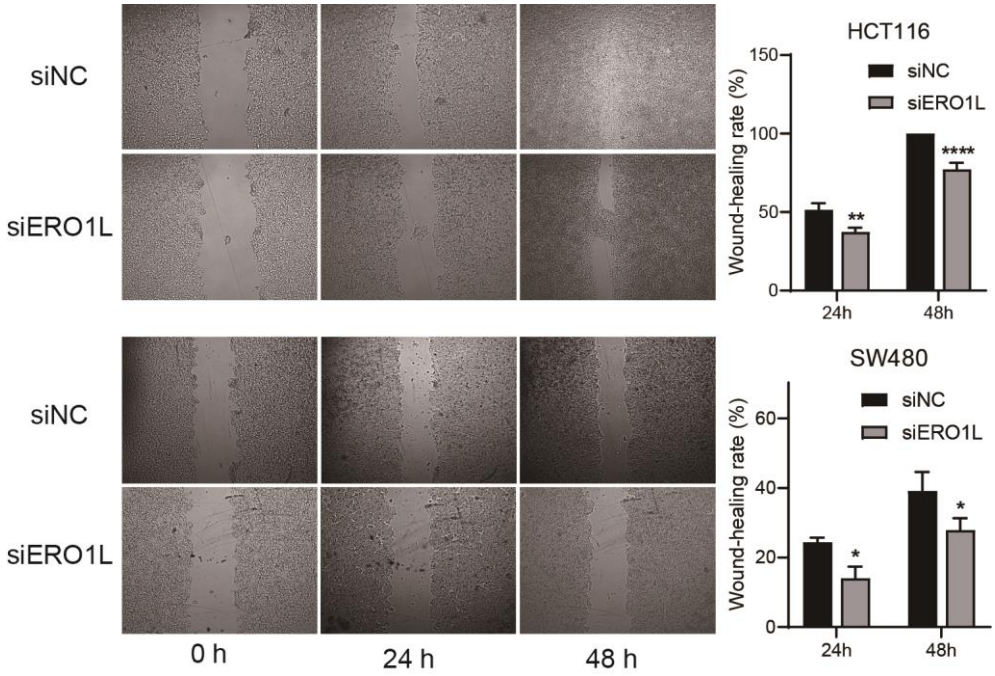

Figure 26: ERO1L inhibition impairs the migration ability of CRC cells. Scratch assay showed that ERO1L deficiency impaired the migration ability of CRC cells. Data are shown as mean ± SD of three independent experiments. *P < 0.05, **P < 0.01, ****P < 0.0001, calculated by two-way ANOVA, Bonferroni's post-hoc test.

Results from Transwell assays also demonstrated that the migration and invasion potential were limited in ERO1L knockdown CRC cells (Figure 3D). Finally, we observed that silencing ERO1L impaired the clonogenic ability of CRC cells (Fig. 27).

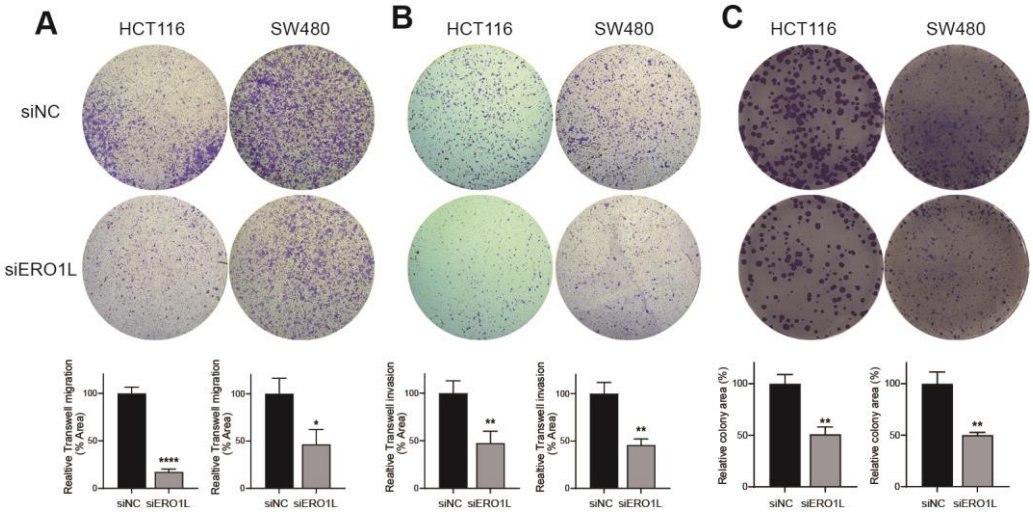

Figure 27: ERO1L deficiency inhibits the migration, invasion and colony formation ability. Transwell and colony formation assay indicated that ERO1L inhibition weakened the migration **(A)**, invasive ability **(B)**, and clonogenic capacity **(C)** of CRC cells. Data are

shown as mean ± SD of three independent experiments. *P < 0.05, **P < 0.01, calculated by student's unpaired t test.

Overall, these findings indicate the critical role of ERO1L in CRC promotion, supporting its function as a tumor-supportive gene.

3.2.5 ERO1L inhibition induces apoptosis and autophagy in CRC

Given the established correlations between ER stress, apoptosis, and autophagy, and our above findings that ERO1L inhibition induces ER stress, we investigated whether ERO1L modulates apoptosis and autophagy in CRC.

Apoptosis was firstly assessed using Annexin V/7-AAD double staining. Results showed that ERO1L knockdown significantly increased the proportion of apoptotic cells (Fig. 28).

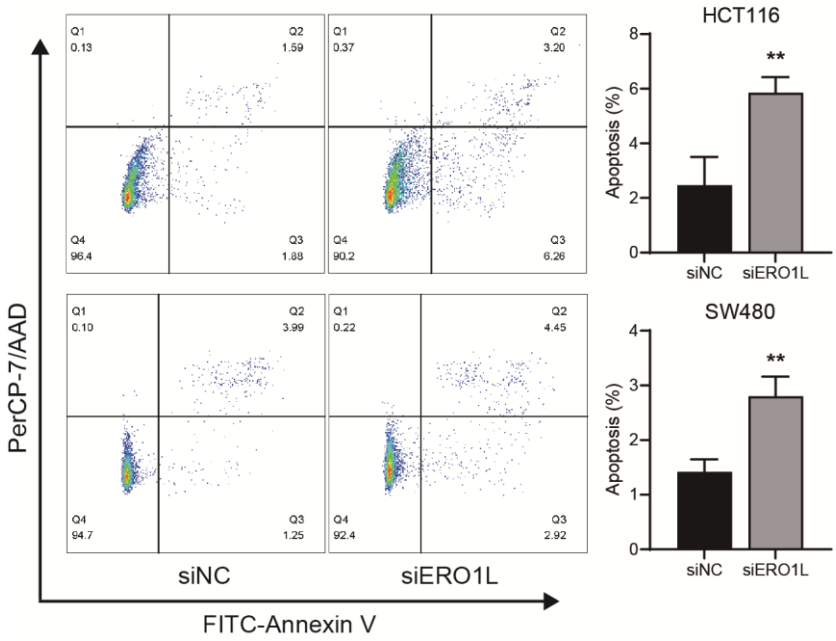

Figure 28: ERO1L inhibition induces apoptosis in CRC cells. AnnexinV/7-AAD apoptosis assay showed that ERO1L inhibition induced apoptosis (AnnexinV+7AAD- cells) in CRC cells. Data are shown as mean ± SD of three independent experiments. **P < 0.01, calculated by student's unpaired t test.

Apoptosis-related proteins were next evaluated using western-blotting (Fig. 29).

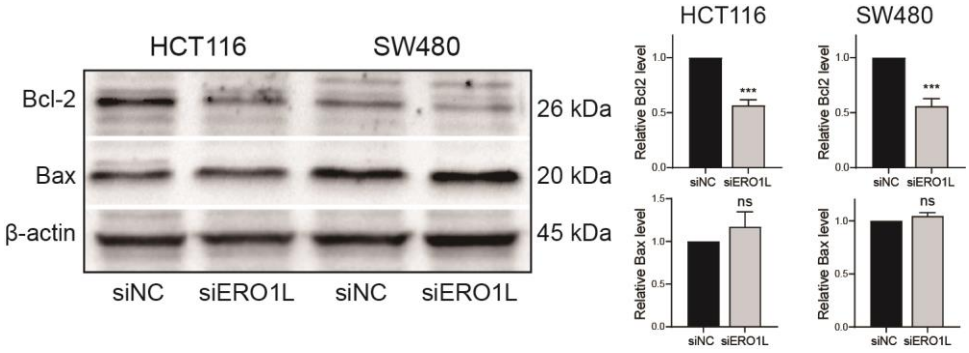

Figure 29: ERO1L inhibition induces apoptosis in CRC cells. Western-blotting assay showed that ERO1L knockdown downregulated anti-apoptotic protein Bcl-2, while had no effect on pro-apoptotic protein Bax. Data are shown as mean ± SD of three independent experiments. ***P < 0.01, ns, no significance, calculated by student's unpaired t test.

To explore the involvement of caspases in ERO1L inhibition-induced apoptosis, we measured the activation of caspase 3/7 and caspase 9, both of which were upregulated (Fig. 30).

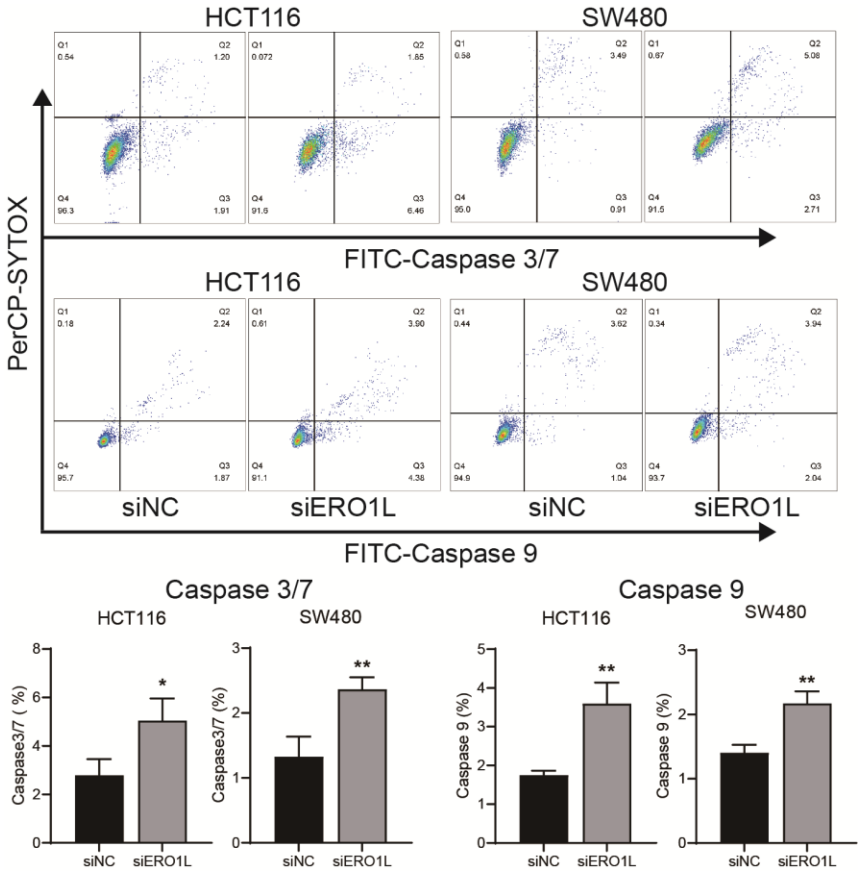

Figure 30: ERO1L knockdown activates caspases in CRC cells. ERO1L inhibition upregulated caspase 3/7 and caspase 9 in CRC cells. Data were shown as mean ± SD of

three independent experiments. *P < 0.05, **P < 0.01, calculated by student's unpaired t test.

Furthermore, we observed that treatment with z-VAD-FMK, a pan-caspase inhibitor, partially reversed apoptosis, indicating that ERO1L knockdown-induced apoptosis was caspase dependent (Fig. 31).

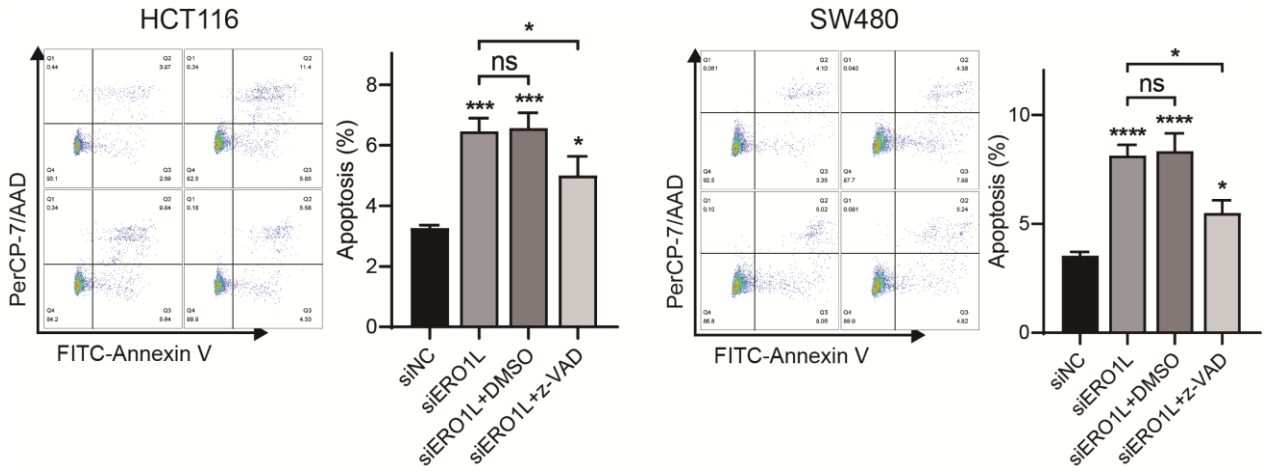

Figure 31: ERO1L knockdown-induced apoptosis is caspase-dependent. Treatment of z-VAD, a pan-caspase inhibitor, partially restored the ERO1L knockdown-induced apoptosis. Data were shown as mean ± SD of three independent experiments. *P < 0.05, ***P < 0.001, ****P < 0.0001, ns, not significant, calculated byone-way ANOVA, Bonferroni's post-hoc test.

Subsequently, we revealed that ERO1L deficiency also activated autophagy, as indicated by the upregulation of LC3-II and Beclin-1 (Fig. 32A). Since autophagy is a dynamic process involving autophagosome formation and degradation (Loos et al., 2014), we monitored autophagy flux using chloroquine (CHQ), a classic autophagosome degradation inhibitor, to distinguish them. CHQ treatment of ERO1L knockdown CRC cells further elevated autophagy levels compared to CHQ treatment of CRC cells, indicating that ERO1L inhibition mediated autophagy primarily through enhanced autophagosome formation (Fig. 32B).

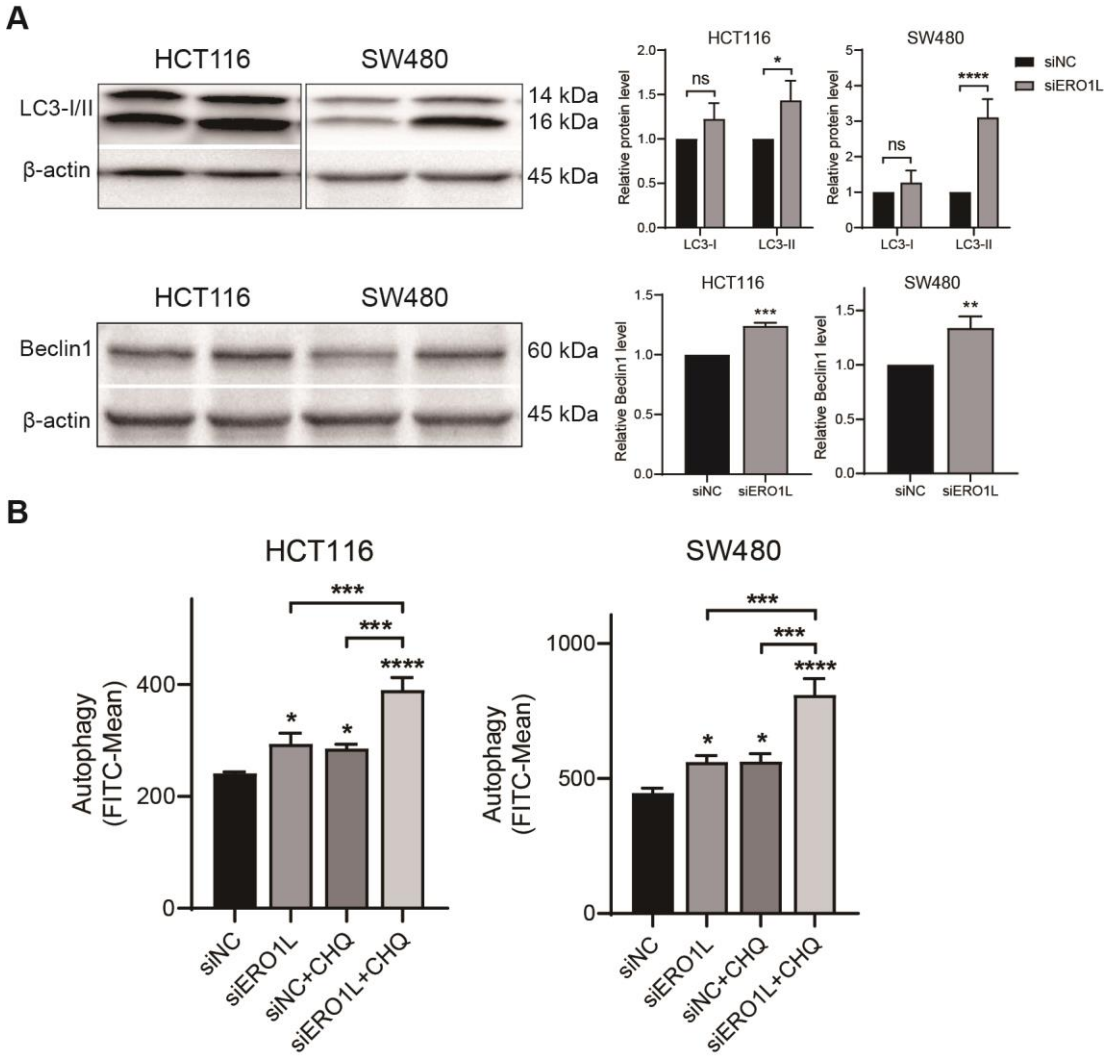

Figure 32: ERO1L inhibition induces autophagy in CRC cells. (A) Autophagy-related protein LC3-I/II and Beclin1 were upregulated upon ERO1L inhibition in CRC cells. **(B)** Autophagy flux measurement with autophagosome degradation inhibitor CHQ. Data were shown as mean ± SD of three independent experiments. *P < 0.05, **P < 0.01, ***P < 0.001, ****P < 0.0001, ns, not significant, calculated by student's unpaired t test (A), one-way (B) and two-way (A) ANOVA, Bonferroni's post-hoc test.

To investigate whether ERO1L inhibition-induced apoptosis and autophagy were driven by ER stress, we treated CRC cells with TUDCA, a well-characterized ER stress inhibitor. The results showed that TUDCA treatment completely or partially reversed ERO1L knockdown-induced apoptosis and autophagy (Fig. 33A and B).

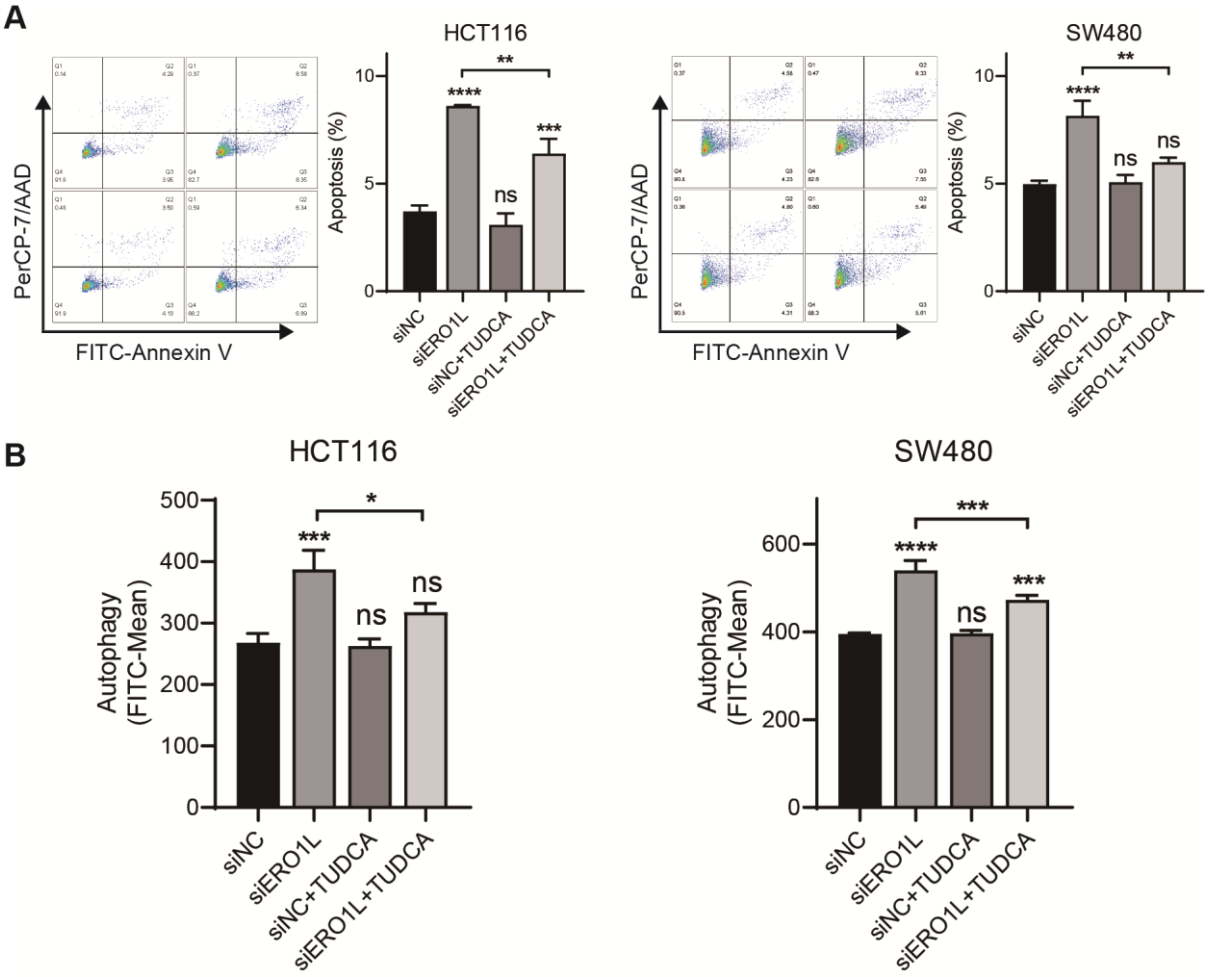

Figure 33: ERO1L knockdown-induced apoptosis and autophagy are mediated by Er stress. ERO1L knockdown-induced apoptosis **(A)** and autophagy **(B)** were blocked by the treatment of TUDCA. Data were shown as mean ± SD of three independent experiments. *P < 0.05, **P < 0.01, ***P < 0.001, ****P < 0.0001, ns, not significant, calculated by one-way ANOVA, Bonferroni's post-hoc test.

Collectively, these findings indicate that ERO1L inhibition triggers ER stress, which subsequently mediates both caspase-dependent apoptosis and autophagy in CRC cells.

3.2.6 ERO1L mediates apoptosis and autophagy via the ERK1/2 pathway

To identify the signaling pathways involved in ERO1L knockdown-mediated apoptosis and autophagy, we evaluated phosphorylated signaling molecules using flow cytometry. A series of signaling proteins known to regulate apoptosis and autophagy were investigated. Mammalian target of rapamycin (mTOR), a central mediator of both apoptosis and autophagy (Xie et al., 2023), showed a significant reduction in phosphorylation levels upon ERO1L knockdown (Fig. 34). Interestingly, we observed a mild increase in the

phosphorylation levels of JNK 1/2, p38 mitogen-activated protein kinase (MAPK), and protein kinase B (AKT). In contrast, the extracellular signal-regulated kinase (ERK)1/2 phosphorylation levels exhibited a marked decrease (Fig. 34). Given that these molecules function upstream of mTOR, we suggested that the reduction in mTOR phosphorylation reflected an integrated outcome of their combined effects. Additionally, the phosphorylation levels of adenosine monophosphate-activated protein kinase α (AMPKα), p53, and NF-κB showed no significant changes (Fig. 34).

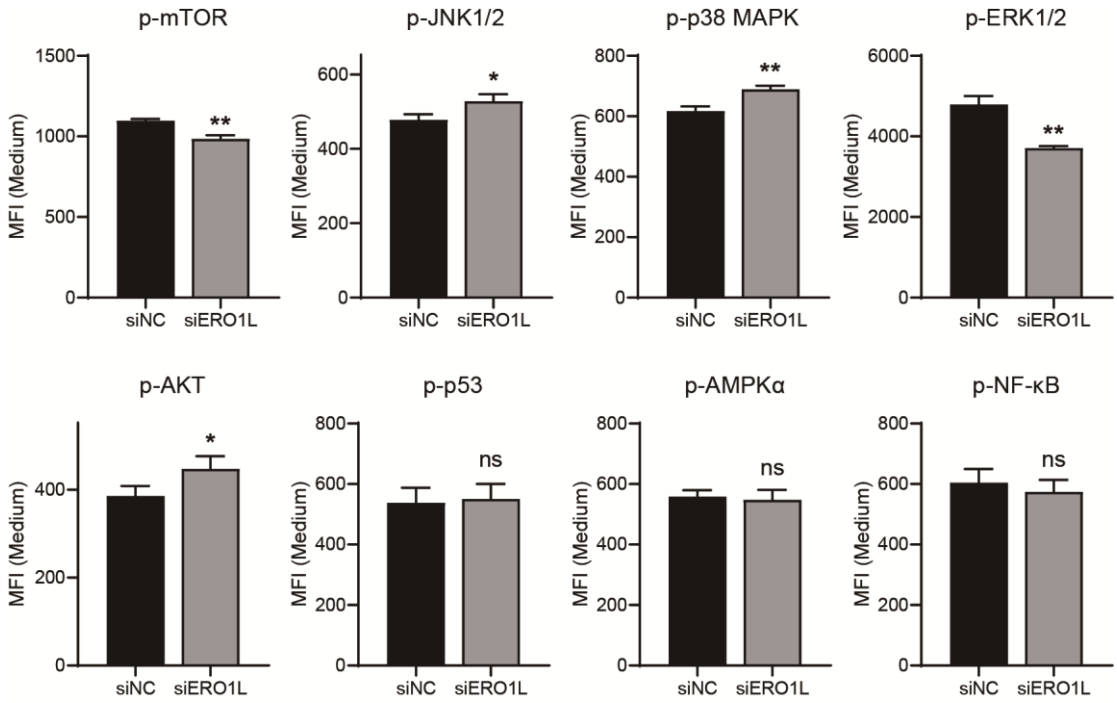

Figure 34: The signaling pathways involved in ERO1L knockdown. The JNK1/2, p38 MAPK, and AKT pathways were activaed after ERO1L inhibition, while the mTOR and ERK1/2 were inhibited. Data were shown as mean ± SD of three independent experiments. *P < 0.05, **P < 0.01, ns, not significant, calculated by student's unpaired t test.

To further investigate the involvement of p38 MAPK, JNK1/2, and AKT, we treated CRC cells with specific inhibitors. The results showed that the inhibition of p38 MAPK, JNK1/2, and AKT did not reduce apoptosis or autophagy in ERO1L knockdown cells, indicating that the activation of these pathways was not responsible for the induced apoptosis and autophagy (Fig. 35A and B). Interestingly, AKT inhibition in ERO1L knockdown cells significantly enhanced apoptosis rather than reversing it, indicating a potential synergistic

interaction between ERO1L deficiency and AKT inhibition in promoting apoptosis (Fig. 35B).

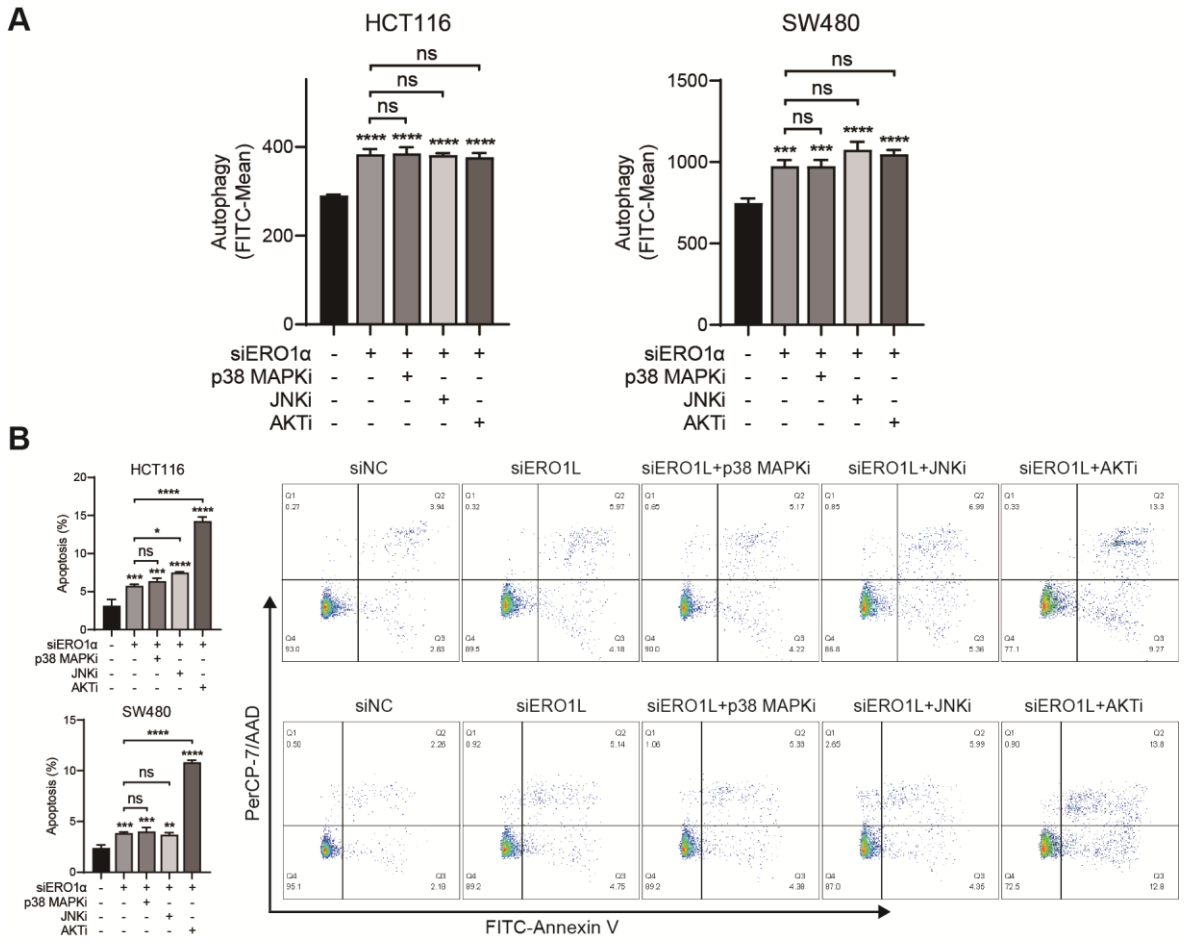

Figure 35: The JNK1/2, p38 MAPK, and AKT pathways are not responsible for ERO1L inhibition-induced apoptosis and autophagy. The treatment of the specific inhibitors of the p38 MAPK, JNK, and AKT did not restore the upregulated apoptosis and autophagy upon ERO1L knockdown. Data were shown as mean ± SD of three independent experiments. *P < 0.05, **P < 0.01, ***P < 0.001, ****P < 0.0001, ns, not significant, calculated by one-way ANOVA, Bonferroni's post-hoc test.

Furthermore, to explore the role of ERK1/2, we conducted a rescue experiment using ACA-28, an ERK1/2 agonist known for its anti-tumor capacity by hyperactivating ERK1/2 (Satoh et al., 2020). Treatment with a low concentration (1 μM) of ACA-28 completely reversed autophagy in both cell lines, while apoptosis was fully reversed in HCT116 cells and partially reversed in SW480 cells (Fig. 36A and B). However, a higher concentration (10 μM) significantly enhanced both autophagy and apoptosis (Fig. 36A and B).

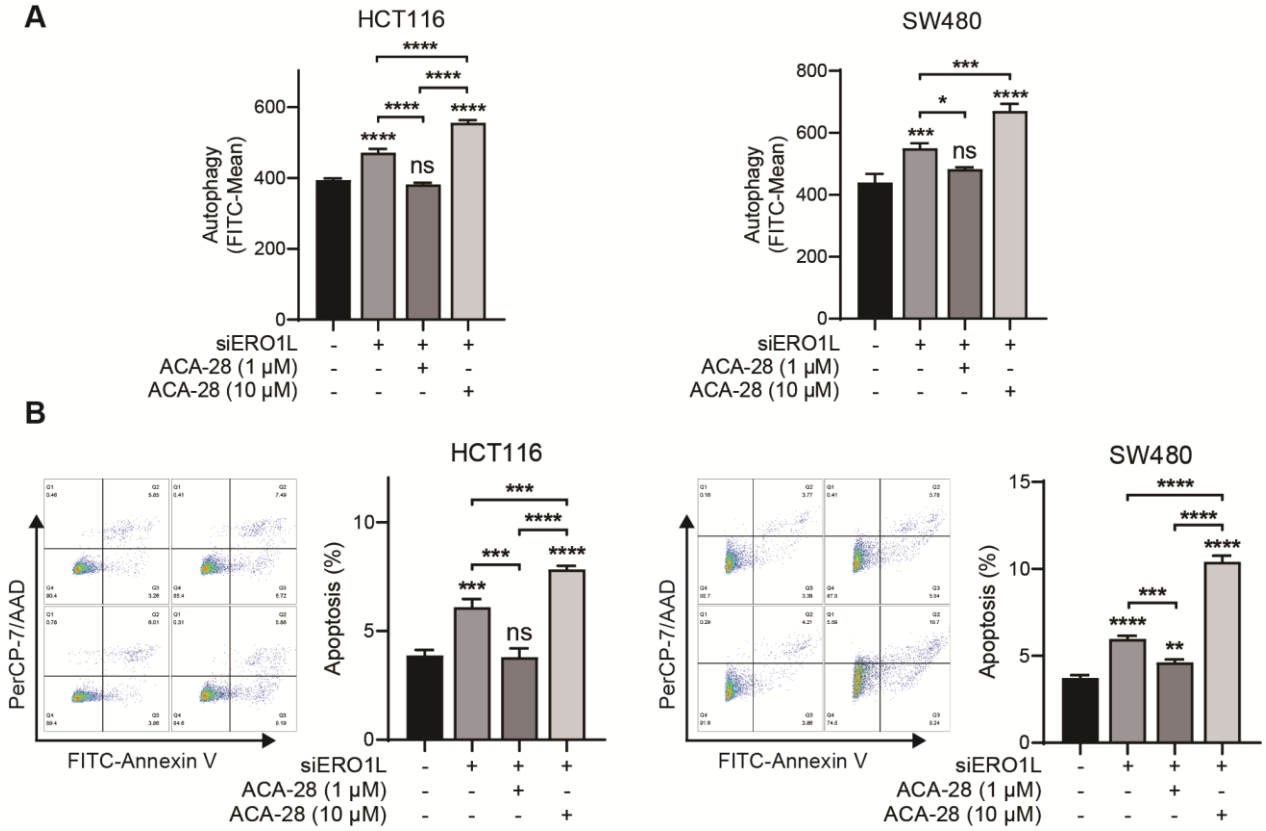

Figure 36: The ERK1/2 pathway is involved in ERO1L knockdown-induced apoptosis and autophagy in CRC. Treatment with low concentration of ACA-28 (1 μM) reversed apoptosis and autophagy while high concentration of ACA-28 (10 μM) reinforced autophagy **(A)** and apoptosis **(B)** in ERO1L knockdown CRC cells. Data were shown as mean ± SD of three independent experiments. *P < 0.05, **P < 0.01, ***P < 0.001, ****P < 0.0001, ns, not significant, calculated by one-way ANOVA, Bonferroni's post-hoc test.

Phosphorylation analysis of ERK1/2 after ACA-28 treatment using flow cytometry and western-blotting confirmed that 1 μM ACA-28 reversed the reduced ERK1/2 phosphorylation, while 10 μM ACA28 markedly increased ERK1/2 phosphorylation in ERO1L knockdown cells (Fig. 37).

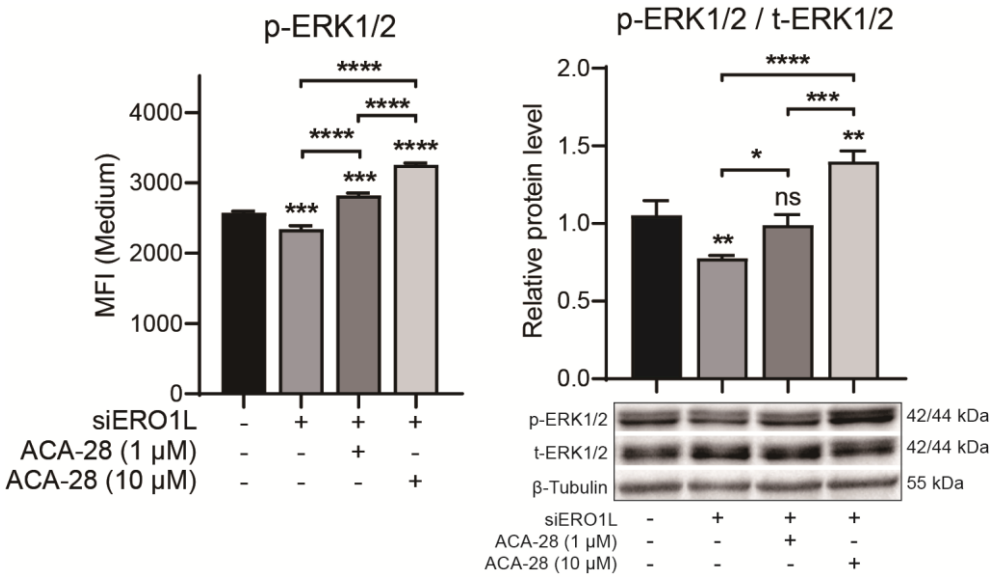

Figure 37: Treatment with ACA-28 reverses ERK1/2 phosphorylation in ERO1L knockdown CRC cells. Treatment with low concentration of ACA-28 (1 μM) reversed the phosphorylation level of ERK1/2 while high concentration of ACA-28 (10 μM) significantli enhanced it in ERO1L knockdown CRC cells. The phosphorylation level of ERK1/2 was measured by flow cytometry (left) or western-blotting (right). Data were shown as mean ± SD of three independent experiments. *P < 0.05, **P < 0.01, ***P < 0.001, ****P < 0.0001, ns, not significant, calculated by one-way ANOVA, Bonferroni's post-hoc test.

Collectively, these findings illustrate the involvement of the ERK1/2 pathway in ERO1L inhibition-induced apoptosis and autophagy.

3.2.7 Combination treatment of ERO1L inhibition with ER stress-inducing therapies

As shown above, ERO1L inhibition induced ER stress and increased the vulnerability of CRC cells to ER stress (Fig. 23 and 24). Considering that the UPR pathway is a critical mechanism employed by tumor cells to mitigate ER stress, we hypothesized that ERO1L inhibition would render CRC cells more susceptible to therapies targeting the UPR pathway. To test this hypothesis, cell viability was measured following treatment with UPR-targeting inhibitors. Among the three inhibitors tested, the PERK inhibitor (GSK2606414) and the ATF6 inhibitor (Ceapin-A7) significantly reduced cell viability compared to negative controls, suggesting a potential synergistic interaction between ERO1L inhibition and UPR-targeting therapies (Fig. 38A and C). However, treatment with the IRE1α inhibitor (4μ8c) did not show a comparable effect (Fig. 38B).

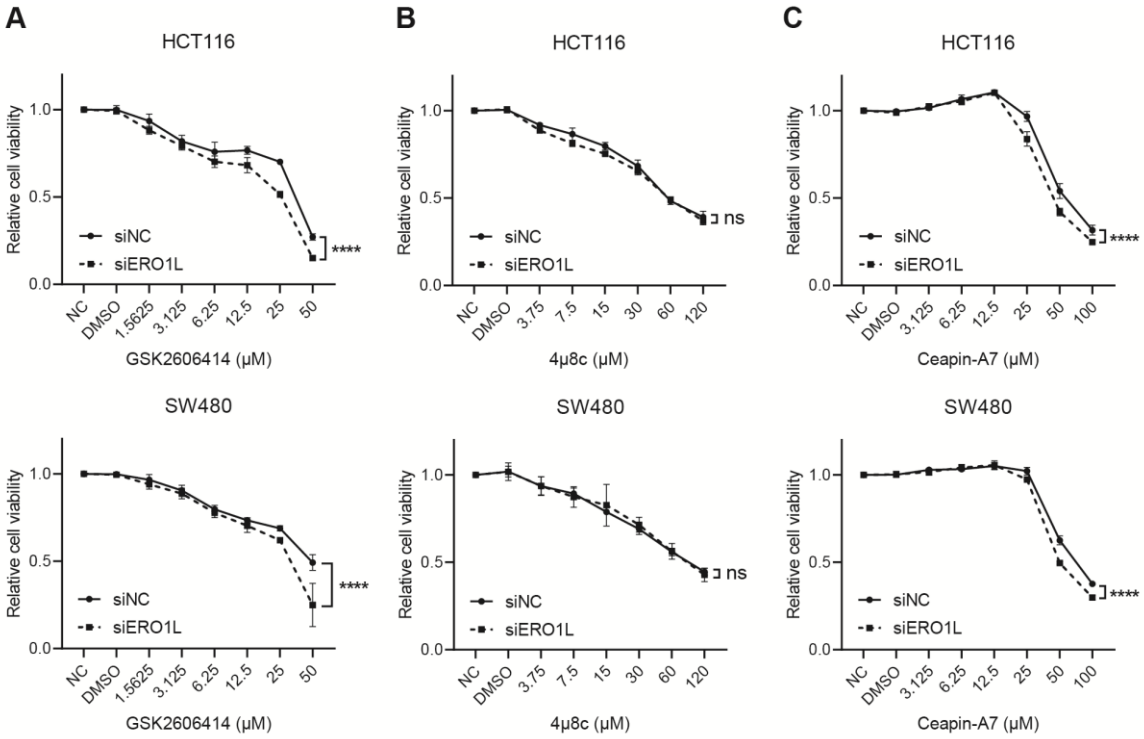

Figure 38: Combination therapy of ERO1L inhibition with UPR-targeting drugs shows potent anti-tumor potentials. ERO1L inhibition combined with PERK inhibitor **(A)** and ATF6 inhibitor **(C)** showed higher anti-cancer efficacy, while ERO1L knockdown did not increase the susceptibility of CRC cells to IRE1 inhibitor **(B)**. Data are shown as mean ± SD of three independent experiments. ****P < 0.0001, ns, not significant, calculated by two-way ANOVA, Bonferroni's post-hoc test.

In addition to UPR inhibitors, we also evaluated proteasome inhibitors MG132, which can induce ER stress by blocking protein degradation (Paniagua Soriano et al., 2014). As illustrated in Fig. 39, ERO1L knockdown significantly enhanced the susceptibility of SW480 cells to MG132, while HCT116 cells exhibited a marginal increase in sensitivity to MG132 upon ERO1L knockdown, but not statistically significant.

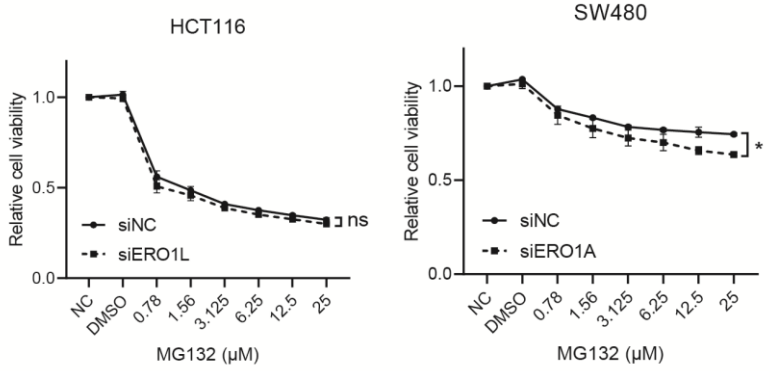

Figure 39: Combination of ERO1L inhibition with proteasome inhibitor shows enhanced anti-tumor potentials. ERO1L deficiency in SW480 cells exhibited a higher sensitivity to proteasome inhibitor while HCT116 did not. Data are shown as mean ± SD of three independent experiments. *P < 0.05, ns, not significant, calculated by two-way ANOVA, Bonferroni's post-hoc test.

Collectively, these data illustrate that ERO1L inhibition may potentiate the efficacy of ER stress-inducing therapies, providing a promising combinatorial strategy to improve anti-tumor outcomes in CRC.

4. Discussion

4.1 Study 1: Pro-inflammatory cytokines augment the cytotoxicity of CIK cells

The crosstalk between inflammation and tumor cells in the TME is highly intricate and multifaced. Inflammation within the TME is widely recognized to promote tumorigenesis by interfering with anti-tumor immunity, reshaping the TME towards a tumor-supportive niche, and acting as tumor-promoting signals for epithelial and cancer cells (Greten and Grivennikov, 2019). However, the specific role of pro-inflammatory cytokines in the TME appears to be more nuanced, as they often exhibit dual and seemingly opposing effects in tumor immunity. As demonstrated in this study, we showed that macrophage-derived pro-inflammatory cytokines reinforce the NKG2D-MICA/B axis and therefore enhance the cytotoxicity of CIK cells against MM cells. However, the pro-inflammatory cytokines concurrently upregulate PD-L1 expression on tumor cells and impair the cytotoxicity of CIK cells. Our findings reveal a novel mechanism by which pro-inflammatory cytokines enhance anti-tumor immunity and propose a combination treatment with PD-L1 blockade during macrophage reprogramming therapy.

4.1.1 Dual roles of pro-inflammatory cytokines in tumors

Pro-inflammatory cytokines, such as IL-1β, IL-6, and TNF-α, play intricate and even opposing roles in the TME. These cytokines can both promote and inhibit tumor progression, depending on factors such as tumor type, surrounding microenvironment, cytokine concentration, and expression patterns. Understanding these dual functions is vital for uncovering the immunopathology of tumor and developing targeted therapeutic strategies. The complex interplay between these cytokines and the TME underscores their importance in tumor biology.

Pro-inflammatory cytokines promote tumor progression through a variety of mechanisms that enhance tumor cell survival, proliferation, invasion, and angiogenesis (Dinarello, 2006). IL-1β is a key player in activating the NF-κB signaling pathway, which induces the expression of pro-inflammatory mediators such as IL-6 and TGF-β (Dinarello, 2006; Pei et al., 2016). These factors enhance tumor cell proliferation, survival, and resistance to

apoptosis. IL-1β also promotes the degradation of the ECM by upregulating MMPs, thereby facilitating tumor invasion and metastasis (Huang et al., 2014). Furthermore, IL-1β stimulates inflammasomes in tumor-infiltrating macrophages, promoting the secretion of cytokines like IL-6 and VEGF, which further facilitate tumor progression (Weichand et al., 2017). IL-6 is another major contributor to tumor promotion. It activates the STAT3 signaling pathway, driving the expression of genes involved in cell proliferation, angiogenesis, and immune evasion (Johnson et al., 2018). IL-6 also induces metabolic remodeling in cancer cells by promoting aerobic glycolysis and suppressing oxidative phosphorylation, providing the energy necessary for rapid tumor growth (Ando et al., 2010; Yi et al., 2019). Moreover, IL-6 contributes to immune suppression by recruiting MDSCs and promoting the differentiation of TAMs into the immunosuppressive M2 phenotype (Briukhovetska et al., 2021). TNF-α, known for its pleiotropic effects, enhances chronic inflammation in the TME by activating the NF-κB and AP-1 pathways, which upregulate the production of pro-inflammatory cytokines (Arnott et al., 2002; Hirano and Kataoka, 2013). These effects create a favorable environment for tumor growth and metastasis. TNF-α also increases vascular permeability and promotes angiogenesis by upregulating VEGF and other angiogenic factors (Hong et al., 2016; Ryuto et al., 1996). Through its ability to induce EMT, TNF-α promotes the migratory and invasive capabilities of tumor cells, further supporting metastatic spread (Chen et al., 2019; Wang et al., 2013).

Despite their tumor-promoting roles, pro-inflammatory cytokines can also exhibit anti-tumor properties under specific conditions. Members of IL-1 family, such as IL-1β, have been extensively investigated in cancer with anti-tumorigenic functions. The majority studies highlighte the ability of IL-1β to induces Th1 and Th17 immune responses, contributing to anti-tumorigenic effects (North et al., 1988). Additionally, IL-1β activates tumor-specific Th1 responses, which play a critical role in suppressing B cell myeloma and lymphoma (Haabeth et al., 2016). Through IL-1 signaling in myeloid cells, particularly neutrophils, it regulates tumor-infiltrating microbial populations, preventing local dysbiosis and excessive production of pro-tumorigenic inflammatory cytokines (Dmitrieva-Posocco et al., 2019). In the context of breast cancer, IL-1β prevents metastatic cells from establishing themselves at distant sites by maintaining these cells in a ZEB1-positive differentiation state (Castano et al., 2018). Furthermore, high expression levels of IL-1β in primary tumors are reported to associated with improved overall survival and distant

metastasis-free survival in breast cancer patients (Castano et al., 2018). While the prevailing view of IL-6 in cancer is as a major driver of malignancy, there is a second face of IL-6 that has attracted interest due to its favorable role in promoting anti-tumor immunity (Fridman et al., 2012). IL-6 enhances T cell activation, proliferation and survival in lymph nodes, generating a robust adaptive immune response (Hope et al., 1995; Leal et al., 2001). IL-6 trans-signaling helps to redirect $CD4^+$ T cells away from Tregs towards Th17 cells, alleviating immunosuppression and supporting anti-tumor $CD8^+$ T cell priming (Sharma et al., 2010). In addition, IL-6 promotes lymphocyte trafficking by increasing the expression of adhesion molecules such as ICAM-1 on high endothelial venules (HEVs), facilitating immune cell migration to lymph nodes and tumour sites (Chen et al., 2009; Chen et al., 2006). Within the TME, IL-6 trans-signaling enhances $CD8^+$ T cell infiltration by upregulating endothelial adhesion molecules, thereby improving tumor cell targeting and reducing tumor growth (Chen et al., 2004; Fisher et al., 2011). The anti-tumor effects of TNF-α have been widely reported. TNF-α exerts its anti-tumor effects primarily through the induction of apoptosis and necrosis in cancer cells. TNF-α triggers apoptotic cell death via the tumor necrosis factor receptor 1 (TNFR1), forming signaling complexes that activate caspase pathways, leading to both extrinsic and intrinsic apoptotic processes (Lin et al., 2004; Wang et al., 2008). TNF-α can also induce necrosis through the accumulation of reactive oxygen species (ROS) and receptor interacting protein kinase 1 (RIPK1)-mediated pathways (Holler et al., 2000). Additionally, TNF-α enhances anti-tumor immune responses by activating tumor-infiltrating macrophages and dendritic cells, promoting cytotoxic T lymphocyte activity and adaptive immunity (Dace et al., 2007; Larmonier et al., 2007). TNF-α also inhibits tumor angiogenesis via TNFR2-mediated nitric oxide production, which disrupts tumor blood supply (Zhao et al., 2007).

In summary, IL-1β, IL-6, and TNF-α play multifaceted roles in cancer progression and suppression, acting as both drivers of tumor growth and agents of tumor destruction. Their dual functions are highly context-dependent, influenced by factors such as cytokine concentration, cellular origin, and the nature of the TME. This complexity presents both challenges and opportunities for cancer therapy. Targeting these pro-inflammatory cytokines requires a nuanced understanding of their roles in specific tumor types and stages. Future research should focus on developing strategies to harness the anti-tumor

effects of these cytokines while mitigating their tumor-promoting activities, potentially through the combination of cytokine-based therapies and immune checkpoint inhibitors.

4.1.2 Targeting TAMs in anti-tumor treatment

TAMs are the most abundant immune cells in the TME and play a crucial role in tumor progression and immune evasion (Balkwill and Mantovani, 2001). TAMs typically represent an M2-like phenotype, characterized by the facilitation of angiogenesis, immunosuppression, and tumor survival. By contrast, macrophages with an M1-like phenotype are considered to exhibit pro-inflammatory properties with secreting pro-inflammatory cytokines, such as IL-1β, IL-6, and TNF-α, enhancing antigen presentation, and also directly killing tumor cells (Murray et al., 2014). With the growing understanding of the interaction between TAMs, TME, and tumor cells, increasing TAM-targeting investigations have been carried out for anti-tumor treatment, including inhibition of monocyte recruitment to the TME, elimination of M2-like TAMs, inhibition of conversion of M1-like anti-tumor TAMs to M2-like pro-tumor TAMs, promotion of conversion of M2-like TAMs to M1-like TAMs, and metabolic reprogramming of TAMs (Klug et al., 2013).

4.1.2.1 Inhibition the recruitment of precursor TAMs

One strategy to target TAMs involves inhibiting the recruitment of TAM precursors, such as monocytes, into tumor tissues and preventing their activation into M2-like TAMs. The colony-stimulating factor 1 (CSF-1)/CSF-1 receptor (CSF-1R) signaling axis plays a critical role in attracting monocytes to the TME and supporting M2-TAMs survival and proliferation. Blocking this pathway with CSF-1R inhibitors, such as PLX3397 and BLZ945, or antibodies, including RG7155 and IMCCS4, has demonstrated efficacy in reducing TAMs accumulation and altering the immunosuppressive environment (Edwards et al., 2018; Quail et al., 2016). Additionally, targeting the C-C motif chemokine ligand 2 (CCL-2)/ C-C motif chemokine receptor 2 (CCR-2) axis can disrupt monocyte recruitment, with inhibitors such as PF-04136309 showing promise in preclinical models (Yang et al., 2020). Despite these advancements, compensatory mechanisms within the TME, such as the upregulation of alternative chemokines, present challenges to achieving consistent clinical efficacy.

4.1.2.2 Clearance of M2-like TAMs in the TME

Direct elimination of M2-like TAMs represents a straightforward and effective immunotherapeutic approach. Methods include utilizing clodronate liposomes (Clo-LipoDOTAP), which are internalized by TAMs and release cytotoxic metabolites to inhibit mitochondrial function, leading to selective M2-like TAMs apoptosis. Experimental studies have demonstrated that this approach effectively reduces M2-like TAMs populations and improves survival in murine tumor models (Goulielmaki et al., 2018; Wang et al., 2023). Other innovative methods include the use of M2pep, a pro-apoptotic peptide with high affinity for M2-like TAMs and Trabectedin (ET743), a DNA-damaging alkaloid approved for ovarian cancer and soft tissue sarcoma treatment, which also selectively targets M2-like TAMs (Gordon et al., 2016; Tian et al., 2023). While these strategies exhibit specificity and efficacy, their associated toxic side effects remain a critical obstacle to broader clinical application.

4.1.2.3 TAM reprogramming therapy

One of the major findings about TAMs is their high plasticity, which means that the category of TAMs can be switched by external interventions. Currently, the therapeutic strategy of reprogramming TAMs involves converting their M2-like phenotype into the M1-like phenotype to restore their anti-tumor capabilities and reestablish immune surveillance (Mantovani et al., 2017). This approach exploits the plasticity of macrophages, which are highly responsive to local environmental signals, including cytokines, chemokines, and metabolic signals within the TME.

In recent years, there are significant advances in TAM-targeted reprogramming therapies. One prominent strategy involves the use of small molecule inhibitors to modulate macrophage survival and recruitment. For instance, inhibitors targeting the CSF1-CSF1R signaling axis have been shown to suppress the recruitment of M2-like TAMs while reducing their immunosuppressive effects (Zhu et al., 2014). Similarly, inhibiting phosphoinositide 3-kinase gamma (PI3K-γ) signaling to reduce TAMs immunosuppressive activity and redirect TAMs towards a pro-inflammatory phenotype by altering downstream signaling pathways (Kaneda et al., 2016). Another promising avenue is immune checkpoint modulation, with therapies such as anti-CD47 antibodies, which block the “don’t eat me” signal on tumor cells and allow TAMs to resume macrophage-

mediated phagocytosis. CD47 blockade has demonstrated efficacy in multiple preclinical tumor models, including non-small cell lung cancer and glioblastoma (Chao et al., 2012; Liu et al., 2015). Furthermore, toll-like receptor (TLR) agonists, such as imiquimod (TLR7 ligand) and IMO-2055 (TLR9 ligand), can shift TAMs phenotypes toward M1-like activation, enhancing their anti-tumor functions (Le Mercier et al., 2013; Rodell et al., 2018). Nanotechnology has also emerged as a powerful tool for TAM reprogramming, enabling the precision delivery of drugs, genetic material (e.g., siRNA or mRNA), or cytokines directly to macrophages within the TME and providing an innovative tool to achieve M2-to-M1 reprogramming while minimizing off-target effects (Lee et al., 2016; Ortega et al., 2016; Zimel et al., 2017). For example, nanoparticles loaded with IFN-γ or IL-12 have been shown to successfully repolarize TAMs toward an M1 phenotype, promoting anti-tumor immunity (Wang et al., 2017).

Additionally, the metabolic activity of TAMs is intricately linked to their functional phenotypes, making metabolic reprogramming a viable immunotherapeutic strategy. Targeting glucose metabolism with agents such as rapamycin, which inhibits mTOR signaling (Huang et al., 2016), or 2-deoxyglucose, a glycolysis inhibitor, can effectively alter the tumor-promoting phenotype of M2-TAMs (Penny et al., 2016). Similarly, interventions in lipid metabolism, such as inhibiting arachidonic acid pathways mediated by cyclooxygenase (COX) and lipoxygenase (LOX) enzymes, have shown potential in reducing M2-like TAMs activation (Wen et al., 2015; Xu et al., 2021). Additionally, targeting arginine metabolism, particularly by inhibiting arginase-1 (ARG1) with agents like L-Norvaline, can suppress M2-like TAMs proliferation (Szlosarek et al., 2013). These strategies demonstrate the potential of metabolic interventions to reprogram TAMs phenotypes and enhance anti-tumor immunity. However, the molecular mechanisms underlying these metabolic changes require further exploration, and their application in diverse tumor settings needs validation

4.1.2.4 Combing PD-L1 blockade and TAM-targeted therapy

Immunotherapy has emerged as a standard strategy for cancer treatment (Murciano-Goroff et al., 2020). ICIs, including drugs targeting CTLA-4 and PD-1/PD-L1, have been approved as potent treatment options for patients with multiple tumor types (Murciano-Goroff et al., 2020). Notably, the response rate of patients treated with single PD-1/PD-L1

immunotherapy in clinical practice is only about 30 %, which is due to the heterogeneity of PD-L1 expression in tumour tissues, as well as the cellular and molecular components in the TME (e.g., TAMs, MDSCs, cytokines, tumor cell secretions, etc.) that significantly limit the responsiveness of ICIs (Petitprez et al., 2020). In addition to the expression on tumor cells, PD-L1 is also expressed on TAMs and is involved in tumor immune escape (Hartley et al., 2018). It has been well-demonstrated that PD-L1 induces TAMs to polarize toward an M2-like phenotype, and M2-like TAMs in turn contribute to PD-1/PD-L1 blockade resistance by inducing T-cell exclusion and by inhibiting T-cell functions (Chen et al., 2021; Li et al., 2022).

Furthermore, studies have revealed that PD-L1 expression on macrophages also increases following reprogramming therapies, thereby contributing to immune evasion (Cai et al., 2021). Interestingly, in addition to TAMs, our results also indicated that pro-inflammatory cytokines secreted by M1 macrophages increase PD-L1 expression on tumor cells, suggesting that the efficacy of TAM reprogramming therapy may be compromised by the upregulation of PD-L1 on tumour cells. Therefore, we propose that including PD-L1 blockade within TAM reprogramming therapies could effectively mitigate PD-L1-mediated immunosuppression while enhancing the anti-tumor efficacy.

In addition, our findings demonstrated that the pro-inflammatory cytokines utilize the JAK/STAT3, MAPK, and PI3K/AKT signaling pathways to modulate MICA/B expression. Notably, these pathways are widely considered as tumor-favoring signals that drive tumorigenesis and progression, with aberrant hyperactivation observed in the majority of human malignancies and correlated with poor clinical outcomes (Arora et al., 2018; Thorpe et al., 2015; Yaeger and Corcoran, 2019). Consequently, the development of targeted inhibitors for these pathways has become a critical approach of anti-tumor therapies, yielding promising clinical results (Johnson et al., 2018; Thorpe et al., 2015; Yaeger and Corcoran, 2019). However, our data highlighte a paradox: inhibition of these pathways may inadvertently suppress MICA/B expression, thereby impairing innate immune responses against tumors. Regarding PD-L1, these pathways have been revealed to contribute to augment PD-L1 in tumors (Jiang et al., 2013; Song et al., 2018; Yamaguchi et al., 2022). In this context, inhibitors targeting these pathways may also act as PD-L1 suppressants. Nevertheless, we recommend prioritizing the use of PD-L1 antibodies over signaling inhibitors or cytokine-targeted therapies in the combination

treatment, as the latter could downregulate MICA/B, potentially compromising anti-tumor immunity.

4.1.2.5 Challenges and prospects for TAM-targeted therapy

TAM-targeted therapies face several significant challenges. First, TAMs are highly heterogeneous, with diverse phenotypes influenced by tumor type, stage, and local microenvironmental factors. This heterogeneity complicates the identification of universal targets and requires context-specific strategies. Second, the lack of specificity of many therapeutic agents can lead to off-target effects, potentially disrupting immune homeostasis in healthy tissues. Third, the TME is highly dynamic and immunosuppressive, with multiple redundant pathways that can counteract the effects of TAM reprogramming approaches. Lastly, tumors often develop resistance mechanisms, including the recruitment of alternative immunosuppressive cells or the upregulation of compensatory signaling pathways.

To address these challenges, future research must prioritize the identification of TAMs subpopulations using advanced tools such as single-cell RNA sequencing and multiplex imaging, enabling precise therapeutic targeting (Papalexi and Satija, 2018). Combination therapies integrating TAM reprogramming with immune checkpoint inhibitors, radiotherapy, or chemotherapy are likely to overcome the limitations of monotherapies and provide synergistic benefits (Kapp et al., 2019; Wu et al., 2020). Additionally, the development of predictive biomarkers will be crucial for selecting patients who are most likely to respond to TAM-targeted therapies and for monitoring therapeutic efficacy. Advances in synthetic biology and nanotechnology also show great potential for designing TME-specific delivery systems that minimize off-target effects and improve drug stability and efficacy. (Andon et al., 2017).

In summary, TAM-targeting therapy offers a compelling strategy to disrupt the immunosuppressive TME and restore anti-tumor immunity. While significant progress has been made, overcoming the current challenges will require interdisciplinary collaboration and the integration of emerging technologies. By addressing these barriers, TAM-targeted therapies could become a cornerstone of next-generation cancer immunotherapy.

4.1.3 Limitations

In this study, we utilized only M1 macrophages under in vitro conditions, further in-depth in vivo and in vitro studies are required to validate these observations by using macrophage reprogramming approaches, such as small molecules drugs or gene editing techniques.

4.2 Study 2: Inhibition of ERO1L mediates autophagy and apoptosis via ER stress

The ER plays a pivotal role in protein folding, modification, lipid synthesis, and calcium homeostasis (Schwarz and Blower, 2016). In tumor cells, the high metabolic demands and adverse microenvironment often disrupt ER homeostasis, resulting in the accumulation of misfolded or unfolded proteins, a condition referred to as ER stress (Chen and Cubillos-Ruiz, 2021). To cope with this stress, cells activate the UPR, a conserved signaling network (Schroder, 2008). This system balances adaptive and cell death processes, enabling tumor cells to survive under hostile conditions, or inducing cell death when ER stress is excessive. Given the crucial role of ERO1L in protein folding, understanding the crosstalk between ERO1L and ER stress, as well as their involvement in tumor promotion, is critical for exploring potential therapeutic strategies.

4.2.1 ER stress in tumors: Formation and functional roles

The ER is a central mediator in various cellular processes, particularly in protein folding. It is the primary site for the synthesis and proper folding of secretory and membrane proteins, which undergo post-translational modifications such as glycosylation and disulfide bond formation to attain their functional conformations (Schwarz and Blower, 2016). Molecular chaperones, such as BiP/GRP78, and enzymes like PDI assist in this process (Inaba et al., 2010; Schroder, 2008). The ER also ensures protein quality control by identifying misfolded proteins and targeting them for degradation through the ERAD pathway, thereby preventing the accumulation of defective proteins (Kopito, 1997).

ER stress arises when the the capacity of ER to fold, modify, and process proteins is overwhelmed, leading to the accumulation of misfolded or unfolded proteins (Chen and

Cubillos-Ruiz, 2021). In tumor cells, several factors inherent to their rapid growth and hostile microenvironment contribute to ER stress. The heightened protein synthesis required for uncontrolled proliferation increases the burden on the ER's folding machinery. Additionally, hypoxia, a hallmark of the TME, disrupts oxidative protein folding, while glucose deprivation impairs glycosylation, a critical post-translational modification (Keith and Simon, 2007; May et al., 2005). Oxidative stress, commonly observed in tumor cells, exacerbates protein misfolding by damaging ER-resident proteins (Zhang et al., 2017). Moreover, dysregulated calcium homeostasis, another characteristic of cancer cells, destabilizes ER function, further promoting protein misfolding and ER stress (Krebs et al., 2015; Zheng et al., 2023).

The advancement of tumors is invariably influenced by a spectrum of factors intrinsic to the TME, including hypoxia, pH fluctuations, reactive oxygen species (ROS), and a variety of cellular metabolites. In this milieu, the ER stress is a key response generated by the ER in response to external stimuli. In response to ER stress, tumor cells activate the UPR, a conserved signaling pathway aimed at restoring ER homeostasis. Through adaptive mechanisms, the UPR reduces protein synthesis, enhances the expression of molecular chaperones, and facilitates the degradation of misfolded proteins (Schroder, 2008). These adaptations allow tumor cells to survive under adverse conditions, supporting their growth and metastasis. Studies have shown that moderate ER stress can promote tumor progression by multiple pathways. ER stress is reported to promote tumor progression by facilitating tumor proliferation, invasion, cellular metabolism, chemoresistance, angiogenesis, metastasis, and stemness maintenance, as well as reprogramming the function of immune cells in the TME (Cubillos-Ruiz et al., 2017; Liang et al., 2021; Urra et al., 2016).

However, the duration and intensity of ER stress play a key role in determining its ultimate function. Prolonged or severe ER stress can lead to tumor cell death through several mechanisms (Mohamed et al., 2017). These include the dysregulation of the UPR, which shifts from a protective to a pro-apoptotic state by upregulating factors like CHOP and inhibiting anti-apoptotic proteins (Galehdar et al., 2010; Puthalakath et al., 2007). Excessive ER stress also disrupts calcium homeostasis, leading to mitochondrial overload and activation of the intrinsic apoptosis pathway through cytochrome C release and Bcl-2 family proteins (Bahar et al., 2016; Pinton et al., 2008). Excessive ER stress may induce

necrotic cell death due to ER swelling and structural damage, as well as autophagic cell death via overactivation of autophagy-related genes like Beclin-1 through PERK and IRE1 pathways (Bhardwaj et al., 2020; Rashid et al., 2015). Additionally, ER stress can promote immunogenic cell death (ICD) by exposing molecules like calreticulin and releasing HMGB1, triggering anti-tumor immune responses (Feng et al., 2023; Mandula et al., 2022). These mechanisms make ER stress both a natural tumor-suppressing process and a therapeutic target for cancer treatment.

4.2.2 Induction of lethal ER stress contributes to anti-tumor treatment

Given the dual role of ER stress in tumor promotion, enhancing the duration and intensity of ER stress in tumors is a potential anti-tumor strategy. Conceptually, ER stress can be targeted pharmacologically in two ways: either by directly affecting the accumulation of misfolded proteins within the ER, or else by modulating UPR signalling by ER stress sensors or the enzymes that mediate their downstream effects.

Chaperones in the ER are essential for ensuring proper protein folding, assembly, and modification, preventing misfolding and aggregation (Hendershot et al., 2024). Key chaperones like GRP78 and GRP94 also support ERAD to maintain protein homeostasis (Cesaratto et al., 2019; Eletto et al., 2010). Tumor cells, which experience high levels of ER stress due to rapid growth and metabolic demands, heavily rely on these chaperones for survival. Targeting chemical chaperones disrupts this balance by inhibiting their function to impair protein folding and induce uncontrolled ER stress, leading to cell death (Luo and Lee, 2013). GRP78 is a central regulator of ER function due to its roles in protein folding and assembly, targeting misfolded protein for degradation, and controlling the activation of trans-membrane ER stress sensors. Furthermore, due to its anti-apoptotic property, the induction of GRP78 represents an important pro-survival component of the UPR (Reddy et al., 2003; Zhou et al., 2011). In recent years, a variety of anti-tumour chemistries targeting GRP78 have been reported (Liu et al., 2013; Rauschert et al., 2008). HA15, a thiazole benzenesulfonamide compound targeting GRP78 and inhibiting its ATPase activity (Cerezo et al., 2016), has been reported to play an anti-tumor role in melanoma, breast, pancreatic and adrenocortical carcinoma, even overcoming drug resistance (Cerezo et al., 2016; Ruggiero et al., 2018). Epigallocatechin gallate (EGCG) is shown to bind GRP78 and inhibits its folding function while activating the ER stress

pathway to induce tumour cell death (Ermakova et al., 2006). In addition, small molecular inhibitor OSU-03012 is reported to target GRP78 and induce ER stress and cell death by regulating the AKT pathway (Booth et al., 2014). Furthermore, there are also inhibitors targeting other chaperones, such as HSP90, HSP70, and GRP94, showing promising outcomes (Crowley et al., 2017; Duerfeldt et al., 2012; Park et al., 2014).

Apart from chaperones, targeting the primary sensors of the UPR is also an approach. Upon recognizing the accumulation of unfolded or misfolded proteins in the ER, the ER stress sensors PERK, ATF4, and IRE1α are activated and attampt to restore the ER protein homeostasis by attenuating ER protein synthesis and by enhancing chaperones expression, ERAD components and expanding the amount of ER. Therefore, targeting UPR to disrupt this protective mechanism of ER stress in tumor cells is a effective strategy. The specific PERK inhibitor GSK2656157 can limit cancer growth via impaired angiogenesis and amino acid metabolism (Atkins et al., 2013). HC4, a perk-specific inhibitor, is reported to block metastatic progression by limiting integrated stress response-dependent survival of quiescent cancer cells (Calvo et al., 2023). IRE1α inhibition can attenuate the protective UPR and induce ER stress-related apoptosis by blocking the production of XBP1s. IRE1α inhibitors 4μ8C, MKC-3946, and STF-083010, show anti-cancer activity in myeloma and breast cancer (Gao et al., 2020; Li et al., 2017; Mimura et al., 2012; Raymundo et al., 2020). Ceapins, a class of isoxazole ring-containing pyrazole amides, that selectively block ATF6α signalling in response to ER stress. Inhibition of ATF6 with specific inhibitors has been shown to limit cancer promotion in a variety of tumors (Benedetti et al., 2022; Zhao et al., 2022).

Lethal ER stress in tumor cells can be induced by inhibiting the degradation of proteins. ERAD is the major pathway for the degradation of unfolded proteins in the ER. Unfolded proteins in the ER lumen are recognized by chaperones and then retrotransported to the cytosol where they are degraded by the ubiquitin proteasome system (UPS) (McCracken and Brodsky, 1996). Impressive results have been noticed anti-tumor treatment by inhibiting UPS-induced excessive ER stress. The most successful examples are the use of proteasome inhibitors such as bortezomib, carfilzomib and ixazomib (Manasanch and Orlowski, 2017). Bortezomib is a classic proteasome inhibitor that is widely used in the clinic and has significantly improved remission rates and patient survival (Scott et al., 2016). Current studies suggest that Bortezomib triggers ER stress by blocking

proteasomal degradation and activates the PERK-eIF2α-ATF4-CHOP pathway in the UPR, ultimately inducing apoptosis in tumour cells (Fels et al., 2008; Nawrocki et al., 2005). Carfilzomib and Ixazomib are second-generation inhibitors that are more potent but have fewer side effects (Deng et al., 2020; Moreau et al., 2021). Proteasome inhibitors are currently used in tumor cells with high proliferation rates and high protein synthesis and secretion, particularly in myeloma. Inhibiting ERAD at the stage of recognition and transport of unfolded proteins is an alternative approach. Eeyarestain I (EerI) targets the retrotransport channels, such as Sec61, during ERAD, preventing the retrotransport of unfolded or misfolded proteins from the ER lumen into the cytoplasm for degradation (Cross et al., 2009). Kifunensine inhibits α-mannosidase I in the ER, blocking glycan chain pruning of misfolded proteins and interfering with their recognition by ERAD (Avezov et al., 2008). The accumulation of ungraded proteins activates excessive ER stress and cell death.

For more efficient induction of ER stress, two or more ER stress-inducing agents can be used in combination. This study preliminarily demonstrated the potential of combination therapy. Given the role of ERO1L in modulating ER stress, combining ERO1L inhibition with ER stress-inducing agents, such as UPR-targeting inhibitors and proteasome inhibitors, could induce lethal ER stress more effectively in tumor cells, leading to more enhanced outcomes. Actually, the synergistic effect of this dual inhibition has also been confirmed by other studies. ISRIB, a small molecule that inhibits the phosphorylation of eIF2α and removes its inhibition on global protein translation, was found to synergistically interact with the genetic deficiency of ERO1L and to impair breast tumor growth and spread (Varone et al., 2022). However, the in vivo availability and utility of the dual inhibition strategy remain unclear, given the current absence of clinically available ERO1L inhibitors. Therefore, the development of highly specific and efficient ERO1L-targeting drugs is a critical objective. Meanwhile, exploring broader combination approaches that integrate ERO1L inhibition with other anti-tumor strategies, such as immunotherapy or adoptive cellular immunotherapy, may yield promising results.

4.2.3 The crosstalk between ERO1L and ER stress

As a critical mediator of oxidative protein folding, ERO1L plays a pivotal role in preventing the accumulation of misfolded and unfolded proteins in the ER. Our results revealed that

ER stress upregulated ERO1L expression in CRC, aligning with previous findings. For instance, Marciniak et al. and Song et al. reported that ER stress reinforced ERO1L expression via the CHOP pathway, though their observations were based on non-tumor settings (Marciniak et al., 2004; Song et al., 2008). Notably, we demonstrated for the first time that ERO1L inhibition also induced ER stress in CRC, highlighting a negative feedback loop between ER stress and ERO1L. These insights suggest that tumor cells may alleviate ER stress by upregulating ERO1L to enhance protein folding capacity.

4.2.4 Targeting ERO1L in tumor treatment

The expression pattern of ERO1L and its tumor-supportive role highlight its potential as an attractive target for CRC treatment. Our recent study explored the therapeutic benefits of targeting ERO1L in anti-tumor therapy (Chen et al., 2024). However, few pharmacological inhibitors are available for further validation and none are approved for clinical use. The challenge predominately arises from the highly conserved structure of the FAD cofactor-binding domain across enzymes, suggesting that inhibitors not only recognize the FAD domain in ERO1L, but also other FAD-containing enzymes, such as lysine specific demethylase 1 (LSD-1), monoamine oxidases A and B (MAO-A and MAO-B) (Hayes et al., 2019). To date, several compounds have been reported to target ERO1L in mammals. EN460 and QM295 stand as the first two identified ERO1L inhibitors through a biochemical high-throughput screen and have been shown to interact with reduced ERO1L and prevent re-oxidation (Hayes et al., 2019). PB-EN-10 is an azide derivative of EN460 and shows similar effects (Hayes et al., 2019). Erodoxin, a dinitrobromobenzene compound, acts as a selective inhibitor of yeast ERO1, but has somewhat weaker activity against mouse ERO1L (Blais et al., 2010). However, these inhibitors lack selectivity for ERO1L, and indeed, they inhibit other FAD-containing enzymes as well (Hayes et al., 2019). Recently, Brennan et al. reported a novel ERO1L inhibitor named T151742, a sulfuretin derivative, showing heightened activity (IC_{50}: 8.27 μM) compared to EN460 (IC_{50}: 16.46 μM) and isozyme specificity for ERO1L as compared to that for ERO1β and no detectable binding to the FAD-containing enzyme LSD-1 (Johnson et al., 2022). However, further investigations are warranted to determine its in vivo efficacy and safety.

Given that PDI directly interacts with ERO1L, targeting PDI would also be a viable approach to block oxidative protein folding. In fact, PDI has also been shown to be up-

regulated in a variety of cancer types and exhibit pro-tumoral roles (Rahman et al., 2022). Various chemical inhibitors of PDI have been identified and some of them showed potential anti-tumor effect (Powell and Foster, 2021). However, the presence of over 20 structurally similar PDI homologues in eukaryotes limits the development of specific inhibitors. Considering the inextricable interplay between ERO1L and PDI, a more effective and specific strategy involves developing inhibitors that disrupt the interaction between ERO1L and PDI. Recently, Zhang et al. reported that valine (Val) 101, a hydrophobic residue in the active site-containing loop of ERO1L, is crucial for the recognition of PDI catalytic domain (Zhang et al., 2019). Mutation of Val101 weaken the activity of ERO1L in oxidative protein folding, and more importantly, impaired tumor progression. This finding not only provides a reliable target site for inhibitor development, but also a paradigm for targeting the ERO1L-PDI interface.

The highly conserved structure of the FAD-binding domain limits the development of ERO1L inhibitors. In recent years, proteolysis-targeting chimera (PROTAC) has been emerged as a novel technology for targeted protein degradation (Bekes et al., 2022). PROTAC is a bifunctional molecule consists of three domains: a protein of interest (POI) ligand, a E3 ubiquitin ligase ligand, and a linker which covalently interconnects with these two ligands. Upon binding to the target protein, the PROTAC molecule can recruit E3 ubiquitin ligase for protein ubiquitination, which is subjected to proteasome-mediated degradation (Sakamoto et al., 2001). Therefore, with respect to ERO1L, the development of PROTAC molecules does not require targeting the active center of ERO1L, but only the ability to specifically recognize ERO1L protein, which would greatly help to avoid off-target effects of the current ERO1L inhibitors. Notably, however, there are also some challenges for PROTAC to be a successful drug development approach (Zeng et al., 2021).

4.2.5 Apoptosis and autophagy

Autophagy is a conserved mechanism where cells degrade and recycle damaged organelles, proteins, and other components via autophagosomes and lysosomes, particularly during stress or nutrient deprivation. The process involves key steps, including initiation by the unc-51-like kinase 1 (ULK1) complex, autophagosome formation, fusion with lysosomes, and degradation of cargo (Glick et al., 2010). Apoptosis, on the other hand, is a form of programmed cell death aimed at eliminating damaged or unwanted cells

without triggering inflammation. It is mediated by two primary pathways: the extrinsic pathway, activated by death receptors and caspase-8, and the intrinsic pathway, involving mitochondrial cytochrome c release and caspase-9 activation. These pathways converge on effector caspases, leading to cell dismantling (Taylor et al., 2008). As the two main types of programmed cell death in tumors, there has been a demonstrated complex interplay between apoptosis and autophagy (Wang et al., 2021). Generally, apoptosis and autophagy are thought to have an antagonistic relationship. In tumor settings, autophagy can block apoptosis by the autophagic clearance of apoptosis-related caspases, while the activation of caspases can also cleave several essential autophagic proteins, such as Beclin-1, autophagy related 3 (ATG3), and ATG5, thereby limiting autophagy (Das et al., 2021). However, in some cases, autophagy has also been reported to activate apoptosis (Song et al., 2017). Consistent with previous studies, our results demonstrated that the deletion of ERO1L induced apoptosis (Young et al., 2012; Yousefi et al., 2006). We further revealed that ERO1L inhibition also induced autophagy, and these activated apoptosis and autophagy were mediated by ER stress. However, the crosstalk between them is not yet clear. Further studies focusing on the interplay between apoptosis and autophagy will help to deepen our understanding of the role of ERO1L in regulating ER stress adaptation mechanisms in tumor cells.

4.2.6 The ERK1/2 signaling pathway in tumors

The ERK1/2 pathway is activated in the majority of tumors and is well known for its role in tumor initiation and progression (Ullah et al., 2022). The ERK1/2 pathway is a key component of the MAPK cascade, plays a critical role in cell proliferation, differentiation, survival, and migration (Meloche and Pouyssegur, 2007). Aberrant activation of ERK1/2 is frequently observed in various cancers due to mutations in upstream regulators, such as RAS, RAF, and MEK (Balmanno and Cook, 2009). This hyperactivation drives oncogenic processes, including uncontrolled cell growth, evasion of apoptosis, and metastasis, making the ERK1/2 pathway a crucial target for anti-cancer therapies. Current ERK-targeting therapeutic strategies focus on targeting components of the pathway, including RAF inhibitors (e.g., vemurafenib for BRAF-mutated cancers), MEK inhibitors (e.g., trametinib), and ERK inhibitors (e.g., ulixertinib) (Kidger et al., 2018; Samatar and Poulikakos, 2014). Despite initial success, resistance often develops due to pathway

reactivation, alternative signaling compensation, or secondary mutations. Recent advancements aim to overcome resistance by combining ERK pathway inhibitors with agents targeting other oncogenic pathways (e.g., PI3K/AKT, immune checkpoints) or utilizing novel dual inhibitors (Bahar et al., 2023; Morante et al., 2022). Additionally, efforts are underway to develop inhibitors with improved selectivity and reduced toxicity. While challenges remain, continued research into the ERK1/2 signalling pathway is expected to improve therapeutic efficacy and expand treatment options for cancer.

In this study, we found that ERK1/2 was involved in ERO1L knockdown-induced apoptosis and autophagy, suggesting that overexpressed ERO1L in CRC may promote tumor progression by activating ERK1/2. To further confirm the involvement of ERK1/2, we performed rescue experiments using ACA-28, the only reported ERK1/2 agonist with anti-tumor activity by hyperactivating ERK1/2. At a low concentration, ACA-28 reversed both the apoptosis and autophagy induced by ERO1L knockdown, indicating the involvement of ERK1/2 in these processes. In contrast, a high concentration of ACA-28 significantly enhanced apoptosis and autophagy, demonstrating its anti-tumor activity through ERK1/2 hyperactivation. While the involvement of the AKT pathway was excluded, treatment with AKT inhibitor markedly enhanced apoptosis, indicating a potential synergistic effect when combining ERO1L inhibition with AKT pathway blockade.

4.2.7 Limitations

There are some limitations for this study. Although the involvement of ERK1/2 has been confirmed, the interaction between ERO1L and ERK1/2 remains unclear. Further investigations are warranted to determine whether ERO1L directly interacts with ERK1/2 or mediates its effects through other intermediaries. In addition, the mechanistic interplay between ERO1L and ER stress has not been fully elucidated. Finally, additional in vivo studies are required to validate the role of ERO1L in CRC.

5. Abstract

Background: Inflammation and ER stress are two prominent hallmarks of tumors, both exhibiting distinct dual roles in tumor promotion. The duration and intensity of inflammation and ER stress can drive divergent, or even opposite outcomes in tumor development. However, evolving tumors usually adapt and escape from inflammation and ER stress by forming delicate balances between them. Disrupting the balances by modulating inflammation and ER stress can impair this adapbility and induce tumor cell death.

Purposes: This dissertation aims to illustrate the potential and mechanisms of regulating inflammation and ER stress in tumor treatment.

Methods: We confirmed the derivation of pro-inflammatory cytokines from M1 macrophages, and illustrated the roles of pro-inflammatory cytokines in enhancing the cytotoxicity of CIK cells against MM and its mechanisms using flow cytometry. For the investigations on ER stress, we demonstrated the expression profile of ERO1L and a bidirection regulatory loop between ERO1L and ER stress in CRC by RT-qPCR and western-blotting. Furthermore, We elucidated the regulatory role of ERO1L on autophagy and apoptosis in tumour cells by flow cytometry, and resolved the responsible signalling pathways.

Results: We found that M1 macrophages produced high levels of pro-inflammatory cytokines, including TNF-α, IL-1β, and IL-6. Pro-inflammatory cytokines enhanced the cytotoxicity of CIK cells towards MM cells by augmenting the expression of killing-dependent MICA/B. For ER stress, we revealed that ERO1L was overexpressed in CRC and found a negative regulatory feedback between ER stress and ERO1L. Inhibition of ERO1L induced apoptosis and autophagy via the induction of ER stress and the ERK1/2 pathway. In addtion, combining ERO1L inhibition with other ER stress-inducing agents showed a synergistic effect in CRC treatment.

Conclusions: M1 macrophage-derived pro-inflammatory cytokines reinforce the cytotoxicity of CIK cells agianst MM cells by up-regulating the MICA/B-NKG2D axis. Inhibition of ERO1L mediates apoptosis and autophagy via the induction of ER stress in CRC.

6. List of figures

7. List of tables

8. References

Aguilar-Cazares D, Chavez-Dominguez R, Carlos-Reyes A, Lopez-Camarillo C, Hernadez de la Cruz ON, Lopez-Gonzalez JS. Contribution of Angiogenesis to Inflammation and Cancer. Front Oncol 2019; 9: 1399

Ando M, Uehara I, Kogure K, Asano Y, Nakajima W, Abe Y, Kawauchi K, Tanaka N. Interleukin 6 enhances glycolysis through expression of the glycolytic enzymes hexokinase 2 and 6-phosphofructo-2-kinase/fructose-2,6-bisphosphatase-3. J Nippon Med Sch 2010; 77(2): 97-105

Andon FT, Digifico E, Maeda A, Erreni M, Mantovani A, Alonso MJ, Allavena P. Targeting tumor associated macrophages: The new challenge for nanomedicine. Semin Immunol 2017; 34: 103-113

Araki K,Inaba K. Structure, mechanism, and evolution of Ero1 family enzymes. Antioxid Redox Signal 2012; 16(8): 790-799

Arnott CH, Scott KA, Moore RJ, Hewer A, Phillips DH, Parker P, Balkwill FR, Owens DM. Tumour necrosis factor-alpha mediates tumour promotion via a PKC alpha- and AP-1-dependent pathway. Oncogene 2002; 21(31): 4728-4738

Arora L, Kumar AP, Arfuso F, Chng WJ, Sethi G. The Role of Signal Transducer and Activator of Transcription 3 (STAT3) and Its Targeted Inhibition in Hematological Malignancies. Cancers (Basel) 2018; 10(9): 327

Atkins C, Liu Q, Minthorn E, Zhang SY, Figueroa DJ, Moss K, Stanley TB, Sanders B, Goetz A, Gaul N, Choudhry AE, Alsaid H, Jucker BM, Axten JM, Kumar R. Characterization of a novel PERK kinase inhibitor with antitumor and antiangiogenic activity. Cancer Res 2013; 73(6): 1993-2002

Avezov E, Frenkel Z, Ehrlich M, Herscovics A, Lederkremer GZ. Endoplasmic reticulum (ER) mannosidase I is compartmentalized and required for N-glycan trimming to Man5-6GlcNAc2 in glycoprotein ER-associated degradation. Mol Biol Cell 2008; 19(1): 216-225

Bahar E, Kim H, Yoon H. ER Stress-Mediated Signaling: Action Potential and Ca(2+) as Key Players. Int J Mol Sci 2016; 17(9): 1558

Bahar ME, Kim HJ, Kim DR. Targeting the RAS/RAF/MAPK pathway for cancer therapy: from mechanism to clinical studies. Signal Transduct Target Ther 2023; 8(1): 455

Balkwill F,Mantovani A. Inflammation and cancer: back to Virchow? Lancet 2001; 357(9255): 539-545

Balmanno K,Cook SJ. Tumour cell survival signalling by the ERK1/2 pathway. Cell Death Differ 2009; 16(3): 368-377

Bekes M, Langley DR, Crews CM. PROTAC targeted protein degraders: the past is prologue. Nat Rev Drug Discov 2022; 21(3): 181-200

Benedetti R, Romeo MA, Arena A, Gilardini Montani MS, Di Renzo L, D'Orazi G, Cirone M. ATF6 prevents DNA damage and cell death in colon cancer cells undergoing ER stress. Cell Death Discov 2022; 8(1): 295

Bhardwaj M, Leli NM, Koumenis C, Amaravadi RK. Regulation of autophagy by canonical and non-canonical ER stress responses. Semin Cancer Biol 2020; 66: 116-128

Bied M, Ho WW, Ginhoux F, Bleriot C. Roles of macrophages in tumor development: a spatiotemporal perspective. Cell Mol Immunol 2023; 20(9): 983-992

Blais JD, Chin KT, Zito E, Zhang Y, Heldman N, Harding HP, Fass D, Thorpe C, Ron D. A small molecule inhibitor of endoplasmic reticulum oxidation 1 (ERO1) with selectively reversible thiol reactivity. J Biol Chem 2010; 285(27): 20993-21003

Booth L, Roberts JL, Cruickshanks N, Grant S, Poklepovic A, Dent P. Regulation of OSU-03012 toxicity by ER stress proteins and ER stress-inducing drugs. Mol Cancer Ther 2014; 13(10): 2384-2398

Bozyk A, Wojas-Krawczyk K, Krawczyk P, Milanowski J. Tumor Microenvironment-A Short Review of Cellular and Interaction Diversity. Biology (Basel) 2022; 11(6): 929

Bray F, Laversanne M, Sung H, Ferlay J, Siegel RL, Soerjomataram I, Jemal A. Global cancer statistics 2022: GLOBOCAN estimates of incidence and mortality worldwide for 36 cancers in 185 countries. CA Cancer J Clin 2024; 74(3): 229-263

Briukhovetska D, Dorr J, Endres S, Libby P, Dinarello CA, Kobold S. Interleukins in cancer: from biology to therapy. Nat Rev Cancer 2021; 21(8): 481-499

Bulleid NJ. Disulfide bond formation in the mammalian endoplasmic reticulum. Cold Spring Harb Perspect Biol 2012; 4(11): a013219

Cai H, Zhang Y, Wang J, Gu J. Defects in Macrophage Reprogramming in Cancer Therapy: The Negative Impact of PD-L1/PD-1. Front Immunol 2021; 12: 690869

Calvo V, Zheng W, Adam-Artigues A, Staschke KA, Huang X, Cheung JF, Nobre AR, Fujisawa S, Liu D, Fumagalli M, Surguladze D, Stokes ME, Nowacek A, Mulvihill M, Farias EF, Aguirre-Ghiso JA. A PERK-Specific Inhibitor Blocks Metastatic Progression by Limiting Integrated Stress Response-Dependent Survival of Quiescent Cancer Cells. Clin Cancer Res 2023; 29(24): 5155-5172

Cappel C, Huenecke S, Suemmerer A, Erben S, Rettinger E, Pfirrmann V, Heinze A, Zimmermann O, Klingebiel T, Ullrich E, Bader P, Bremm M. Cytotoxic potential of IL-15-activated cytokine-induced killer cells against human neuroblastoma cells. Pediatr Blood Cancer 2016; 63(12): 2230-2239

Castano Z, San Juan BP, Spiegel A, Pant A, DeCristo MJ, Laszewski T, Ubellacker JM, Janssen SR, Dongre A, Reinhardt F, Henderson A, Del Rio AG, Gifford AM, Herbert ZT, Hutchinson JN, Weinberg RA, Chaffer CL, McAllister SS. IL-1beta inflammatory response driven by primary breast cancer prevents metastasis-initiating cell colonization. Nat Cell Biol 2018; 20(9): 1084-1097

Castro F, Cardoso AP, Goncalves RM, Serre K, Oliveira MJ. Interferon-Gamma at the Crossroads of Tumor Immune Surveillance or Evasion. Front Immunol 2018; 9: 847

Cerezo M, Lehraiki A, Millet A, Rouaud F, Plaisant M, Jaune E, Botton T, Ronco C, Abbe P, Amdouni H, Passeron T, Hofman V, Mograbi B, Dabert-Gay AS, Debayle D, Alcor D, Rabhi N, Annicotte JS, Heliot L, Gonzalez-Pisfil M, Robert C, Morera S, Vigouroux A, Gual P, Ali MMU, Bertolotto C, Hofman P, Ballotti R, Benhida R, Rocchi S. Compounds Triggering ER Stress Exert Anti-Melanoma Effects and Overcome BRAF Inhibitor Resistance. Cancer Cell 2016; 30(1): 183

Cesaratto F, Sasset L, Myers MP, Re A, Petris G, Burrone OR. BiP/GRP78 Mediates ERAD Targeting of Proteins Produced by Membrane-Bound Ribosomes Stalled at the STOP-Codon. J Mol Biol 2019; 431(2): 123-141

Chang TK, Lawrence DA, Lu M, Tan J, Harnoss JM, Marsters SA, Liu P, Sandoval W, Martin SE, Ashkenazi A. Coordination between Two Branches of the Unfolded Protein Response Determines Apoptotic Cell Fate. Mol Cell 2018; 71(4): 629-636

Chao MP, Weissman IL, Majeti R. The CD47-SIRPalpha pathway in cancer immune evasion and potential therapeutic implications. Curr Opin Immunol 2012; 24(2): 225-232

Chen P, Sharma A, Weiher H, Schmidt-Wolf IGH. Biological mechanisms and clinical significance of endoplasmic reticulum oxidoreductase 1 alpha (ERO1alpha) in human cancer. J Exp Clin Cancer Res 2024; 43(1): 71

Chen Q, Appenheimer MM, Muhitch JB, Fisher DT, Clancy KA, Miecznikowski JC, Wang WC, Evans SS. Thermal facilitation of lymphocyte trafficking involves temporal induction of intravascular ICAM-1. Microcirculation 2009; 16(2): 143-158

Chen Q, Fisher DT, Clancy KA, Gauguet JM, Wang WC, Unger E, Rose-John S, von Andrian UH, Baumann H, Evans SS. Fever-range thermal stress promotes lymphocyte trafficking across high endothelial venules via an interleukin 6 trans-signaling mechanism. Nat Immunol 2006; 7(12): 1299-1308

Chen Q, Wang WC, Bruce R, Li H, Schleider DM, Mulbury MJ, Bain MD, Wallace PK, Baumann H, Evans SS. Central role of IL-6 receptor signal-transducing chain gp130 in activation of L-selectin adhesion by fever-range thermal stress. Immunity 2004; 20(1): 59-70

Chen X,Cubillos-Ruiz JR. Endoplasmic reticulum stress signals in the tumour and its microenvironment. Nat Rev Cancer 2021; 21(2): 71-88

Chen X, Gao A, Zhang F, Yang Z, Wang S, Fang Y, Li J, Wang J, Shi W, Wang L, Zheng Y, Sun Y. ILT4 inhibition prevents TAM- and dysfunctional T cell-mediated immunosuppression and enhances the efficacy of anti-PD-L1 therapy in NSCLC with EGFR activation. Theranostics 2021; 11(7): 3392-3416

Chen XW,Zhou SF. Inflammation, cytokines, the IL-17/IL-6/STAT3/NF-kappaB axis, and tumorigenesis. Drug Des Devel Ther 2015; 9: 2941-2946

Chen Y, Wen H, Zhou C, Su Q, Lin Y, Xie Y, Huang Y, Qiu Q, Lin J, Huang X, Tan W, Min C, Wang C. TNF-alpha derived from M2 tumor-associated macrophages promotes epithelial-mesenchymal transition and cancer stemness through the Wnt/beta-catenin pathway in SMMC-7721 hepatocellular carcinoma cells. Exp Cell Res 2019;378(1): 41-50

Chevrier S, Levine JH, Zanotelli VRT, Silina K, Schulz D, Bacac M, Ries CH, Ailles L, Jewett MAS, Moch H, van den Broek M, Beisel C, Stadler MB, Gedye C, Reis B, Pe'er D, Bodenmiller B. An Immune Atlas of Clear Cell Renal Cell Carcinoma. Cell 2017; 169(4): 736-749

Cornelius J, Cavarretta I, Pozzi E, Lavorgna G, Locatelli I, Tempio T, Montorsi F, Mattei A, Sitia R, Salonia A, Anelli T. Endoplasmic reticulum oxidoreductase 1 alpha modulates prostate cancer hallmarks. Transl Androl Urol 2021; 10(3): 1110-1120

Cowan AJ, Green DJ, Kwok M, Lee S, Coffey DG, Holmberg LA, Tuazon S, Gopal AK, Libby EN. Diagnosis and Management of Multiple Myeloma: A Review. JAMA 2022; 327(5): 464-477

Cross BC, McKibbin C, Callan AC, Roboti P, Piacenti M, Rabu C, Wilson CM, Whitehead R, Flitsch SL, Pool MR, High S, Swanton E. Eeyarestatin I inhibits Sec61-mediated protein translocation at the endoplasmic reticulum. J Cell Sci 2009; 122(Pt 23): 4393-4400

Crowley VM, Huard DJE, Lieberman RL, Blagg BSJ. Second Generation Grp94-Selective Inhibitors Provide Opportunities for the Inhibition of Metastatic Cancer. Chemistry 2017; 23(62): 15775-15782

Cubillos-Ruiz JR, Bettigole SE, Glimcher LH. Tumorigenic and Immunosuppressive Effects of Endoplasmic Reticulum Stress in Cancer. Cell 2017; 168(4): 692-706

Dace DS, Chen PW, Niederkorn JY. CD8+ T cells circumvent immune privilege in the eye and mediate intraocular tumor rejection by a TNF-alpha-dependent mechanism. J Immunol 2007; 178(10): 6115-6122

Das S, Shukla N, Singh SS, Kushwaha S, Shrivastava R. Mechanism of interaction between autophagy and apoptosis in cancer. Apoptosis 2021; 26(9-10): 512-533

Dekker E, Tanis PJ, Vleugels JLA, Kasi PM, Wallace MB. Colorectal cancer. Lancet 2019; 394(10207): 1467-1480

Deng L, Meng T, Chen L, Wei W, Wang P. The role of ubiquitination in tumorigenesis and targeted drug discovery. Signal Transduct Target Ther 2020; 5(1): 11

Dinarello CA. The paradox of pro-inflammatory cytokines in cancer. Cancer Metastasis Rev 2006; 25(3): 307-313

Dmitrieva-Posocco O, Dzutsev A, Posocco DF, Hou V, Yuan W, Thovarai V, Mufazalov IA, Gunzer M, Shilovskiy IP, Khaitov MR, Trinchieri G, Waisman A, Grivennikov SI. Cell-Type-Specific Responses to Interleukin-1 Control Microbial Invasion and Tumor-Elicited Inflammation in Colorectal Cancer. Immunity 2019; 50(1): 166-180 e167

Duerfeldt AS, Peterson LB, Maynard JC, Ng CL, Eletto D, Ostrovsky O, Shinogle HE, Moore DS, Argon Y, Nicchitta CV, Blagg BS. Development of a Grp94 inhibitor. J Am Chem Soc 2012; 134(23): 9796-9804

Durrieu L, Lemieux W, Dieng MM, Fontaine F, Duval M, Le Deist F, Haddad E. Implication of different effector mechanisms by cord blood-derived and peripheral blood-derived cytokine-induced killer cells to kill precursor B acute lymphoblastic leukemia cell lines. Cytotherapy 2014; 16(6): 845-856

Edwards VD, Sweeney DT, Ho H, Eide CA, Rofelty A, Agarwal A, Liu SQ, Danilov AV, Lee P, Chantry D, McWeeney SK, Druker BJ, Tyner JW, Spurgeon SE, Loriaux MM. Targeting of colony-stimulating factor 1 receptor (CSF1R) in the CLL microenvironment yields antineoplastic activity in primary patient samples. Oncotarget 2018; 9(37): 24576-24589

Eletto D, Dersh D, Argon Y. GRP94 in ER quality control and stress responses. Semin Cell Dev Biol 2010; 21(5): 479-485

Ermakova SP, Kang BS, Choi BY, Choi HS, Schuster TF, Ma WY, Bode AM, Dong Z. (-)-Epigallocatechin gallate overcomes resistance to etoposide-induced cell death by targeting the molecular chaperone glucose-regulated protein 78. Cancer Res 2006; 66(18): 9260-9269

Fels DR, Ye J, Segan AT, Kridel SJ, Spiotto M, Olson M, Koong AC, Koumenis C. Preferential cytotoxicity of bortezomib toward hypoxic tumor cells via overactivation of endoplasmic reticulum stress pathways. Cancer Res 2008; 68(22): 9323-9330

Feng X, Lin T, Chen D, Li Z, Yang Q, Tian H, Xiao Y, Lin M, Liang M, Guo W, Zhao P, Guo Z. Mitochondria-associated ER stress evokes immunogenic cell death through the ROS-PERK-eIF2alpha pathway under PTT/CDT combined therapy. Acta Biomater 2023; 160: 211-224

Fisher DT, Chen Q, Skitzki JJ, Muhitch JB, Zhou L, Appenheimer MM, Vardam TD, Weis EL, Passanese J, Wang WC, Gollnick SO, Dewhirst MW, Rose-John S, Repasky EA, Baumann H, Evans SS. IL-6 trans-signaling licenses mouse and human tumor microvascular gateways for trafficking of cytotoxic T cells. J Clin Invest 2011; 121(10): 3846-3859

Fridman WH, Pages F, Sautes-Fridman C, Galon J. The immune contexture in human tumours: impact on clinical outcome. Nat Rev Cancer 2012;12(4): 298-306

Galehdar Z, Swan P, Fuerth B, Callaghan SM, Park DS, Cregan SP. Neuronal apoptosis induced by endoplasmic reticulum stress is regulated by ATF4-CHOP-mediated induction of the Bcl-2 homology 3-only member PUMA. J Neurosci 2010; 30(50): 16938-16948

Gao Q, Li XX, Xu YM, Zhang JZ, Rong SD, Qin YQ, Fang J. IRE1alpha-targeting downregulates ABC transporters and overcomes drug resistance of colon cancer cells. Cancer Lett 2020; 476: 67-74

Glick D, Barth S, Macleod KF. Autophagy: cellular and molecular mechanisms. J Pathol 2010; 221(1): 3-12

Gordon EM, Sankhala KK, Chawla N, Chawla SP. Trabectedin for Soft Tissue Sarcoma: Current Status and Future Perspectives. Adv Ther 2016;33(7): 1055-1071

Goulielmaki E, Bermudez-Brito M, Andreou M, Tzenaki N, Tzardi M, de Bree E, Tsentelierou E, Makrigiannakis A, Papakonstanti EA. Pharmacological inactivation of the PI3K p110delta prevents breast tumour progression by targeting cancer cells and macrophages. Cell Death Dis 2018; 9(6): 678

Greten FR,Grivennikov SI. Inflammation and Cancer: Triggers, Mechanisms, and Consequences. Immunity 2019; 51(1): 27-41

Grivennikov SI, Greten FR, Karin M. Immunity, inflammation, and cancer. Cell 2010; 140(6): 883-899

Guo Q, Jin Y, Chen X, Ye X, Shen X, Lin M, Zeng C, Zhou T, Zhang J. NF-kappaB in biology and targeted therapy: new insights and translational implications. Signal Transduct Target Ther 2024; 9(1): 53

Haabeth OA, Lorvik KB, Yagita H, Bogen B, Corthay A. Interleukin-1 is required for cancer eradication mediated by tumor-specific Th1 cells. Oncoimmunology 2016; 5(1): e1039763

Han D, Lerner AG, Vande Walle L, Upton JP, Xu W, Hagen A, Backes BJ, Oakes SA, Papa FR. IRE1alpha kinase activation modes control alternate endoribonuclease outputs to determine divergent cell fates. Cell 2009; 138(3): 562-575

Han F, Xu Q, Zhao J, Xiong P, Liu J. ERO1L promotes pancreatic cancer cell progression through activating the Wnt/catenin pathway. J Cell Biochem 2018; 119(11): 8996-9005

Hartley GP, Chow L, Ammons DT, Wheat WH, Dow SW. Programmed Cell Death Ligand 1 (PD-L1) Signaling Regulates Macrophage Proliferation and Activation. Cancer Immunol Res 2018; 6(10): 1260-1273

Hayes KE, Batsomboon P, Chen WC, Johnson BD, Becker A, Eschrich S, Yang Y, Robart AR, Dudley GB, Geldenhuys WJ, Hazlehurst LA. Inhibition of the FAD containing ER oxidoreductin 1 (Ero1) protein by EN-460 as a strategy for treatment of multiple myeloma. Bioorg Med Chem 2019; 27(8): 1479-1488

Hendershot LM, Buck TM, Brodsky JL. The Essential Functions of Molecular Chaperones and Folding Enzymes in Maintaining Endoplasmic Reticulum Homeostasis. J Mol Biol 2024; 436(14): 168418

Hirano S,Kataoka T. Deoxynivalenol induces ectodomain shedding of TNF receptor 1 and thereby inhibits the TNF-alpha-induced NF-kappaB signaling pathway. Eur J Pharmacol 2013; 701(1-3): 144-151

Holler N, Zaru R, Micheau O, Thome M, Attinger A, Valitutti S, Bodmer JL, Schneider P, Seed B, Tschopp J. Fas triggers an alternative, caspase-8-independent cell death pathway using the kinase RIP as effector molecule. Nat Immunol 2000; 1(6): 489-495

Hong H, Jiang L, Lin Y, He C, Zhu G, Du Q, Wang X, She F, Chen Y. TNF-alpha promotes lymphangiogenesis and lymphatic metastasis of gallbladder cancer through the ERK1/2/AP-1/VEGF-D pathway. BMC Cancer 2016; 16: 240

Hope JC, Cumberbatch M, Fielding I, Dearman RJ, Kimber I, Hopkins SJ. Identification of dendritic cells as a major source of interleukin-6 in draining lymph nodes following skin sensitization of mice. Immunology 1995; 86(3): 441-447

Huang Q, Lan F, Wang X, Yu Y, Ouyang X, Zheng F, Han J, Lin Y, Xie Y, Xie F, Liu W, Yang X, Wang H, Dong L, Wang L, Tan J. IL-1beta-induced activation of p38 promotes

metastasis in gastric adenocarcinoma via upregulation of AP-1/c-fos, MMP2 and MMP9. Mol Cancer 2014; 13: 18

Huang SC, Smith AM, Everts B, Colonna M, Pearce EL, Schilling JD, Pearce EJ. Metabolic Reprogramming Mediated by the mTORC2-IRF4 Signaling Axis Is Essential for Macrophage Alternative Activation. Immunity 2016; 45(4): 817-830

Ikeda H, Old LJ, Schreiber RD. The roles of IFN gamma in protection against tumor development and cancer immunoediting. Cytokine Growth Factor Rev 2002; 13(2): 95-109

Inaba K, Masui S, Iida H, Vavassori S, Sitia R, Suzuki M. Crystal structures of human Ero1alpha reveal the mechanisms of regulated and targeted oxidation of PDI. EMBO J 2010; 29(19): 3330-3343

Itoh K, Shiiba K, Shimizu Y, Suzuki R, Kumagai K. Generation of activated killer (AK) cells by recombinant interleukin 2 (rIL 2) in collaboration with interferon-gamma (IFN-gamma). J Immunol 1985; 134(5): 3124-3129

Jayaraj GG, Hipp MS, Hartl FU. Functional Modules of the Proteostasis Network. Cold Spring Harb Perspect Biol 2020; 12(1): a033951

Jiang X, Zhou J, Giobbie-Hurder A, Wargo J, Hodi FS. The activation of MAPK in melanoma cells resistant to BRAF inhibition promotes PD-L1 expression that is reversible by MEK and PI3K inhibition. Clin Cancer Res 2013; 19(3): 598-609

Johnson BD, Kaulagari S, Chen WC, Hayes K, Geldenhuys WJ, Hazlehurst LA. Identification of Natural Product Sulfuretin Derivatives as Inhibitors for the Endoplasmic Reticulum Redox Protein ERO1alpha. ACS Bio Med Chem Au 2022; 2(2): 161-170

Johnson DE, O'Keefe RA, Grandis JR. Targeting the IL-6/JAK/STAT3 signalling axis in cancer. Nat Rev Clin Oncol 2018; 15(4): 234-248

Joimel U, Gest C, Soria J, Pritchard LL, Alexandre J, Laurent M, Blot E, Cazin L, Vannier JP, Varin R, Li H, Soria C. Stimulation of angiogenesis resulting from cooperation between macrophages and MDA-MB-231 breast cancer cells: proposed molecular mechanism and effect of tetrathiomolybdate. BMC Cancer 2010; 10: 375

Kaneda MM, Messer KS, Ralainirina N, Li H, Leem CJ, Gorjestani S, Woo G, Nguyen AV, Figueiredo CC, Foubert P, Schmid MC, Pink M, Winkler DG, Rausch M, Palombella VJ, Kutok J, McGovern K, Frazer KA, Wu X, Karin M, Sasik R, Cohen EE, Varner JA. PI3Kgamma is a molecular switch that controls immune suppression. Nature 2016; 539(7629): 437-442

Kanemura S, Sofia EF, Hirai N, Okumura M, Kadokura H, Inaba K. Characterization of the endoplasmic reticulum-resident peroxidases GPx7 and GPx8 shows the higher oxidative activity of GPx7 and its linkage to oxidative protein folding. J Biol Chem 2020; 295(36): 12772-12785

Kapp K, Volz B, Oswald D, Wittig B, Baumann M, Schmidt M. Beneficial modulation of the tumor microenvironment and generation of anti-tumor responses by TLR9 agonist lefitolimod alone and in combination with checkpoint inhibitors. Oncoimmunology 2019; 8(12): e1659096

Keith B,Simon MC. Hypoxia-inducible factors, stem cells, and cancer. Cell 2007; 129(3): 465-472

Kidger AM, Sipthorp J, Cook SJ. ERK1/2 inhibitors: New weapons to inhibit the RAS-regulated RAF-MEK1/2-ERK1/2 pathway. Pharmacol Ther 2018; 187: 45-60

Klug F, Prakash H, Huber PE, Seibel T, Bender N, Halama N, Pfirschke C, Voss RH, Timke C, Umansky L, Klapproth K, Schakel K, Garbi N, Jager D, Weitz J, Schmitz-Winnenthal H, Hammerling GJ, Beckhove P. Low-dose irradiation programs macrophage

differentiation to an iNOS(+)/M1 phenotype that orchestrates effective T cell immunotherapy. Cancer Cell 2013; 24(5): 589-602

Kopito RR. ER quality control: the cytoplasmic connection. Cell 1997; 88(4): 427-430

Krebs J, Agellon LB, Michalak M. Ca(2+) homeostasis and endoplasmic reticulum (ER) stress: An integrated view of calcium signaling. Biochem Biophys Res Commun 2015; 460(1): 114-121

Larmonier N, Cathelin D, Larmonier C, Nicolas A, Merino D, Janikashvili N, Audia S, Bateman A, Thompson J, Kottke T, Hartung T, Katsanis E, Vile R, Bonnotte B. The inhibition of TNF-alpha anti-tumoral properties by blocking antibodies promotes tumor growth in a rat model. Exp Cell Res 2007; 313(11): 2345-2355

Le Mercier I, Poujol D, Sanlaville A, Sisirak V, Gobert M, Durand I, Dubois B, Treilleux I, Marvel J, Vlach J, Blay JY, Bendriss-Vermare N, Caux C, Puisieux I, Goutagny N. Tumor promotion by intratumoral plasmacytoid dendritic cells is reversed by TLR7 ligand treatment. Cancer Res 2013; 73(15): 4629-4640

Leal IS, Florido M, Andersen P, Appelberg R. Interleukin-6 regulates the phenotype of the immune response to a tuberculosis subunit vaccine. Immunology 2001; 103(3): 375-381

Lee S, Lee E, Ko E, Ham M, Lee HM, Kim ES, Koh M, Lim HK, Jung J, Park SY, Moon A. Tumor-associated macrophages secrete CCL2 and induce the invasive phenotype of human breast epithelial cells through upregulation of ERO1-alpha and MMP-9. Cancer Lett 2018; 437: 25-34

Lee SJ, Kim MJ, Kwon IC, Roberts TM. Delivery strategies and potential targets for siRNA in major cancer types. Adv Drug Deliv Rev 2016; 104: 2-15

Li W, Wu F, Zhao S, Shi P, Wang S, Cui D. Correlation between PD-1/PD-L1 expression and polarization in tumor-associated macrophages: A key player in tumor immunotherapy. Cytokine Growth Factor Rev 2022; 67: 49-57

Li XX, Zhang HS, Xu YM, Zhang RJ, Chen Y, Fan L, Qin YQ, Liu Y, Li M, Fang J. Knockdown of IRE1alpha inhibits colonic tumorigenesis through decreasing beta-catenin and IRE1alpha targeting suppresses colon cancer cells. Oncogene 2017; 36(48): 6738-6746

Liang D, Khoonkari M, Avril T, Chevet E, Kruyt FAE. The unfolded protein response as regulator of cancer stemness and differentiation: Mechanisms and implications for cancer therapy. Biochem Pharmacol 2021; 192: 114737

Lin Y, Choksi S, Shen HM, Yang QF, Hur GM, Kim YS, Tran JH, Nedospasov SA, Liu ZG. Tumor necrosis factor-induced nonapoptotic cell death requires receptor-interacting protein-mediated cellular reactive oxygen species accumulation. J Biol Chem 2004; 279(11): 10822-10828

Lin Y, Xu J, Lan H. Tumor-associated macrophages in tumor metastasis: biological roles and clinical therapeutic applications. J Hematol Oncol 2019; 12(1): 76

Liu L, Li S, Qu Y, Bai H, Pan X, Wang J, Wang Z, Duan J, Zhong J, Wan R, Fei K, Xu J, Yuan L, Wang C, Xue P, Zhang X, Ma Z, Wang J. Ablation of ERO1A induces lethal endoplasmic reticulum stress responses and immunogenic cell death to activate anti-tumor immunity. Cell Rep Med 2023; 4(10): 101206

Liu L, Wang C, Li S, Qu Y, Xue P, Ma Z, Zhang X, Bai H, Wang J. ERO1L Is a Novel and Potential Biomarker in Lung Adenocarcinoma and Shapes the Immune-Suppressive Tumor Microenvironment. Front Immunol 2021; 12: 677169

Liu R, Li X, Gao W, Zhou Y, Wey S, Mitra SK, Krasnoperov V, Dong D, Liu S, Li D, Zhu G, Louie S, Conti PS, Li Z, Lee AS, Gill PS. Monoclonal antibody against cell surface

GRP78 as a novel agent in suppressing PI3K/AKT signaling, tumor growth, and metastasis. Clin Cancer Res 2013; 19(24): 6802-6811

Liu X, Pu Y, Cron K, Deng L, Kline J, Frazier WA, Xu H, Peng H, Fu YX, Xu MM. CD47 blockade triggers T cell-mediated destruction of immunogenic tumors. Nat Med 2015; 21(10): 1209-1215

Liu Z, Zhang K, Zhao Z, Qin Z, Tang H. Prognosis-related autophagy genes in female lung adenocarcinoma. Medicine (Baltimore) 2022; 101(1): e28500

Loos B, du Toit A, Hofmeyr JH. Defining and measuring autophagosome flux-concept and reality. Autophagy 2014; 10(11): 2087-2096

Lu M, Lawrence DA, Marsters S, Acosta-Alvear D, Kimmig P, Mendez AS, Paton AW, Paton JC, Walter P, Ashkenazi A. Opposing unfolded-protein-response signals converge on death receptor 5 to control apoptosis. Science 2014; 345(6192): 98-101

Luo B,Lee AS. The critical roles of endoplasmic reticulum chaperones and unfolded protein response in tumorigenesis and anticancer therapies. Oncogene 2013; 32(7): 805-818

Manasanch EE,Orlowski RZ. Proteasome inhibitors in cancer therapy. Nat Rev Clin Oncol 2017; 14(7): 417-433

Mandula JK, Chang S, Mohamed E, Jimenez R, Sierra-Mondragon RA, Chang DC, Obermayer AN, Moran-Segura CM, Das S, Vazquez-Martinez JA, Prieto K, Chen A, Smalley KSM, Czerniecki B, Forsyth P, Koya RC, Ruffell B, Cubillos-Ruiz JR, Munn DH, Shaw TI, Conejo-Garcia JR, Rodriguez PC. Ablation of the endoplasmic reticulum stress kinase PERK induces paraptosis and type I interferon to promote anti-tumor T cell responses. Cancer Cell 2022; 40(10): 1145-1160

Mantovani A, Marchesi F, Malesci A, Laghi L, Allavena P. Tumour-associated macrophages as treatment targets in oncology. Nat Rev Clin Oncol 2017; 14(7): 399-416

Mantovani A, Sozzani S, Locati M, Allavena P, Sica A. Macrophage polarization: tumor-associated macrophages as a paradigm for polarized M2 mononuclear phagocytes. Trends Immunol 2002; 23(11): 549-555

Marciniak SJ, Yun CY, Oyadomari S, Novoa I, Zhang Y, Jungreis R, Nagata K, Harding HP, Ron D. CHOP induces death by promoting protein synthesis and oxidation in the stressed endoplasmic reticulum. Genes Dev 2004; 18(24): 3066-3077

May D, Itin A, Gal O, Kalinski H, Feinstein E, Keshet E. Ero1-L alpha plays a key role in a HIF-1-mediated pathway to improve disulfide bond formation and VEGF secretion under hypoxia: implication for cancer. Oncogene 2005; 24(6): 1011-1020

McCracken AA,Brodsky JL. Assembly of ER-associated protein degradation in vitro: dependence on cytosol, calnexin, and ATP. J Cell Biol 1996; 132(3): 291-298

McCullough KD, Martindale JL, Klotz LO, Aw TY, Holbrook NJ. Gadd153 sensitizes cells to endoplasmic reticulum stress by down-regulating Bcl2 and perturbing the cellular redox state. Mol Cell Biol 2001; 21(4): 1249-1259

Meloche S,Pouyssegur J. The ERK1/2 mitogen-activated protein kinase pathway as a master regulator of the G1- to S-phase transition. Oncogene 2007; 26(22): 3227-3239

Mimura N, Fulciniti M, Gorgun G, Tai YT, Cirstea D, Santo L, Hu Y, Fabre C, Minami J, Ohguchi H, Kiziltepe T, Ikeda H, Kawano Y, French M, Blumenthal M, Tam V, Kertesz NL, Malyankar UM, Hokenson M, Pham T, Zeng Q, Patterson JB, Richardson PG, Munshi NC, Anderson KC. Blockade of XBP1 splicing by inhibition of IRE1alpha is a promising therapeutic option in multiple myeloma. Blood 2012; 119(24): 5772-5781

Mohamed E, Cao Y, Rodriguez PC. Endoplasmic reticulum stress regulates tumor growth and anti-tumor immunity: a promising opportunity for cancer immunotherapy. Cancer Immunol Immunother 2017; 66(8): 1069-1078

Morante M, Pandiella A, Crespo P, Herrero A. Immune Checkpoint Inhibitors and RAS-ERK Pathway-Targeted Drugs as Combined Therapy for the Treatment of Melanoma. Biomolecules 2022; 12(11): 1562

Moreau P, Dimopoulos MA, Mikhael J, Yong K, Capra M, Facon T, Hajek R, Spicka I, Baker R, Kim K, Martinez G, Min CK, Pour L, Leleu X, Oriol A, Koh Y, Suzuki K, Risse ML, Asset G, Mace S, Martin T, group Is. Isatuximab, carfilzomib, and dexamethasone in relapsed multiple myeloma (IKEMA): a multicentre, open-label, randomised phase 3 trial. Lancet 2021; 397(10292): 2361-2371

Morgan E, Arnold M, Gini A, Lorenzoni V, Cabasag CJ, Laversanne M, Vignat J, Ferlay J, Murphy N, Bray F. Global burden of colorectal cancer in 2020 and 2040: incidence and mortality estimates from GLOBOCAN. Gut 2023; 72(2): 338-344

Movahedi K, Laoui D, Gysemans C, Baeten M, Stange G, Van den Bossche J, Mack M, Pipeleers D, In't Veld P, De Baetselier P, Van Ginderachter JA. Different tumor microenvironments contain functionally distinct subsets of macrophages derived from Ly6C(high) monocytes. Cancer Res 2010; 70(14): 5728-5739

Murciano-Goroff YR, Warner AB, Wolchok JD. The future of cancer immunotherapy: microenvironment-targeting combinations. Cell Res 2020; 30(6): 507-519

Murray PJ, Allen JE, Biswas SK, Fisher EA, Gilroy DW, Goerdt S, Gordon S, Hamilton JA, Ivashkiv LB, Lawrence T, Locati M, Mantovani A, Martinez FO, Mege JL, Mosser DM, Natoli G, Saeij JP, Schultze JL, Shirey KA, Sica A, Suttles J, Udalova I, van Ginderachter JA, Vogel SN, Wynn TA. Macrophage activation and polarization: nomenclature and experimental guidelines. Immunity 2014; 41(1): 14-20

Nawrocki ST, Carew JS, Dunner K, Jr., Boise LH, Chiao PJ, Huang P, Abbruzzese JL, McConkey DJ. Bortezomib inhibits PKR-like endoplasmic reticulum (ER) kinase and induces apoptosis via ER stress in human pancreatic cancer cells. Cancer Res 2005; 65(24): 11510-11519

Nguyen VD, Saaranen MJ, Karala AR, Lappi AK, Wang L, Raykhel IB, Alanen HI, Salo KE, Wang CC, Ruddock LW. Two endoplasmic reticulum PDI peroxidases increase the efficiency of the use of peroxide during disulfide bond formation. J Mol Biol 2011; 406(3): 503-515

Nie H, Luo C, Liao K, Xu J, Cheng XX, Wang X. Seven Glycolysis-Related Genes Predict the Prognosis of Patients With Pancreatic Cancer. Front Cell Dev Biol 2021; 9: 647106
North RJ, Neubauer RH, Huang JJ, Newton RC, Loveless SE. Interleukin 1-induced, T cell-mediated regression of immunogenic murine tumors. Requirement for an adequate level of already acquired host concomitant immunity. J Exp Med 1988; 168(6): 2031-2043

Nyiramana MM, Cho SB, Kim EJ, Kim MJ, Ryu JH, Nam HJ, Kim NG, Park SH, Choi YJ, Kang SS, Jung M, Shin MK, Han J, Jang IS, Kang D. Sea Hare Hydrolysate-Induced Reduction of Human Non-Small Cell Lung Cancer Cell Growth through Regulation of Macrophage Polarization and Non-Apoptotic Regulated Cell Death Pathways. Cancers (Basel) 2020; 12(3): 726

Olmeda D, Jorda M, Peinado H, Fabra A, Cano A. Snail silencing effectively suppresses tumour growth and invasiveness. Oncogene 2007; 26(13): 1862-1874

Ortega RA, Barham W, Sharman K, Tikhomirov O, Giorgio TD, Yull FE. Manipulating the NF-kappaB pathway in macrophages using mannosylated, siRNA-delivering nanoparticles can induce immunostimulatory and tumor cytotoxic functions. Int J Nanomedicine 2016; 11: 2163-2177

Paniagua Soriano G, De Bruin G, Overkleeft HS, Florea BI. Toward understanding induction of oxidative stress and apoptosis by proteasome inhibitors. Antioxid Redox Signal 2014; 21(17): 2419-2443

Papalexi E,Satija R. Single-cell RNA sequencing to explore immune cell heterogeneity. Nat Rev Immunol 2018; 18(1): 35-45

Park HK, Lee JE, Lim J, Kang BH. Mitochondrial Hsp90s suppress calcium-mediated stress signals propagating from mitochondria to the ER in cancer cells. Mol Cancer 2014; 13: 148

Pei HP, Feng Bo T, Li L, Nan Hui Y, Hong Z. IL-1beta/NF-kb signaling promotes colorectal cancer cell growth through miR-181a/PTEN axis. Arch Biochem Biophys 2016; 604: 20-26

Penny HL, Sieow JL, Adriani G, Yeap WH, See Chi Ee P, San Luis B, Lee B, Lee T, Mak SY, Ho YS, Lam KP, Ong CK, Huang RY, Ginhoux F, Rotzschke O, Kamm RD, Wong SC. Warburg metabolism in tumor-conditioned macrophages promotes metastasis in human pancreatic ductal adenocarcinoma. Oncoimmunology 2016; 5(8): e1191731

Petitprez F, Meylan M, de Reynies A, Sautes-Fridman C, Fridman WH. The Tumor Microenvironment in the Response to Immune Checkpoint Blockade Therapies. Front Immunol 2020; 11: 784

Pickup MW, Mouw JK, Weaver VM. The extracellular matrix modulates the hallmarks of cancer. EMBO Rep 2014; 15(12): 1243-1253

Pievani A, Borleri G, Pende D, Moretta L, Rambaldi A, Golay J, Introna M. Dual-functional capability of CD3+CD56+ CIK cells, a T-cell subset that acquires NK function and retains TCR-mediated specific cytotoxicity. Blood 2011; 118(12): 3301-3310

Pinton P, Giorgi C, Siviero R, Zecchini E, Rizzuto R. Calcium and apoptosis: ER-mitochondria Ca2+ transfer in the control of apoptosis. Oncogene 2008; 27(50): 6407-6418

Powell LE,Foster PA. Protein disulphide isomerase inhibition as a potential cancer therapeutic strategy. Cancer Med 2021; 10(8): 2812-2825

Puthalakath H, O'Reilly LA, Gunn P, Lee L, Kelly PN, Huntington ND, Hughes PD, Michalak EM, McKimm-Breschkin J, Motoyama N, Gotoh T, Akira S, Bouillet P, Strasser A. ER stress triggers apoptosis by activating BH3-only protein Bim. Cell 2007; 129(7): 1337-1349

Qian BZ,Pollard JW. Macrophage diversity enhances tumor progression and metastasis. Cell 2010; 141(1): 39-51

Quail DF, Bowman RL, Akkari L, Quick ML, Schuhmacher AJ, Huse JT, Holland EC, Sutton JC, Joyce JA. The tumor microenvironment underlies acquired resistance to CSF-1R inhibition in gliomas. Science 2016; 352(6288): aad3018

Rahma OE,Hodi FS. The Intersection between Tumor Angiogenesis and Immune Suppression. Clin Cancer Res 2019; 25(18): 5449-5457

Rahman NSA, Zahari S, Syafruddin SE, Firdaus-Raih M, Low TY, Mohtar MA. Functions and mechanisms of protein disulfide isomerase family in cancer emergence. Cell Biosci 2022; 12(1): 129

Ranganathan AC, Adam AP, Zhang L, Aguirre-Ghiso JA. Tumor cell dormancy induced by p38SAPK and ER-stress signaling: an adaptive advantage for metastatic cells? Cancer Biol Ther 2006; 5(7): 729-735

Rao B, Wang Q, Yao D, Xia Y, Li W, Xie Y, Li S, Cao M, Shen Y, Qin A, Zhao J, Cao Y. The cryo-EM structure of the human ERAD retrotranslocation complex. Sci Adv 2023; 9(41): eadi5656

Rashid HO, Yadav RK, Kim HR, Chae HJ. ER stress: Autophagy induction, inhibition and selection. Autophagy 2015; 11(11): 1956-1977

Raulet DH, Gasser S, Gowen BG, Deng W, Jung H. Regulation of ligands for the NKG2D activating receptor. Annu Rev Immunol 2013; 31: 413-441

Rauschert N, Brandlein S, Holzinger E, Hensel F, Muller-Hermelink HK, Vollmers HP. A new tumor-specific variant of GRP78 as target for antibody-based therapy. Lab Invest 2008; 88(4): 375-386

Raymundo DP, Doultsinos D, Guillory X, Carlesso A, Eriksson LA, Chevet E. Pharmacological Targeting of IRE1 in Cancer. Trends Cancer 2020; 6(12): 1018-1030

Reddy RK, Mao C, Baumeister P, Austin RC, Kaufman RJ, Lee AS. Endoplasmic reticulum chaperone protein GRP78 protects cells from apoptosis induced by topoisomerase inhibitors: role of ATP binding site in suppression of caspase-7 activation. J Biol Chem 2003; 278(23): 20915-20924

Rigo A, Gottardi M, Zamo A, Mauri P, Bonifacio M, Krampera M, Damiani E, Pizzolo G, Vinante F. Macrophages may promote cancer growth via a GM-CSF/HB-EGF paracrine loop that is enhanced by CXCL12. Mol Cancer 2010; 9: 273

Rodell CB, Arlauckas SP, Cuccarese MF, Garris CS, Li R, Ahmed MS, Kohler RH, Pittet MJ, Weissleder R. TLR7/8-agonist-loaded nanoparticles promote the polarization of tumour-associated macrophages to enhance cancer immunotherapy. Nat Biomed Eng 2018; 2(8): 578-588

Ruggiero C, Doghman-Bouguerra M, Ronco C, Benhida R, Rocchi S, Lalli E. The GRP78/BiP inhibitor HA15 synergizes with mitotane action against adrenocortical carcinoma cells through convergent activation of ER stress pathways. Mol Cell Endocrinol 2018; 474: 57-64

Ryuto M, Ono M, Izumi H, Yoshida S, Weich HA, Kohno K, Kuwano M. Induction of vascular endothelial growth factor by tumor necrosis factor alpha in human glioma cells. Possible roles of SP-1. J Biol Chem 1996; 271(45): 28220-28228

Sakamoto KM, Kim KB, Kumagai A, Mercurio F, Crews CM, Deshaies RJ. Protacs: chimeric molecules that target proteins to the Skp1-Cullin-F box complex for ubiquitination and degradation. Proc Natl Acad Sci U S A 2001; 98(15): 8554-8559

Salvagno C, Mandula JK, Rodriguez PC, Cubillos-Ruiz JR. Decoding endoplasmic reticulum stress signals in cancer cells and antitumor immunity. Trends Cancer 2022; 8(11): 930-943

Samatar AA,Poulikakos PI. Targeting RAS-ERK signalling in cancer: promises and challenges. Nat Rev Drug Discov 2014; 13(12): 928-942

Satoh R, Hamada N, Yamada A, Kanda Y, Ishikawa F, Takasaki T, Tanabe G, Sugiura R. Discovery of new benzhydrol biscarbonate esters as potent and selective apoptosis inducers of human melanomas bearing the activated ERK pathway: SAR studies on an ERK MAPK signaling modulator, ACA-28. Bioorg Chem 2020; 103: 104137

Schmeel LC, Schmeel FC, Coch C, Schmidt-Wolf IG. Cytokine-induced killer (CIK) cells in cancer immunotherapy: report of the international registry on CIK cells (IRCC). J Cancer Res Clin Oncol 2015; 141(5): 839-849

Schmidt-Wolf IG, Lefterova P, Mehta BA, Fernandez LP, Huhn D, Blume KG, Weissman IL, Negrin RS. Phenotypic characterization and identification of effector cells involved in

tumor cell recognition of cytokine-induced killer cells. Exp Hematol 1993; 21(13): 1673-1679

Schmidt-Wolf IG, Negrin RS, Kiem HP, Blume KG, Weissman IL. Use of a SCID mouse/human lymphoma model to evaluate cytokine-induced killer cells with potent antitumor cell activity. J Exp Med 1991; 174(1): 139-149

Schroder M. Endoplasmic reticulum stress responses. Cell Mol Life Sci 2008; 65(6): 862-894

Schwarz DS,Blower MD. The endoplasmic reticulum: structure, function and response to cellular signaling. Cell Mol Life Sci 2016; 73(1): 79-94

Scott K, Hayden PJ, Will A, Wheatley K, Coyne I. Bortezomib for the treatment of multiple myeloma. Cochrane Database Syst Rev 2016; 4(4): CD010816

Seol SY, Kim C, Lim JY, Yoon SO, Hong SW, Kim JW, Choi SH, Cho JY. Overexpression of Endoplasmic Reticulum Oxidoreductin 1-alpha (ERO1L) Is Associated with Poor Prognosis of Gastric Cancer. Cancer Res Treat 2016; 48(4): 1196-1209

Sharma MD, Hou DY, Baban B, Koni PA, He Y, Chandler PR, Blazar BR, Mellor AL, Munn DH. Reprogrammed foxp3(+) regulatory T cells provide essential help to support cross-presentation and CD8(+) T cell priming in naive mice. Immunity 2010; 33(6): 942-954

Song B, Scheuner D, Ron D, Pennathur S, Kaufman RJ. Chop deletion reduces oxidative stress, improves beta cell function, and promotes cell survival in multiple mouse models of diabetes. J Clin Invest 2008; 118(10): 3378-3389

Song S, Tan J, Miao Y, Li M, Zhang Q. Crosstalk of autophagy and apoptosis: Involvement of the dual role of autophagy under ER stress. J Cell Physiol 2017; 232(11): 2977-2984

Song TL, Nairismagi ML, Laurensia Y, Lim JQ, Tan J, Li ZM, Pang WL, Kizhakeyil A, Wijaya GC, Huang DC, Nagarajan S, Chia BK, Cheah D, Liu YH, Zhang F, Rao HL, Tang T, Wong EK, Bei JX, Iqbal J, Grigoropoulos NF, Ng SB, Chng WJ, Teh BT, Tan SY, Verma NK, Fan H, Lim ST, Ong CK. Oncogenic activation of the STAT3 pathway drives PD-L1 expression in natural killer/T-cell lymphoma. Blood 2018; 132(11): 1146-1158

Szlosarek PW, Luong P, Phillips MM, Baccarini M, Stephen E, Szyszko T, Sheaff MT, Avril N. Metabolic response to pegylated arginine deiminase in mesothelioma with promoter methylation of argininosuccinate synthetase. J Clin Oncol 2013; 31(7): e111-113

Tanaka T, Kajiwara T, Torigoe T, Okamoto Y, Sato N, Tamura Y. Cancer-associated oxidoreductase ERO1-alpha drives the production of tumor-promoting myeloid-derived suppressor cells via oxidative protein folding. J Immunol 2015; 194(4): 2004-2010

Tanaka T, Kutomi G, Kajiwara T, Kukita K, Kochin V, Kanaseki T, Tsukahara T, Hirohashi Y, Torigoe T, Okamoto Y, Hirata K, Sato N, Tamura Y. Cancer-associated oxidoreductase ERO1-alpha drives the production of VEGF via oxidative protein folding and regulating the mRNA level. Br J Cancer 2016; 114(11): 1227-1234

Tanaka T, Kutomi G, Kajiwara T, Kukita K, Kochin V, Kanaseki T, Tsukahara T, Hirohashi Y, Torigoe T, Okamoto Y, Hirata K, Sato N, Tamura Y. Cancer-associated oxidoreductase ERO1-alpha promotes immune escape through up-regulation of PD-L1 in human breast cancer. Oncotarget 2017; 8(15): 24706-24718

Tay AHM, Cinotti R, Sze NSK, Lundqvist A. Inhibition of ERO1a and IDO1 improves dendritic cell infiltration into pancreatic ductal adenocarcinoma. Front Immunol 2023; 14: 1264012

Taylor RC, Cullen SP, Martin SJ. Apoptosis: controlled demolition at the cellular level. Nat Rev Mol Cell Biol 2008; 9(3): 231-241

Teichmann JV, Ludwig WD, Seibt-Jung H, Thiel E. Induction of lymphokine-activated killer cell against human leukemia cells in vitro. Blut 1989; 59(1): 21-24

Thorpe LM, Yuzugullu H, Zhao JJ. PI3K in cancer: divergent roles of isoforms, modes of activation and therapeutic targeting. Nat Rev Cancer 2015; 15(1): 7-24

Tian Y, Xiao H, Yang Y, Zhang P, Yuan J, Zhang W, Chen L, Fan Y, Zhang J, Cheng H, Deng T, Yang L, Wang W, Chen G, Wang P, Gong P, Niu X, Zhang X. Crosstalk between 5-methylcytosine and N(6)-methyladenosine machinery defines disease progression, therapeutic response and pharmacogenomic landscape in hepatocellular carcinoma. Mol Cancer 2023; 22(1): 5

Ullah R, Yin Q, Snell AH, Wan L. RAF-MEK-ERK pathway in cancer evolution and treatment. Semin Cancer Biol 2022; 85: 123-154

Urano F, Wang X, Bertolotti A, Zhang Y, Chung P, Harding HP, Ron D. Coupling of stress in the ER to activation of JNK protein kinases by transmembrane protein kinase IRE1. Science 2000; 287(5453): 664-666

Urra H, Dufey E, Avril T, Chevet E, Hetz C. Endoplasmic Reticulum Stress and the Hallmarks of Cancer. Trends Cancer 2016; 2(5): 252-262

Varone E, Decio A, Barbera MC, Bolis M, Di Rito L, Pisati F, Giavazzi R, Zito E. Endoplasmic reticulum oxidoreductin 1-alpha deficiency and activation of protein translation synergistically impair breast tumour resilience. Br J Pharmacol 2022; 179(23): 5180-5195

Varone E, Decio A, Chernorudskiy A, Minoli L, Brunelli L, Ioli F, Piotti A, Pastorelli R, Fratelli M, Gobbi M, Giavazzi R, Zito E. The ER stress response mediator ERO1 triggers cancer metastasis by favoring the angiogenic switch in hypoxic conditions. Oncogene 2021; 40(9): 1721-1736

Verneris MR, Karimi M, Baker J, Jayaswal A, Negrin RS. Role of NKG2D signaling in the cytotoxicity of activated and expanded CD8+ T cells. Blood 2004; 103(8): 3065-3072
Voronov E, Carmi Y, Apte RN. The role IL-1 in tumor-mediated angiogenesis. Front Physiol 2014; 5: 114

Walton PD, Airey JA, Sutko JL, Beck CF, Mignery GA, Sudhof TC, Deerinck TJ, Ellisman MH. Ryanodine and inositol trisphosphate receptors coexist in avian cerebellar Purkinje neurons. J Cell Biol 1991; 113(5): 1145-1157

Wang D,DuBois RN. Immunosuppression associated with chronic inflammation in the tumor microenvironment. Carcinogenesis 2015; 36(10): 1085-1093

Wang G, Han J, Wang G, Wu X, Huang Y, Wu M, Chen Y. ERO1alpha mediates endoplasmic reticulum stress-induced apoptosis via microRNA-101/EZH2 axis in colon cancer RKO and HT-29 cells. Hum Cell 2021; 34(3): 932-944

Wang H, Wang HS, Zhou BH, Li CL, Zhang F, Wang XF, Zhang G, Bu XZ, Cai SH, Du J. Epithelial-mesenchymal transition (EMT) induced by TNF-alpha requires AKT/GSK-3beta-mediated stabilization of snail in colorectal cancer. PLoS One 2013; 8(2): e56664
Wang L, Du F, Wang X. TNF-alpha induces two distinct caspase-8 activation pathways. Cell 2008; 133(4): 693-703

Wang M,Kaufman RJ. The impact of the endoplasmic reticulum protein-folding environment on cancer development. Nat Rev Cancer 2014; 14(9): 581-597

Wang Y, Lin YX, Qiao SL, An HW, Ma Y, Qiao ZY, Rajapaksha RP, Wang H. Polymeric nanoparticles promote macrophage reversal from M2 to M1 phenotypes in the tumor microenvironment. Biomaterials 2017; 112: 153-163

Wang Y, Zhai W, Yang L, Cheng S, Cui W, Li J. Establishments and evaluations of post‐operative adhesion animal models. Advanced Therapeutics 2023; 6(4): 2200297

Weichand B, Popp R, Dziumbla S, Mora J, Strack E, Elwakeel E, Frank AC, Scholich K, Pierre S, Syed SN, Olesch C, Ringleb J, Oren B, Doring C, Savai R, Jung M, von Knethen A, Levkau B, Fleming I, Weigert A, Brune B. S1PR1 on tumor-associated macrophages promotes lymphangiogenesis and metastasis via NLRP3/IL-1beta. J Exp Med 2017; 214(9): 2695-2713

Wen Z, Liu H, Li M, Li B, Gao W, Shao Q, Fan B, Zhao F, Wang Q, Xie Q, Yang Y, Yu J, Qu X. Increased metabolites of 5-lipoxygenase from hypoxic ovarian cancer cells promote tumor-associated macrophage infiltration. Oncogene 2015; 34(10): 1241-1252

Whiteside TL. The tumor microenvironment and its role in promoting tumor growth. Oncogene 2008; 27(45): 5904-5912

Wu X, Sharma A, Oldenburg J, Weiher H, Essler M, Skowasch D, Schmidt-Wolf IGH. NKG2D Engagement Alone Is Sufficient to Activate Cytokine-Induced Killer Cells While 2B4 Only Provides Limited Coactivation. Front Immunol 2021; 12: 731767

Wu X, Singh R, Hsu DK, Zhou Y, Yu S, Han D, Shi Z, Huynh M, Campbell JJ, Hwang ST. A Small Molecule CCR2 Antagonist Depletes Tumor Macrophages and Synergizes with Anti-PD-1 in a Murine Model of Cutaneous T-Cell Lymphoma (CTCL). J Invest Dermatol 2020; 140(7): 1390-1400

Wu X, Zhang Y, Li Y, Schmidt-Wolf IGH. Increase of Antitumoral Effects of Cytokine-Induced Killer Cells by Antibody-Mediated Inhibition of MICA Shedding. Cancers (Basel) 2020; 12(7):1818

Wynn TA, Chawla A, Pollard JW. Macrophage biology in development, homeostasis and disease. Nature 2013; 496(7446): 445-455

Xie Y, Lei X, Zhao G, Guo R, Cui N. mTOR in programmed cell death and its therapeutic implications. Cytokine Growth Factor Rev 2023; 71-72: 66-81

Xu M, Wang X, Li Y, Geng X, Jia X, Zhang L, Yang H. Arachidonic Acid Metabolism Controls Macrophage Alternative Activation Through Regulating Oxidative Phosphorylation in PPARgamma Dependent Manner. Front Immunol 2021; 12: 618501

Yaeger R,Corcoran RB. Targeting Alterations in the RAF-MEK Pathway. Cancer Discov 2019; 9(3): 329-341

Yamaguchi H, Hsu JM, Yang WH, Hung MC. Mechanisms regulating PD-L1 expression in cancers and associated opportunities for novel small-molecule therapeutics. Nat Rev Clin Oncol 2022; 19(5): 287-305

Yang H, Zhang Q, Xu M, Wang L, Chen X, Feng Y, Li Y, Zhang X, Cui W, Jia X. CCL2-CCR2 axis recruits tumor associated macrophages to induce immune evasion through PD-1 signaling in esophageal carcinogenesis. Mol Cancer 2020; 19(1): 41

Yang Q, Guo N, Zhou Y, Chen J, Wei Q, Han M. The role of tumor-associated macrophages (TAMs) in tumor progression and relevant advance in targeted therapy. Acta Pharm Sin B 2020; 10(11): 2156-2170

Yi M, Ban Y, Tan Y, Xiong W, Li G, Xiang B. 6-Phosphofructo-2-kinase/fructose-2,6-biphosphatase 3 and 4: A pair of valves for fine-tuning of glucose metabolism in human cancer. Mol Metab 2019; 20: 1-13

Young MM, Takahashi Y, Khan O, Park S, Hori T, Yun J, Sharma AK, Amin S, Hu CD, Zhang J, Kester M, Wang HG. Autophagosomal membrane serves as platform for intracellular death-inducing signaling complex (iDISC)-mediated caspase-8 activation and apoptosis. J Biol Chem 2012; 287(15): 12455-12468

Yousefi S, Perozzo R, Schmid I, Ziemiecki A, Schaffner T, Scapozza L, Brunner T, Simon HU. Calpain-mediated cleavage of Atg5 switches autophagy to apoptosis. Nat Cell Biol 2006; 8(10): 1124-1132

Yuri P, Hendri AZ, Danarto R. Association between tumor-associated macrophages and microvessel density on prostate cancer progression. Prostate Int 2015; 3(3): 93-98

Zeisberger SM, Odermatt B, Marty C, Zehnder-Fjallman AH, Ballmer-Hofer K, Schwendener RA. Clodronate-liposome-mediated depletion of tumour-associated macrophages: a new and highly effective antiangiogenic therapy approach. Br J Cancer 2006; 95(3): 272-281

Zeng S, Huang W, Zheng X, Liyan C, Zhang Z, Wang J, Shen Z. Proteolysis targeting chimera (PROTAC) in drug discovery paradigm: Recent progress and future challenges. Eur J Med Chem 2021; 210: 112981

Zhang J, Pavlova NN, Thompson CB. Cancer cell metabolism: the essential role of the nonessential amino acid, glutamine. EMBO J 2017; 36(10): 1302-1315

Zhang J, Yang J, Lin C, Liu W, Huo Y, Yang M, Jiang SH, Sun Y, Hua R. Endoplasmic Reticulum stress-dependent expression of ERO1L promotes aerobic glycolysis in Pancreatic Cancer. Theranostics 2020; 10(18): 8400-8414

Zhang M, He Y, Sun X, Li Q, Wang W, Zhao A, Di W. A high M1/M2 ratio of tumor-associated macrophages is associated with extended survival in ovarian cancer patients. J Ovarian Res 2014; 7: 19

Zhang Y, Li T, Zhang L, Shangguan F, Shi G, Wu X, Cui Y, Wang X, Wang X, Liu Y, Lu B, Wei T, Wang CC, Wang L. Targeting the functional interplay between endoplasmic reticulum oxidoreductin-1alpha and protein disulfide isomerase suppresses the progression of cervical cancer. EBioMedicine 2019; 41: 408-419

Zhao H, Wu L, Yan G, Chen Y, Zhou M, Wu Y, Li Y. Inflammation and tumor progression: signaling pathways and targeted intervention. Signal Transduct Target Ther 2021; 6(1): 263

Zhao R, Lv Y, Feng T, Zhang R, Ge L, Pan J, Han B, Song G, Wang L. ATF6alpha promotes prostate cancer progression by enhancing PLA2G4A-mediated arachidonic acid metabolism and protecting tumor cells against ferroptosis. Prostate 2022; 82(5): 617-629

Zhao X, Mohaupt M, Jiang J, Liu S, Li B, Qin Z. Tumor necrosis factor receptor 2-mediated tumor suppression is nitric oxide dependent and involves angiostasis. Cancer Res 2007; 67(9): 4443-4450

Zheng S, Wang X, Zhao D, Liu H, Hu Y. Calcium homeostasis and cancer: insights from endoplasmic reticulum-centered organelle communications. Trends Cell Biol 2023; 33(4): 312-323

Zhou H, Zhang Y, Fu Y, Chan L, Lee AS. Novel mechanism of anti-apoptotic function of 78-kDa glucose-regulated protein (GRP78): endocrine resistance factor in breast cancer, through release of B-cell lymphoma 2 (BCL-2) from BCL-2-interacting killer (BIK). J Biol Chem 2011; 286(29): 25687-25696

Zhu J, Wang M, Hu D. Development of an autophagy-related gene prognostic signature in lung adenocarcinoma and lung squamous cell carcinoma. PeerJ 2020; 8: e8288

Zhu Y, Knolhoff BL, Meyer MA, Nywening TM, West BL, Luo J, Wang-Gillam A, Goedegebuure SP, Linehan DC, DeNardo DG. CSF1/CSF1R blockade reprograms tumor-infiltrating macrophages and improves response to T-cell checkpoint immunotherapy in pancreatic cancer models. Cancer Res 2014; 74(18): 5057-5069

Zilli F, Marques Ramos P, Auf der Maur P, Jehanno C, Sethi A, Coissieux MM, Eichlisberger T, Sauteur L, Rouchon A, Bonapace L, Pinto Couto J, Rad R, Jensen MR, Banfi A, Stadler MB, Bentires-Alj M. The NFIB-ERO1A axis promotes breast cancer metastatic colonization of disseminated tumour cells. EMBO Mol Med 2021; 13(4): e13162

Zimel MN, Horowitz CB, Rajasekhar VK, Christ AB, Wei X, Wu J, Wojnarowicz PM, Wang D, Goldring SR, Purdue PE, Healey JH. HPMA-Copolymer Nanocarrier Targets Tumor-

Associated Macrophages in Primary and Metastatic Breast Cancer. Mol Cancer Ther 2017; 16(12): 2701-2710

Zito E. PRDX4, an endoplasmic reticulum-localized peroxiredoxin at the crossroads between enzymatic oxidative protein folding and nonenzymatic protein oxidation. Antioxid Redox Signal 2013; 18(13): 1666-1674

Zito E, Hansen HG, Yeo GS, Fujii J, Ron D. Endoplasmic reticulum thiol oxidase deficiency leads to ascorbic acid depletion and noncanonical scurvy in mice. Mol Cell 2012; 48(1): 39-51

9. Acknowledgements

My four years at the University of Bonn have been an unforgettable and transformative experience. During this time, I learned to conduct independent research, identify and solve scientific problems, and broaden my perspectives through exchange.

I would like to express my sincere gratitude to my supervisor, Prof. Schmidt-Wolf, for giving me the opportunity to study at the University of Bonn, for his invaluable guidance, and for supporting my independent research. I am also thankful to my second supervisor, Prof. Weiher, for his insightful discussions and suggestions during annual committee meetings, as well as for reviewing this dissertation. My appreciation also goes to Prof. Lukacs-Kornek and Prof. Gonzalez-Carmona for serving on my dissertation committee. I am deeply grateful to our secretary, Tanja Schuster, for her kind assistance in various aspects of my academic and daily life. Special thanks to my lab colleagues for their discussions and friendship, and to Maria Fitria Setiawan and Oliver Rudan for their excellent lab management. I also appreciate Jennifer Sonne and Prof. Jaehde for their support with lab facilities and space. Finally, I sincerely thank my family and all my friends for their unwavering support and encouragement throughout this journey.